Ferdowsi University of Mashhad

ISSN 2008-9147
Numbers: 22

JCMR

Journal of Cell and Molecular Research

Volume 11, Number 2, Winter, 2020

بسم الله الرحمن الرحیم

Issuance License No. 124/902-27.05.2008 from Ministry of Culture and Islamic Guidance
Scientific Research Issuance License No. 161675 from the Ministry of Science, Research and Technology, Iran

Journal of Cell and Molecular Research (JCMR)

Volume 11, Number 2, Winter, 2020

JCMR Office: Department of Biology, Faculty of Sciences, Ferdowsi University of Mashhad, Mashhad, Iran.
Postal Code: 9177948953
P.O. Box: 917751436
Tel: +98-513-8804063/+98-9156996326
Fax: +98-513-8795162
E-mail: jcmr@um.ac.ir
Online Submission: http://jcmr.um.ac.ir

Table of Contents

Cost-effective Strategies for Depletion of Endogenous Extracellular Vesicles from Fetal Bovine Serum **42**
Azadeh Haghighitalab, Maryam M. Matin, Fatemeh Khakrah, Ahmad Asoodeh, Ahmad Reza Bahrami

A Rapid Method for Analysis of cDNA Synthesis Using Ion-Pair Reversed-Phase High Performance Liquid Chromatography **55**
Maryam M. Matin, David P. Hornby

Production of Silver Nanoparticles by Marigold Extract **59**
Zohreh Sohrabi Nezhad, Hassan Marashi, Nasrin Moshtaghi

***In silico* Analysis of Determinant Factors in Microbial Protease Thermostability** **66**
Parisa Farrokh, Fatemeh Salimi

Evaluation of IFN-γ and T-bet Expression Levels as Possible Molecular Markers of Schizophrenia **82**
Roghaye Lorestani, Sohrab Boozarpour, Sakineh Alijanpour, Leila Ahangar

Immunosuppressive Effects of Human Chorionic Gonadotropin (hCG) on Mesenchymal Stromal Cells **90**
Sepideh sadat Hosseini, Shadi Mehrzad, Halimeh Hassanzadeh, Hamid Reza Bidkhori, Mahdi Mirahmadi, Madjid Momeni-Moghaddam, Fatemeh Sadeghifar, Moein Farshchian

Vitamin E Pretreatment of Mesenchymal Stem Cells: The Interplay of Oxidative Stress and Inflammation **99**
Shadi Mehrzad, Sepideh sadat Hosseini, Majid Momeni-Moghaddam, Moein Farshchian, Halimeh Hassanzadeh, Mahdi Mirahmadi, Fatemeh Sadeghifar, Hamid Reza Bidkhori

Journal of Cell and Molecular Research (2020) 11 (2), 42-54 DOI: 10.22067/jcmr.v11i2.85209

Research Article

Cost-effective Strategies for Depletion of Endogenous Extracellular Vesicles from Fetal Bovine Serum

Azadeh Haghighitalab[1], Maryam M. Matin[1,2], Fatemeh Khakrah[3], Ahmad Asoodeh[4,5], Ahmad Reza Bahrami[1,5*]

[1] *Department of Biology, Faculty of Science, Ferdowsi University of Mashhad, Mashhad, Iran*
[2] *Novel Diagnostics & Therapeutics Research Group, Institute of Biotechnology, Ferdowsi University of Mashhad, Mashhad, Iran*
[3] *Central laboratory, Ferdowsi University of Mashhad, Mashhad, Iran*
[4] *Department of Chemistry, Faculty of Science, Ferdowsi University of Mashhad, Mashhad, Iran*
[5] *Industrial Biotechnology Research Group, Institute of Biotechnology, Ferdowsi University of Mashhad, Mashhad, Iran*

Received 22 January 2020 Accepted 28 February 2020

Abstract

Despite the prominent therapeutic potentials of stem cells, their use in cell therapy has been challenged with some unreproducible and inconsistent outcomes in addition to the risk of rejection and tumorigenesis. Gaining novel insights to the importance of the conditioned medium, secretory factors and extracellular vesicles as the functional components of the cultured stem cells, suggested the idea of substituting the cells with their cell-free counterparts. Biological properties of these products are influenced by the cues received from their microenvironment. Hence, providing optimal and fully defined culture conditions is essential for their preparation. Fetal bovine serum (FBS), one of the most routine supplements of cell culture, is enriched by endogenous extracellular vesicles (EVs). These EVs will affect the yield, purity and functional features of the cell-free products. Here, we endeavored to examine and compare three different methods including ultrasonication, ultrafiltration and polymer-based precipitation, to deplete EVs from FBS. We chose easy to perform and fast methods with the capacity for high-throughput applications. Based on our observations, although all examined methods were able to deplete EVs from FBS to some extent, polymer-based precipitation could be considered as the method of choice with minimal consequences on the biological requirements of FBS to support cell growth and characteristics. Due to similarities between FBS and some other biological solutions, this strategy would be suitable for EV-depletion from other liquids with high concentrations of proteins and nutrients. Moreover, it could be applied for preparation of optimal culture conditions for nanoparticle applications.

***Keywords*:** Extracellular vesicle-depletion, Exosome, Polyethylene glycol, Ultrafiltration, Ultrasonication, Fetal bovine serum

Introduction

Although, in recent decades stem cell therapy as an advanced scientific research topic has been declared to hold a great promise for untreatable diseases, the fluctuations in the outcome of cell therapy procedures, put some struggle in their application (Choi et al., 2019; Lukomska et al., 2019; Zakrzewski et al., 2019). In recent years, there has been a trend to take advantage of stem cells' benefits by substituting them with their secretome or active components of their conditioned media such as extracellular vesicles (EVs) (Gurunathan et al., 2019; Weiss and Dahlke, 2019; Zhang et al., 2019). These vesicles transfer a wide range of bioactive components such as RNAs, DNAs and proteins while protecting them from environmental insults due to presence of a bilayer membrane (Colombo et al., 2014).

There are a wide range of techniques for isolation of extracellular vesicles from various bioliquids or conditioned media (*see* Gurunathan et al., 2019; Li et al., 2019). The method of choice affects the purity of the final preparations which should be carefully examined according to the guidelines of the International Society of Extracellular Vesicles (ISEV) (Théry et al., 2018).

It is known that application of FBS, as an essential supplement in cell culture, bears a risk of transferring bovine EVs to the culture (Czapla et al., 2019; Eitan et al., 2015; Mannerström et al., 2019; Shelke et al., 2014). A brief literature review indicates the significance of this problem as most studies investigating the functional roles of EVs

*Corresponding author's e-mail address: *ar-bahrami@um.ac.ir*

have been performed under serum-free circumstances, which are not optimal (Lehrich et al., 2019; Théry et al., 2006). In some other studies, exosome-depleted serum prepared by more than 18 h ultracentrifugation at 100000 to 120000 *g* has been applied. Despite the large number of experiments performed based on this method, particle removal was reported to be inefficient (Lehrich et al., 2018). Moreover, long-term ultracentrifugation, by itself, will also remove most of the active components of the serum. It is labor intensive, time consuming and needs expensive infrastructures. Commercial exosome depleted serum batches are also available. However, their application is extremely limited due to the high cost.

Hence, in this study, we investigated the possibility of removing the nano-sized extracellular vesicles from FBS based on the application of cost-effective methods including ultrasonication, ultrafiltration and polymer precipitation to decrease the expenditures of research in the field of EVs, while maintaining its quality. Unlike ultracentrifugation, these methods have the proper capacity for large-scale applications.

Materials and Methods

EV depletion strategies

Probe Sonication (Ultrasonication)

Commercial fetal bovine serum samples (Gibco, Germany), thawed to room temperature, were probe sonicated on ice for 120 sec (10 sec on, 10 sec off) with 20 kHz and 50 W (Ultrasonic probe, Topsonics; Iran). Samples were not heat-inactivated or diluted before sonication. Serum samples were then centrifuged at 600 *g* for 4 min at 4°C, to remove components created during sonication.

Ultrafiltration procedure

Briefly, FBS samples without any modifications or dilutions were centrifuged (400 *g*, 6 min) to remove large suspended particles. Then, they were concentrated from 35 ml to 5 ml using pressure-driven concentrating protocols via Stirred Cell Model 8050 with the application of 100 kDa disposable membranes (PLHK04310, Millipore, USA) using nitrogen gas (<10 psi) at room temperature. The concentrates were applied for downstream applications. EV-depleted serum samples were syringe-filtrated and collected in clean vessels as the final products.

Polymer-based precipitation

In order to deplete EVs from FBS samples, based on the polymer precipitation method, (polyethylene glycol) PEG 4000 (Merck, Germany) sterile solutions were applied. 16% PEG solutions were prepared in sterile deionized water and homogenized via ultrasonic-bath (35 Hz, 4 min, RT; BANDELIN SONOREX, Germany). Fetal bovine sera were thawed and homogenized by mechanical mixing, before the addition of NaCl (0.9%) at a ratio of 1:30 V/V. Then, PEG solutions were added to fetal bovine samples (final ratio of 1 to 4 V/V) and shaken to obtain homogenous solutions. Following 90 min incubation at 4°C, samples were cold-centrifuged (5000 *g*) for 50 min (Sigma, 3-16pk, Germany). The supernatants were collected in new tubes under sterile conditions as the exosome-depleted serum, while white pellets were discarded.

Nanoparticle characterization strategies

Dynamic Light Scattering

EV-depleted serum samples, prepared using different methods, were loaded on Particle Size Analyzer (0.5 nm-10 µm; Vasco3, Cordouan, France) to investigate the distribution pattern of the remaining particles (0-1000 nm) in comparison to the control samples. Measurements were performed based on Cumulants and Pade Laplace modes (wavelength 657 nm) and 3 to 5 repeats were considered for each sample. Measurements were carried out at time intervals of 10.000 µs and number of channels of 400, as device settings. Refractive index of 1.33 and viscosity of 0.891 were considered as dispersant properties during all studies. All particle size analytical experiments were performed at 25°C and data were analyzed using NanoQ Report software.

Zeta potential analysis

Zeta potential was measured to investigate the physical properties of different FBS samples following EV depletion procedures (Zeta Compact, CAD, France). At least three independent measurements were carried out for each sample and reported as mean of zeta potential+/-SEM in each case.

Atomic Force Microscopy

Atomic force microscopy (AFM) was performed to demonstrate the presence of EVs in EV-enriched fraction following the application of polymer-based precipitation procedure. Briefly, diluted EV-

containing solutions in each case were loaded on freshly cleaved mica and air-dried. They were investigated in non-contact mode at different scan size ranges including 3, 5 and 10 µm based on the protocols provided previously (Parisse et al., 2017; Ridolfi et al., 2019; Skliar and Chernyshev, 2019) via Ara Research atomic force microscope (model: Full).

Bicinchoninic Acid Assay

Bicinchoninic Acid (BCA) assay was performed using the BCA protein quantification kit (DNAbioTech life Sciences) to investigate the total protein content of different samples according to manufacturer protocol. Optical densities were recorded at 545 nm by an ELISA reader (Awareness, USA) following 1 h incubation at 60°C. Same procedures were performed for unknown samples in addition to the serial dilutions of albumin as the standard protein.

FBS biosufficiency evaluation Strategies

Mesenchymal stem cells derivation and characterization

Human adipose tissue aspirates, provided by surgeons from healthy volunteers with informed consents, were transferred to the lab and applied for derivation of primary cultures of human MSCs, based on our previously described protocol (Ahmadian Kia et al., 2011). Briefly, after removing the extra blood, adipose tissues were gently washed with phosphate-buffered saline (PBS 1X) and digested with collagenase type I in the absence of bovine serum albumin (BSA) and $CaCl_2$ for 45 min at 37°C. Digestion was stopped by the addition of heat-inactivated-serum-containing medium, and mononuclear cells were separated after centrifugation and washing steps. Cell suspensions were cultured for 48 h at 37°C in low glucose Dulbecco's Modified Eagle's Medium (DMEM) containing 10% FBS in the presence of penicillin/streptomycin. Upon reaching 90 to 100% confluency, cells were sub-cultured. MSCs were applied for downstream applications from passage numbers 3 to 5.

Primary adipose tissue derived mesenchymal stem cells (Ad-MSCs) were also applied for immunophenotyping experiments following 5 days of culture in the presence of medium supplemented with 10% of PEG 4000-mediated EV-depleted FBS. Briefly, for flow cytometric analysis, Ad-MSCs were trypsinized following two rounds of washing with PBS 1X, and after centrifugation steps they were applied for staining procedures with single color antibodies (Supplementary *Table 1*).

MTT assay

Human mesenchymal stem cells were seeded in 96-well plates (8000 cells per well) and 24 h later, upon reaching proper confluency, their media were exchanged with the complete media prepared by application of ultrafiltration- or PEG 4000-mediated EV-depleted serum. In control wells the media were exchanged with the normal FBS-containing media. 24, 48 and 72 h following the treatments, 25 µl of the MTT solution (3-(4,5-dimethylthiazol-2-yl)-2,5-diphenyltetrazolium bromide; Sigma-Aldrich, Germany), was added per well (final concentration of 5 mg/ml). After 3.5 h incubation, the media were discarded from each well and formazan crystals were solved in 200 µl dimethyl sulfoxide (DMSO). Cell viabilities were calculated by dividing the mean of optical densities in the treated-cell groups to the mean of ODs for the cells cultured in the presence of 10% unmodified FBS and reported as the percentage of cell viabilities.

Examination of sample contamination

PEG 4000-mediated exosome-depleted serum was applied to investigate the presence of any contamination using the BHI (Brain Heart Infusion) broth medium (HiMedia, Germany). Serum samples were inoculated in BHI media and incubated for 48 h at 35°C incubator. This medium with high concentrations of nutrients supports the proliferation of a variety of pathogens including aerobic bacteria, anaerobic bacteria, yeast and molds (Atlas, 1993; MacFaddin, 1985; Roseno, 1919; Salfinger and Tortorello, 2015).

Methods presented in this article for removal of EVs from fetal bovine serum samples were registered in the Intellectual Property Center of Iran under Declaration No. 13985014000300973 on 13 December 2019.

Results

Removal of EVs from FBS by probe sonication

Particle size analysis was performed for FBS samples, following the probe sonication method. The efficient removal of endogenous particles in the range of 50-1000 nm was confirmed and compared with commercial FBS (Figure *1A,B*). It was inferred from results that sonication decreases the amount of

poly dispersity index as an indicator of homogeneity from 0.4+/-0.04 to 0.2+/-0.01. Furthermore, a considerable decrease in the count of particles (kcps) was observed following the sonication experiments, based on particle size analysis (laser power 50%; Ctrl: 4735.708+/-962; Sonicates: 1354.931+/-93; 70% depletion; data reported as mean of three independent experiments+/-SEM). Zeta potential means, measured at 23-24°C were equal to -19.83+/-0.596 and -23.27+/-0.384 for control and sonicated serum samples, respectively. This is an indication of homogenously dispersed solutions (Table 1, data are

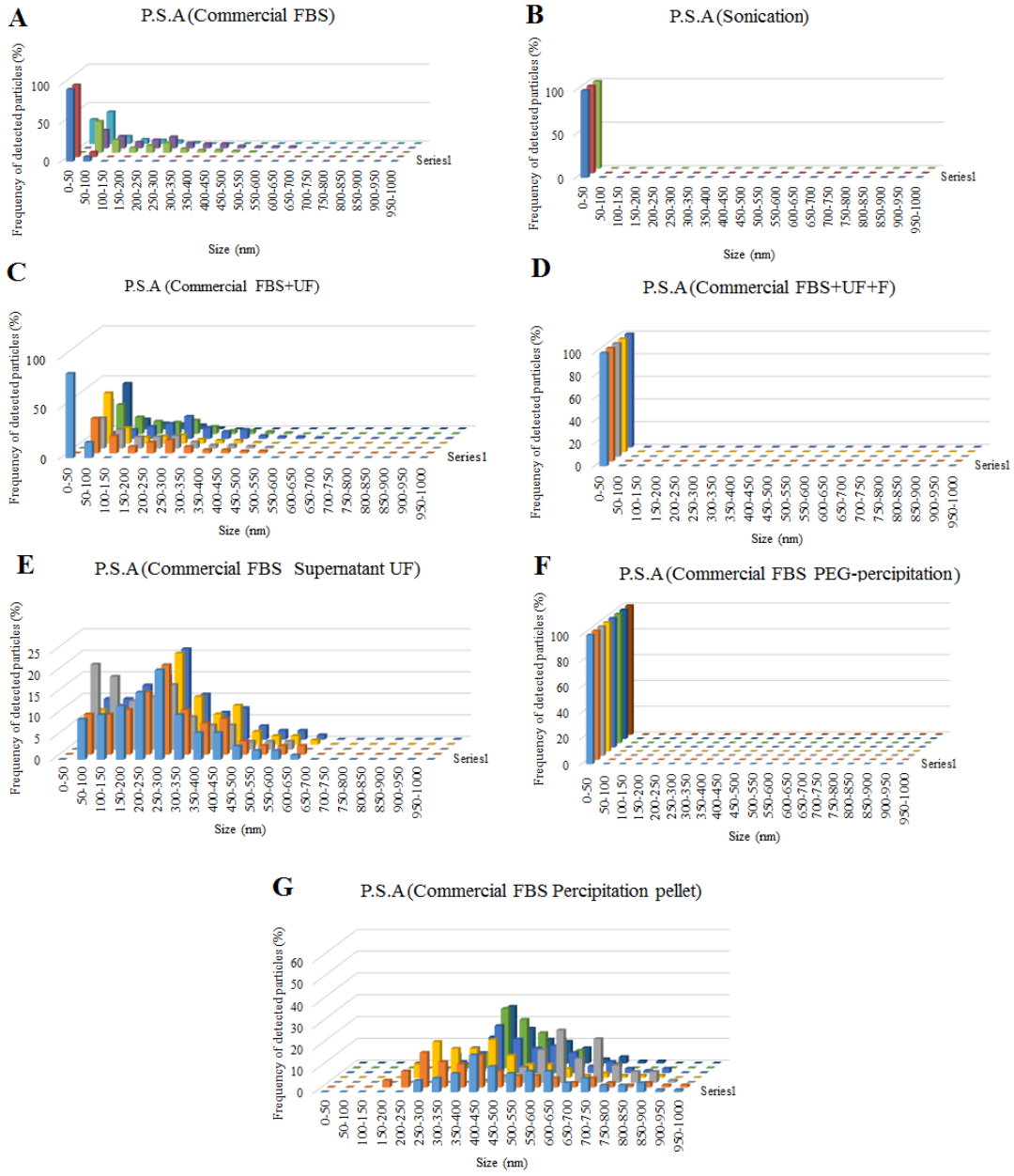

Figure 1. Particle size analysis experiments indicated the removal of desired particles from fetal bovine samples (A) and following the probe sonication (B). Furthermore, consequences of ultrafiltration on the distribution of particles from different size range (0 to 1000 nm) were demonstrated by particle size analysis via dynamic light scattering device: (C) commercial FBS ultrafiltrates, (D) commercial FBS ultrafiltrates followed by one round of syringe filtration (0.22 µm), and (E) supernatant of ultrafiltration. EV depletion was also evident in FBS samples following one round of polymer-based precipitation: (F) commercial FBS following EV depletion steps via PEG 4000 solution. Enrichment of larger particles including extracellular vesicles can be observed in the pellet of the polymer-precipitation procedure (G). As demonstrated 3 to 5 replicates were considered for each experiment.

reported as mean of three independent experiments+/-SEM). No changes were observed in the pH which remained 7.6 for both samples.

Table 1. Comparative biophysical analysis for FBS samples following EV depletion via ultrasonication in comparison to commercial control FBS.

Mean of +/-SEM	FBS Ctrl	EV-depleted FBS
Temperature (°C)	24.42+/-0.02	23.54+/-0.00
Electric Field (V/cm)	8.49+/-0.003	8.57+/-0.003
Conductivity (mS/cm)	0.764+/-0.001	0.335+/-0.00
Dielectric Constant	78.62+/-0.00	78.94+/-0.00
Viscosity (mPas)	0.90+/-0.00	0.92+/-0.00
pH	7.6	7.6
Mobility (µm/s/V/cm)	-1.53+/-0.04	-1.77+/-0.02
Zeta Mean (mV)	-19.83+/-0.59	-23.27+/-0.34
Coefficient	12.96+/-0.00	13.17+/-0.00

Depletion of EVs from FBS by ultrafiltration

Based on particle size analysis, pressure-mediated ultrafiltration accompanied by a round of syringe filtration resulted in efficient depletion of nano-sized particles (50-1000 nm size range; Figure *1C-E*). Ultrafiltrated serum samples indicated significantly lower kcps (17.77+/-0.40) in comparison to control samples (1541.011+/-21.574), which indicates more than 85% particle depletion following ultrafiltration. This method led to some changes in the physical appearance of the samples, i.e. increased light transparency and decreased density of the serum. Furthermore, polydispersity index was increased from 0.28+/-0.016 to 0.63+/-0.037 following the procedure. Mean of zeta potential, measured at 21-22°C, was equal to -19.29+/-0.497 and -14.22+/-3.894 for FBS samples before and after the ultrafiltration, respectively (Table 2). During the Zeta potential analysis, similar noise level of 1-1.05 was considered for all samples. In accordance with probe-sonication, adjacent pH values were measured for ultrafiltrates (7.40) in comparison to the intact FBS samples (7.35). Remarkable depletion of nano-sized particles was observable in the videos recorded by zeta size analyzer (Supplementary Videos, *V1*).

Table 2. Comparative biophysical analysis for FBS samples following EV depletion via ultrafiltration in comparison to commercial control FBS.

	FBS Ctrl	EV-depleted FBS
Temperature (°C)	21.96+/-0.031	22.48+/-0.059
Electric Field (V/cm)	8.54+/-0.013	8.57+/-3.834
Conductivity (mS/cm)	0.255+/-0.002	0.268+/-0.000
Dielectric Constant	79.51+/-0.01	79.32+/-0.02
Viscosity (mPas)	0.95+/-0.00	0.94+/-0.00
pH	7.35	7.40
Mobility (µm/s/V/cm)	-1.42+/-0.35	-1.05+/-0.28
Zeta Mean (mV)	-19.29+/-0.49	-14.22+/-3.89
No. of Tracking	62+/-14.53	12+/-2.21
Coefficient	13.57+/- 0.00	13.44+/-0.01

PEG 4000 solution as the method of choice for EV-depletion

Comparative particle size analysis performed based on the dynamic light scattering detection of particles demonstrated the efficient and reproducible depletion of EVs from FBS samples by PEG 4000 (Figure *1F-G*). Based on the DLS results, more than 91% depletion was observed in kcps for serum samples following the PEG-precipitation (380.958+/-60.456) in comparison to naïve FBS samples (4563.949+/-1187.615). As demonstrated in Figure *1F*, FBS samples were completely cleared from extracellular vesicles following a short-time (90 min) incubation with PEG 4000 solution and low-speed centrifugation (50 min, 5000 *g*). The reproducible depletion of EVs was accompanied by no obvious modification in the physical appearance of FBS samples. In addition, as confirmed by zeta potential analysis, the stability of the samples and their physical properties were not decreased or deteriorated, however, as we expected, number of tracking was decreased in EV-depleted serum samples due to removal of particles from 50 to 1000 nm size range (Table 3). Mean of polydispersity index (PDI) which was variable between 0.234 and 0.920 for unmodified serum samples, was equal to 0.253+/-0.038 for PEG 4000-mediated EV-depleted FBS. This is an indication of a proper level of stability. pH value, recorded at 23°C for control FBS, PEG 4000-mediated EV-depleted FBS and

collected EVs, were equal to 7.75, 7.61 and 6.70, respectively. 10-second videos recorded for EV-depleted FBS samples indicated EV removal as compared to the samples prepared from the pellets (Supplementary Videos, *V2*). Extracellular vesicles enriched from fetal bovine samples were detected via atomic force microscopy as demonstrated in Figure 2.

BCA assay, to investigate the total protein content of FBS samples following the probe sonication, ultrafiltration or PEG-precipitation, demonstrated that while the protein content of FBS remained constant in comparison to control FBS (5163.294+/-0.011) following ultrasonication (5142.223+/-0.004), it was considerably decreased following one round of ultrafiltration accompanied by syringe filtration (1459.223+/-0.018).

EV-depleted FBS samples prepared by polymer precipitating method were negative for bacterial, fungal or mold contaminations at the end of the process, as confirmed by inoculation of the samples in BHI broth medium. Moreover, culturing the cells in the presence of the EV-depleted FBS for 5 days had no considerable effect on cell viability and immune phenotype as demonstrated by morphological observations (Figure *3A*), MTT assay (Figure *3B*) and flow cytometric analysis of the cells.

Table 3. Comparative biophysical analysis for FBS samples following EV depletion via PEG 4000 in comparison to commercial control FBS.

Mean of +/-SEM	FBS Ctrl	EV-depleted FBS
Temperature (°C)	24.45+/-0.023	23.54+/-0.00
Electric Field (V/cm)	8.48+/-0.003	8.57+/-0.003
Conductivity (mS/cm)	0.763+/-0.001	0.335+/-0.000
Dielectric Constant	78.60+/-0.00	78.94+/-0.00
Viscosity (mPas)	0.90+/-0.00	0.92+/-0.00
pH	7.75	7.61
Mobility (µm/s/V/cm)	-1.52+/-0.04	-1.71+/-0.02
Zeta potential (mV)	-19.74+/-0.59	-22.60+/-0.34
No. of Tracking	105+/-7.05	30+/-4.09
Coefficient	12.95+/-0.00	13.17+/-0.00

Cell viabilities of mesenchymal stem cells, treated with EV-depleted serum prepared by PEG method or ultrafiltration were assessed in comparison to reference controls. 91 percent of the primary cells remained viable after 24 h of both treatments. Cell viabilities were equal to 80.85+/-0.60 and 86.72+/-2.16 for PEG group and 86.95+/-3.74 and 93.17+/-0.98 for ultrafiltration method, after 48 and 72 h, respectively. Furthermore, Ad-MSCs showed the common spindle-like morphology of mesenchymal stem cells, when they were exposed to the PEG 4000-mediated EV-depleted FBS. During our experiments cells exposed to these media were frequently sub-cultured and propagated without any technical problem, similar to cells grown in control medium.

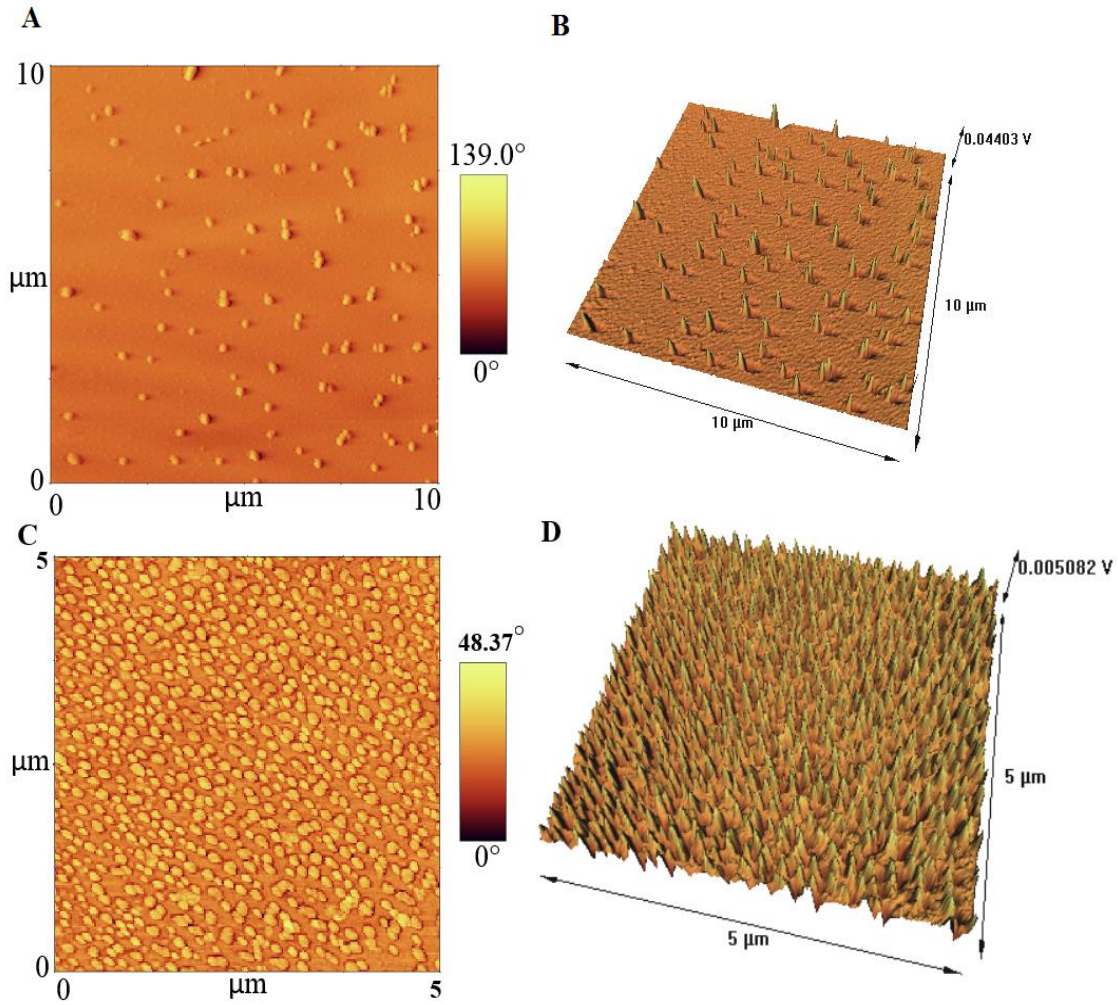

Figure 2. Atomic force microscopic detection of extracellular vesicles enriched from FBS samples. Samples were diluted at least 50 folds before loading on freshly cleaved mica. (A, C) 2D phase and (B, D) 3D amplitude pictures of EV-containing fractions following the application of polymer (PEG 4000) precipitation (A, B) and ultrafiltration (C, D) methods for removal of EVs from FBS.

As demonstrated in Figure 4, primary adipose tissue derived cells indicated high expression levels for CD44 (99.7%), CD105 (99.8%) and CD29 (97.2%), while they were negative for the expression of CD45 (0.93%) and CD11b (0.60%), as markers for hematopoietic and endothelial cells. They were also positive for expression of CD34 (Colter et al., 2000; Harvanová et al., 2011; Pittenger et al., 1999; Riekstina et al., 2008; Tran et al., 2012; Vaculik et al., 2012).

Discussion

Although first cell-based products have been approved by the European Medicines Agency (EMA) in 2018 and despite emerging very recent approvals for therapeutic applications of MSCs, still there are major concerns regarding their short- and long-term consequences. Among which risk of pro-tumorigenic events, stimulation of immune response and reduced differentiation capacity have been highlighted (Chu et al., 2019; Hoogduijn and Lombardo, 2019). Such unique and undeniable superiority of cell-based therapies in comparison to classic therapeutics, led the scientists to find a way for bringing the benefits of the cells to off-the-shelf and cell-free products, by using extracellular vesicles. As this field is yet in its infancy, providing the basic requirements, in an affordable manner, is not easy for many researchers throughout the world.

The presence of endogenous EVs in fetal bovine serum, as well as other biological fluids, is important from different aspects. As previously reported, they

have significant influence on different features of the cells in culture (Beninson and Fleshner, 2015) and encounter with their normal functional properties (Angelini et al., 2016). In this study, we aimed to deplete endogenous EVs present in the FBS by application of widely accessible methods to be applied for large-scale depletion of EVs in an affordable manner. Ultrasonication, ultrafiltration and polymer-precipitation methods were investigated comparatively to achieve this goal.

Ultrasonication was used as a proper method to destruct the lipid bilayer membrane of the extracellular vesicles and was followed by one round of centrifugation to remove the artifacts. Ultrafiltration is considered as a method of choice for isolation of extracellular vesicles from conditioned media or EVs from liquid biopsies including urine, saliva or plasma samples (He et al., 2019; Lobb et al., 2015; Yu et al., 2018). In a previous study, depletion of EVs from FBS was shown, based on ultrafiltration method via the application of ultra-15 centrifugal filters for 55 min at 3000 *g* (Kornilov et al., 2018). Although this method is economically preferred over the commercially available EV-depleted FBS, it does not yet meet the requirements for large-scale EV preparation. Ultrafiltration chambers, working under high pressure conditions, are proper substitutes to deplete the EVs under sterile conditions. In addition, this method is faster than common ultracentrifugation method, which takes more than 18 h. However, due to agglomeration of the vesicles following ultrafiltration of different liquids under pressure, it becomes necessary to add another filtration step to remove larger aggregates. Ideal ultrafiltration membranes are the ones with strong mechanical properties, hydrophobicity, durability, chemical stability and low polymer cost (Dobosz et al., 2017).

The third method investigated here is polymer based precipitation of the EVs by PEG 4000. PEG as a water-excluding polymer, has the capacity for conducting less soluble extracellular vesicles out of the media via binding to water molecules (Li et al., 2017; Patel et al., 2019; Ramasubramanian et al., 2019; Willis et al., 2017; Witwer et al., 2013). Normally PEG 6000 is the chemical of choice for isolation of extracellular vesicles from different biological liquids and conditioned media with an acceptable efficiency (Ludwig et al., 2018). To avoid

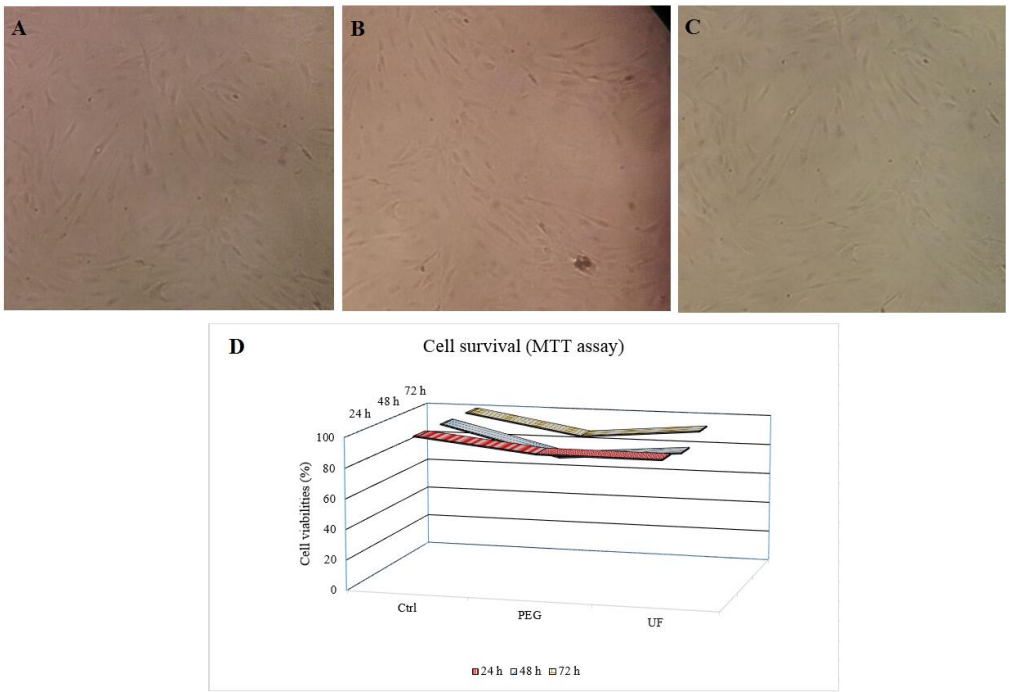

Figure 3. Spindle-like morphology of mesenchymal stem cells propagated in (A) normal medium in comparison to the cells which were conditioned with EV-depleted supplemented media prepared by (B) polymer precipitation or (C) ultrafiltration strategies, as evidenced by light microscopy. Panel **(**D) demonstrates cell viabilities of Ad-MSCs grown in different media (exosome-depleted FBS prepared based on the PEG precipitation or ultrafiltration methods) after 24, 48 and 72 h, as obtained by MTT assay.

strong protein precipitation in FBS samples PEG 6000 was substituted by PEG 4000 and the incubation time was decreased to 90 min. The observations, FBS samples depleted from EVs by PEG 4000 were closely similar to normal FBS regarding their stability in comparison to the ones

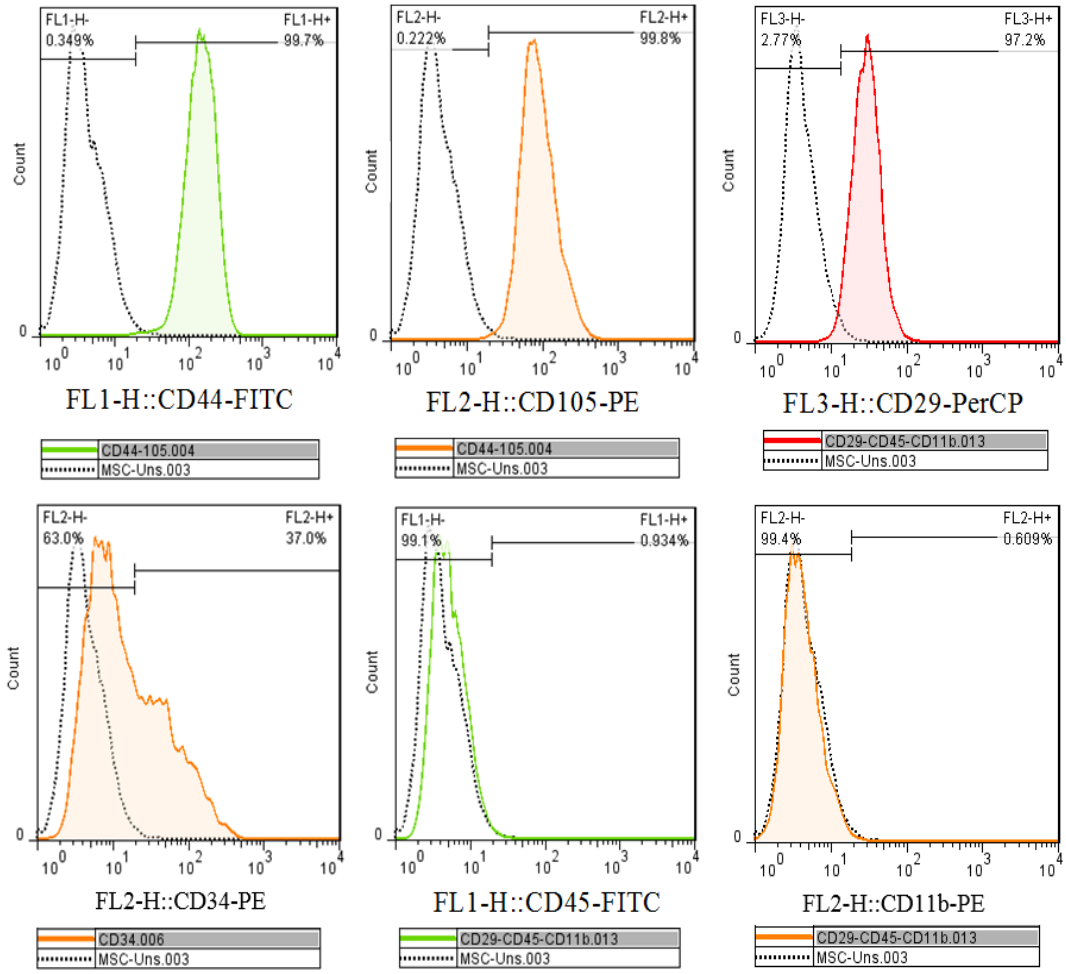

Figure 4. Flow cytometric analysis of primary adipose tissue derived mesenchymal stem cells from passage 3 following 5 days of culture in the presence of the medium supplemented by 10% PEG 4000-mediated EV-depleted serum. As evidenced by these experiments mesenchymal stem cells retained high expression levels for their typical markers including CD44, CD105 and CD29, while, they were negative for CD45 and CD11b as non-mesenchymal cell origin CD markers. 37% of the cells express CD34 (BD FACSCalibur, BD biosciences, USA). Data analysis was performed by FlowJo (version 7.6.1).

efficacy of EV removal was explored based on particle size analysis. Zeta potential experiment was performed to monitor the physico-chemical properties and stability of the FBS samples. Results indicated no considerable change in the primary features of the samples. Solutions with higher magnitude of zeta potential (mV) are less competent for sedimentation or agglomeration during the time (Helwa et al., 2017; Wang et al., 2015). Based on our exposed to rounds of ultrafiltration/filtration.

Our morphological analysis in addition to MTT assay and immunophenotyping of the Ad-MSCs following exposure to the media supplemented with EV-depleted FBS, prepared based on the polymer-precipitation method, demonstrated normal growth and phenotype of the cells. Furthermore, the presence of EVs in the precipitants was approved by atomic force microscopy.

In conclusion, we propose both polymer-precipitation and ultrafiltration can be applied as proper and efficient methods to deplete EVs from FBS samples. These methods are faster and less labor-intensive in comparison to the ultracentrifugation method. Furthermore, unlike more complicated methods such as microfluidics or tangential flow filtration, there is no need for high-tech or advanced instruments and expertise. Based on our experiments application of PEG 4000 for depletion of EVs would simplify the procedure and decrease the expenditures, while, would provide higher efficiency of EV depletion without any side effects on the quality of the FBS. This method would be of special interest for removing the EVs as it supports large-scale requirements and is not dependent on frequent rounds of filtration, centrifugation, preparation of serial dilutions, and application of disposable materials. Due to less overall sensitivity, this method is also proper for culturing a wide range of cancerous cell lines under exosome-depleted condition and its application could be attributed to other fields of nano-therapeutics and targeted drug delivery procedures.

Acknowledgements

This study was supported by the National Institute for Medical Research Development (NIMAD, Grant number 957797) of Iran and Ferdowsi University of Mashhad (Grant number 41827).

References

Ahmadian Kia N., Bahrami A. R., Ebrahimi M., Matin M. M., Neshati Z., Almohaddesin M. R., Aghdami N. and Bidkhori H. R. (2011) Comparative analysis of chemokine receptor's expression in mesenchymal stem cells derived from human bone marrow and adipose tissue. Journal of Molecular Neuroscience 44:178-185.

Angelini F., Ionta V., Rossi F., Miraldi F., Messina E. and Giacomello A. (2016) Foetal bovine serum-derived exosomes affect yield and phenotype of human cardiac progenitor cell culture. Bioimpacts 6:15-24.

Atlas RM. (1993) *Handbook of microbiological media. boca raton, Fla, USA: CRC Press*.

Beninson L. A. and Fleshner M. (2015) Exosomes in fetal bovine serum dampen primary macrophage IL-1beta response to lipopolysaccharide (LPS) challenge. Immunology Letters 163:187-192.

Choi J. R., Yong K. W. and Nam H. Y. (2019) Current status and perspectives of human mesenchymal stem cell therapy. Stem Cells International 2019:4762634.

Chu D. T., Nguyen Thi Phuong T., Tien N. L. B., Tran D. K., Minh L. B., Thanh V. V., Gia Anh P., Pham V. H. and Thi Nga V. (2019) Adipose tissue stem cells for therapy: an update on the progress of isolation, culture, storage, and clinical application. Journal of Clinical Medicine 8: pii: E917 .

Colombo M., Raposo G. and Théry C. (2014) Biogenesis, secretion, and intercellular interactions of exosomes and other extracellular vesicles. Annual Review of Cell and Developmental Biology 30:255-289.

Colter D. C., Class R., DiGirolamo C. M. and Prockop D. J. (2000) Rapid expansion of recycling stem cells in cultures of plastic-adherent cells from human bone marrow. Proceedings of the National Academy of Sciences of the United States of America 97:3213-3218.

Cowper M., Frazier T., Wu X., Curley L., Ma M. H., Mohuiddin O. A., Dietrich M., McCarthy M., Bukowska J. and Gimble J. M. (2019) Human platelet lysate as a functional substitute for fetal bovine serum in the culture of human adipose derived stromal/stem cells. Cells 8: pii: E724.

Czapla J., Matuszczak S., Kulik K., Wisniewska E., Pilny E., Jarosz-Biej M., Smolarczyk R., Sirek T., Zembala M. O., Zembala M., et al. (2019) The effect of culture media on large-scale expansion and characteristic of adipose tissue-derived mesenchymal stromal cells. Stem Cell Research & Therapy 10:235.

Devireddy L. R., Myers M., Screven R., Liu Z. and Boxer L. (2019) A serum-free medium formulation efficiently supports isolation and propagation of canine adipose-derived mesenchymal stem/stromal cells. PLoS One 14:e0210250.

Dobosz K. M., Kuo-Leblanc C. A., Martin T. J. and Schiffman J. D. (2017) Ultrafiltration membranes enhanced with electrospun nanofibers exhibit improved flux and fouling resistance. Industrial & Engineering Chemistry Research 56: 5724-5733.

Dominici M., Le Blanc K., Mueller I., Slaper-Cortenbach I., Marini F., Krause D., Deans R., Keating A., Prockop D. and Horwitz E. (2006) Minimal criteria for defining multipotent mesenchymal stromal cells. The International Society for Cellular Therapy position statement. Cytotherapy 8:315-317.

Eitan E., Zhang S., Witwer K. W. and Mattson M. P. (2015) Extracellular vesicle-depleted fetal bovine and human sera have reduced capacity to support cell growth. Journal of Extracellular Vesicles 4:26373.

Gurunathan S., Kang M. H., Jeyaraj M., Qasim M. and Kim J. H. (2019) Review of the isolation, characterization, biological function, and multifarious therapeutic approaches of exosomes. Cells 8: pii: E307.

Harvanova D., Tothova T., Sarissky M., Amrichova J. and Rosocha J. (2011) Isolation and characterization of synovial mesenchymal stem cells. Folia Biologica (Praha) 57:119-124.

He L., Zhu D., Wang J. and Wu X. (2019) A highly efficient method for isolating urinary exosomes. International Journal of Molecular Medicine 43:83-90.

Helwa I., Cai J., Drewry M. D., Zimmerman A., Dinkins M. B., Khaled M. L., Seremwe M., Dismuke W. M., Bieberich E., Stamer W. D., et al. (2017) A comparative study of serum exosome isolation using differential ultracentrifugation and three commercial reagents. PLoS One 12:e0170628.

Hemeda H., Giebel B. and Wagner W. (2014) Evaluation of human platelet lysate versus fetal bovine serum for culture of mesenchymal stromal cells. Cytotherapy 16:170-180.

Hoogduijn M. J. and Lombardo E. (2019) Mesenchymal stromal cells anno 2019: dawn of the therapeutic era? Concise review. STEM CELLS Translational Medicine 8:1126-1134.

Kornilov R., Puhka M., Mannerstrom B., Hiidenmaa H., Peltoniemi H., Siljander P., Seppanen-Kaijansinkko R. and Kaur S. (2018) Efficient ultrafiltration-based protocol to deplete extracellular vesicles from fetal bovine serum. Journal of Extracellular Vesicles 7:1422674.

Lehrich B. M., Liang Y. and Fiandaca M. S. (2019) Response to "Technical approaches to reduce interference of fetal calf serum derived RNA in the analysis of extracellular vesicle RNA from cultured cells". Journal of Extracellular Vesicles 8:1599681.

Lehrich B. M., Liang Y., Khosravi P., Federoff H. J. and Fiandaca M. S. (2018) Fetal bovine serum-derived extracellular vesicles persist within vesicle-depleted culture media. International Journal of Molecular Sciences 19: pii: E48.

Li P., Kaslan M., Lee S. H., Yao J. and Gao Z. (2017) Progress in exosome isolation techniques. Theranostics 7:789-804.

Li X., Corbett A. L., Taatizadeh E., Tasnim N., Little J. P., Garnis C., Daugaard M., Guns E., Hoorfar M. and Li I. T. S. (2019) Challenges and opportunities in exosome research-perspectives from biology, engineering, and cancer therapy. APL Bioengineering 3:011503.

Lobb R. J., Becker M., Wen S. W., Wong C. S., Wiegmans A. P., Leimgruber A. and Moller A. (2015) Optimized exosome isolation protocol for cell culture supernatant and human plasma. Journal of Extracellular Vesicles 4:27031.

Ludwig A. K., De Miroschedji K., Doeppner T. R., Borger V., Ruesing J., Rebmann V., Durst S., Jansen S., Bremer M., Behrmann E., et al. (2018) Precipitation with polyethylene glycol followed by washing and pelleting by ultracentrifugation enriches extracellular vesicles from tissue culture supernatants in small and large scales. Journal of Extracellular Vesicles 7:1528109.

Mannerstrom B., Paananen R. O., Abu-Shahba A. G., Moilanen J., Seppanen-Kaijansinkko R. and Kaur S. (2019) Extracellular small non-coding RNA

contaminants in fetal bovine serum and serum-free media. Scientific Reports 9:5538.

Parisse P., Rago I., Ulloa Severino L., Perissinotto F., Ambrosetti E., Paoletti P., Ricci M., Beltrami A. P., Cesselli D. and Casalis L. (2017) Atomic force microscopy analysis of extracellular vesicles. European Biophysics Journal 46:813-820.

Patel G. K., Khan M. A., Zubair H., Srivastava S. K., Khushman M., Singh S. and Singh A. P. (2019) Comparative analysis of exosome isolation methods using culture supernatant for optimum yield, purity and downstream applications. Scientific Reports 9:5335.

Pittenger M. F., Mackay A. M., Beck S. C., Jaiswal R. K., Douglas R., Mosca J. D., Moorman M. A., Simonetti D. W., Craig S. and Marshak D. R. (1999) Multilineage potential of adult human mesenchymal stem cells. Science 284:143-147.

Ramasubramanian L., Kumar P. and Wang A. (2019) Engineering extracellular vesicles as nanotherapeutics for regenerative medicine. Biomolecules 10.

Ridolfi A., Brucale M., Montis C., Caselli L., Paolini L., Borup A., Boysen A., Loria F., van Herwijnen M., Kleinjan M., et al. (2019) AFM-based high-throughput nanomechanical screening of single extracellular vesicles. bioRxiv.

Riekstina U., Muceniece R., Cakstina I., Muiznieks I. and Ancans J. (2008) Characterization of human skin-derived mesenchymal stem cell proliferation rate in different growth conditions. Cytotechnology 58:153-162.

Rosenow E. C. (1919) Studies on elective localization focal infection with special reference to oral sepsis'. Journal of Dental Research 1:205-267.

Salfinger Y., and Tortorello M. L. (2015) Compendium of methods for the microbiological examination of foods. Fifth (Ed.), American Public Health Association, Washington, D.C.

Schau H. P. (1986) J. F. MacFaddin, Media for isolation - cultivation - identification - maintenance of medical bacteria, Volume I. XI + 929 S., 163 Abb., 94 Tab. Baltimore, London 1985. Williams and Wilkins. ISBN: 0-683-05316-7. Journal of Basic Microbiology 26:240-240.

Shelke G. V., Lasser C., Gho Y. S. and Lotvall J. (2014) Importance of exosome depletion protocols to eliminate functional and RNA-containing extracellular vesicles from fetal bovine serum. Journal of Extracellular Vesicles 3.

Skliar M. and Chernyshev V. S. (2019) Imaging of extracellular vesicles by atomic force microscopy. The Journal of Visualized Experiments.

Tancharoen W., Aungsuchawan S., Pothacharoen P., Bumroongkit K., Puaninta C., Pangjaidee N., Narakornsak S., Markmee R., Laowanitwattana T. and Thaojamnong C. (2019) Human platelet lysate as an alternative to fetal bovine serum for culture and endothelial differentiation of human amniotic fluid mesenchymal stem cells. Molecular Medicine Reports 19:5123-5132.

Tao S. C., Guo S. C. and Zhang C. Q. (2017) Platelet-derived extracellular vesicles: an emerging therapeutic approach. International Journal of Biological Sciences 13:828-834.

Théry C., Amigorena S., Raposo G. and Clayton A. (2006) Isolation and characterization of exosomes from cell culture supernatants and biological fluids. Current Protocols in Cell Biology 3:22.1-22.29.

Théry C., Witwer K. W., Aikawa E., Alcaraz M. J., Anderson J. D., Andriantsitohaina R., Antoniou A., Arab T., Archer F., Atkin-Smith G. K., et al. (2018) Minimal information for studies of extracellular vesicles 2018 (MISEV2018): a position statement of the International Society for Extracellular Vesicles and update of the MISEV2014 guidelines. Journal of Extracellular Vesicles 7:1535750.

Tran N. T., Trinh Q. M., Lee G. M. and Han Y. M. (2012) Efficient differentiation of human pluripotent stem cells into mesenchymal stem cells by modulating intracellular signaling pathways in a feeder/serum-free system. Stem Cells and Development 21:1165-1175.

Vaculik C., Schuster C., Bauer W., Iram N., Pfisterer K., Kramer G., Reinisch A., Strunk D. and Elbe-Burger A. (2012) Human dermis harbors distinct

mesenchymal stromal cell subsets. Journal of Investigative Dermatology 132:563-574.

Wang Y., Zhang L., Li Y., Chen L., Wang X., Guo W., Zhang X., Qin G., He S. H., Zimmerman A., et al. (2015) Exosomes/microvesicles from induced pluripotent stem cells deliver cardioprotective miRNAs and prevent cardiomyocyte apoptosis in the ischemic myocardium. International Journal of Cardiology 192:61-69.

Weiss A. R. R. and Dahlke M. H. (2019) Immunomodulation by mesenchymal stem cells (MSCs): Mechanisms of action of living, apoptotic, and dead MSCs. Frontiers in Immunology 10:1191.

Willis G. R., Kourembanas S. and Mitsialis S. A. (2017) Toward exosome-based therapeutics: isolation, heterogeneity, and fit-for-purpose potency. Frontiers in Cardiovascular Medicine 4:63.

Witwer K. W., Buzas E. I., Bemis L. T., Bora A., Lasser C., Lotvall J., Nolte-'t Hoen E. N., Piper M. G., Sivaraman S., et al. (2013) Standardization of sample collection, isolation and analysis methods in extracellular vesicle research. Journal of Extracellular Vesicles 2.

Yu L. L., Zhu J., Liu J. X., Jiang F., Ni W. K., Qu L. S., Ni R. Z., Lu C. H. and Xiao M. B. (2018) A comparison of traditional and novel methods for the separation of exosomes from human samples. BioMed Research International 2018:3634563.

Zakrzewski W., Dobrzynski M., Szymonowicz M. and Rybak Z. (2019) Stem cells: past, present, and future. Stem Cell Research & Therapy 10:68.

Zhang Z., Huang S., Wu S., Qi J., Li W., Liu S., Cong Y., Chen H., Lu L., Shi S., et al. (2019) Clearance of apoptotic cells by mesenchymal stem cells contributes to immunosuppression via PGE2. EBioMedicine 45:341-350.

Supplementary Materials:

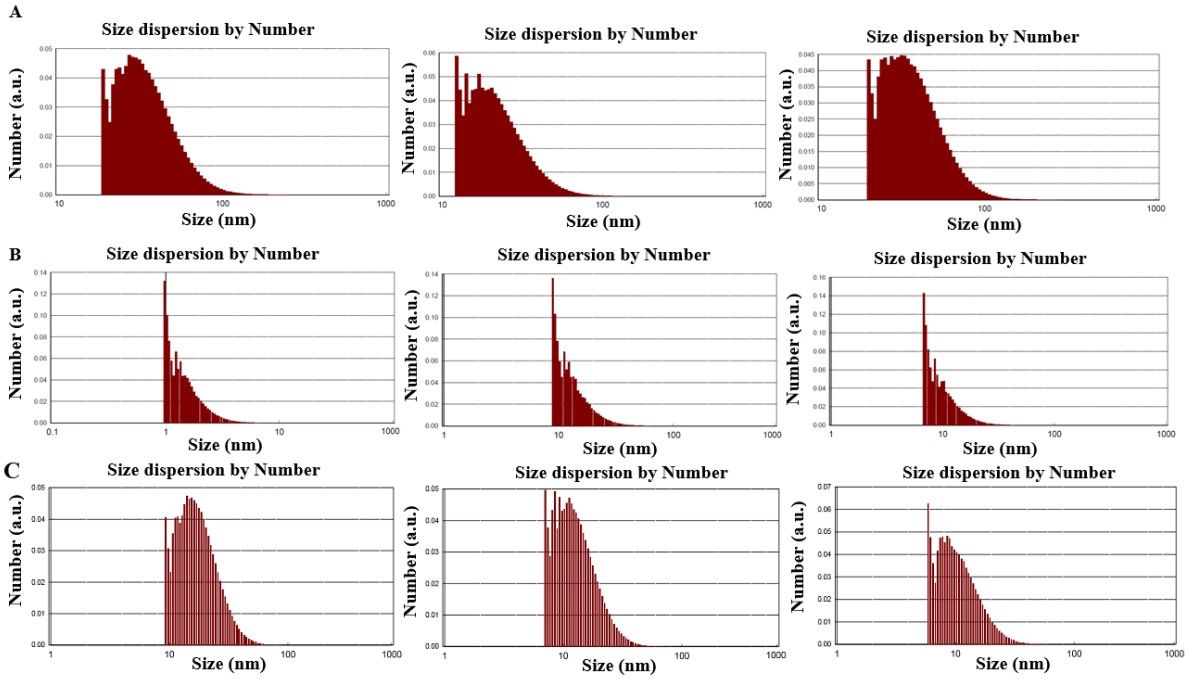

Figure S1. Size distribution of detected particles based on their frequencies (number) during particle size analysis, as demonstrated by DLS device. As seen a wide range of particles detected inside unmodified serum samples in the first row (A), were removed in the second and third rows, which represent ultrafiltration-mediated exosome-depletion (B) and PEG-mediated-exosome-depletion (C), following three rounds of analysis.

Table S1. Antibodies applied during flow cytometric analysis.

No.	Antibody	Company	Cat No.	Isotype	Clone	Reactivity
1	CD44-FITC	Immunostep	114659	IgG2a	HI44a	Human
2	CD105-PE	Exbio	1P-298-T025	IgG2a	MEM-226	Human
3	CD29-PerCP	Immunostep	29PB-100T	IgG2b	VJ1/14	Human
4	CD34-PE	Immunostep	34PE-100T	IgG1	581	Human
5	CD45-FITC	BD Bioscience	560976	IgG1, κ	-	Human
6	CD11b-PE	Biolegend	101207	IgG2b, κ	-	Mouse, Human

Supplementary Videos S1. Depletion of EVs from FBS samples (Ctrl) following the ultrafiltration procedure (UF) was shown for three different samples, as evidenced by zeta potential analysis. (Videos: Ctrl 1, Ctrl 2, Ctrl 3, UF1, UF2, UF3).

Supplementary Videos S2. Endogenous EVs isolated from FBS samples (EVs collected by PEG precipitation) in addition to EV-depleted serum samples (PEG 4000-mediated EV-depleted FBS) were shown for three different samples. Videos were recorded by Zeta Analyzer device. (Videos: endogenous FBS EVs-1, endogenous FBS EVs-2, endogenous FBS EVs-3, EV-Depleted serum-1, EV-Depleted serum-2, EV-Depleted serum-3).

Journal of Cell and Molecular Research (2020) 11 (2), 55-58 DOI: 10.22067/jcmr.v11i2.83212

Research Article

A Rapid Method for Analysis of cDNA Synthesis Using Ion-Pair Reversed-Phase High Performance Liquid Chromatography

Maryam M. Matin[1,2*], David P. Hornby[3*]

[1] *Department of Biology, Faculty of Science, Ferdowsi University of Mashhad, Mashhad, Iran*
[2] *Novel Diagnostics and Therapeutics Research Group, Institute of Biotechnology, Ferdowsi University of Mashhad, Mashhad, Iran*
[3] *The Krebs Institute, Department of Molecular Biology and Biotechnology, University of Sheffield, Western Bank, Sheffield S10 2TN, United Kingdom*

Received 25 September 2019 Accepted 31 January 2020

Abstract

We have developed a rapid, quantitative method for analysing the outcome of the first strand synthesis step in cDNA library preparation, yield and molecular weight range of the final cDNA products are determined after size fractionation. This method involves conventional cDNA library construction including all enzymatic steps usually required, but replaces radioactive labelling of nucleic acids with fluorescence detection. The separation and quantification steps all involve ion-pair reversed-phase high performance liquid chromatography (IP RP HPLC). This quantitative method replaces the use of autoradiography and size exclusion chromatography with combined ion-pair reversed-phase high performance liquid chromatography and in line fluorescence detection. The result of this approach is combination of speed with the generation of reproducible, high quality cDNA libraries.

***Keywords*:** cDNA, library construction, IP RP HPLC, size fractionation

Introduction

The construction of high quality cDNA libraries is of fundamental importance in contemporary molecular biology, since such libraries play a critical role in the analysis of all aspects of gene expression. Several methods for the construction of cDNA libraries have been published (for an overview see Kimmel and Berger, 1987; Ying, 2004; Harbers, 2008) most of which involve a series of enzymatic reactions including first strand synthesis, which is primed by oligo-dT and catalysed by reverse transcriptase; second strand synthesis, catalysed by DNA polymerase I; end filling, catalysed by *Pfu* DNA polymerase, and finally DNA ligation (DNA ligase) into a vector which has often been dephosphorylated (Okayama and Berg, 1982; Gubler and Hoffman, 1983; Bashirdes and Lovett, 2001; Harbers, 2008).

A major problem with this multi-step procedure is the frequent failure, or sub optimal yield of one or more of the steps. In order to insure that all steps have been successful, careful monitoring at all stages is carried out by radiolabeling and autoradiography procedures, which normally take one or two days depending on the specific activity of the labelled material. The other problem is that when a pool of fragments, differing in molecular weight by an order of magnitude, are used for construction of cDNA libraries, the smaller fragments are selectively cloned (Matin and Hornby, 2000; Sambrook and Russell, 2001) and therefore, there is a need for size based fractionation of the cDNA, which is routinely achieved by gel filtration. This prolonged exposure of the cDNA to radioactive nucleotides increases the probability of radiation damage and requires discontinuous analysis, which is usually carried out by gel electrophoresis and an ethidium bromide fluorescence assay, in which part of each fraction is lost.

Ion-pair reversed-phase high performance liquid chromatography (IP RP HPLC) is an applicable conventional method which is currently being used for the analysis of compounds with more than one ionizable group. Since it is hard to retain such compounds on non-polar stationary phases, an ion-pairing reagent has been added to the mobile phase in IP RP HPLC (Peng and Dansereau, 2001). IP RP HPLC has been widely used in pharmaceutical and molecular biology studies as a highly accurate assay system, for instance to quantitatively analyse the gene expression (Doris et al., 1998), to investigate

*Corresponding authors' e-mail address:
matin@um.ac.ir, d.hornby@shef.ac.uk

the metabolism of antisense drugs (Wei et al., 2006), to separate and identify metabolites in cellular extracts (Kiefer et al., 2010), to determine several chemical components in drug agents (Kyriakidesa and Panderi, 2007; Breuzovska et al., 2010; Zhang, 2010) and for proteome analysis (Delmotte et al., 2007) and simultaneous determination of nucleotide sugars (Nakajima et al., 2010).

Here we have combined the qualitative and quantitative analysis of the first strand products and final cDNA products (before or after fractionation) with IP RP HPLC. As a result of this method, the preparation and quality control of cDNA synthesis, for example, for library construction is made more reproducible and control over cDNA fragment sizes is much improved.

Materials and Methods

The WAVE® Nucleic Acid Fragment Analysis System, the DNASep® cartridge (7.8 mm internal diameter and 50 mm length) and triethylammonium acetate (TEAA) were provided by Transgenomic, San Jose, USA. The ZAP Express cDNA synthesis kit and ZAP Express cDNA Gigapack III Gold Cloning kit were purchased from Stratagene. Oligo-dT primer was synthesized at University of Sheffield and labelled with 5'-Tetrachloro-Fluorescein Phosphoramidite (TET, Glen Research): 5'-GAGACTCGAGTTTTTTTTTTTTTTTT-3'.
The chromatography was performed using a two eluent buffer system: buffer A consists of 0.1 M TEAA, pH 7.0 and buffer B consists of 0.1 M TEAA, pH 7.0 and 25% (V/V) acetonitrile (ACN) and the chromatograms were recorded using a fluorescence detector. The analysis was performed using the following gradient conditions at 50ºC: flow rate 0.75 ml/min, 44 to 55% B in 3 min, to 65% B in 8 min, to 70% B in 5 min, to 100% B in 0.5 min, hold at 100% B for 0.5 min, to 44% B in 1 min and hold at 44% B for 1 min. For fractionation of double strand cDNA using the UV detector the following gradient was used at 50ºC and with a flow rate of 0.75 ml/min: 35 to 55% B in 2 min, to 65% B in 8 min, hold at 65% B for 2 min, to 75% B in 5 min, hold at 75% B for 1 min, to 100% B in 1 min, hold at 100% B for 1 min and to 35% B in 1 min.

Chinese Hamster Ovary (CHO) cells were grown in T25 tissue culture plastic flasks (Corning Life Sciences) in a humidified, 95% air: 5% CO_2 atmosphere at 37ºC. The medium was a 1:1 mixture of Ham's F12 and Dulbecco's modified Eagle's medium, supplemented with 5% Foetal Bovine Serum and 2 mM glutamine (all from Sigma, Poole). The medium contained 50 U/ml penicillin and 50 mg/ml streptomycin (Sigma, Poole). Total RNA was extracted from the cells using Trizol reagent (Gibco-BRL) according to the manufacturer's instructions. The messenger RNA (mRNA) was then purified from total RNA using MessageMaker kit (Gibco-BRL).

Results and Discussion

mRNA was primed in the first-strand synthesis reaction with a TET-labelled oligo-dT primer and was reverse transcribed using MMLV-RT using a ZAP express cDNA synthesis kit (Stratagene). In order to analyse first strand synthesis reaction, a small volume of the product was injected on to a DNASep® column and compared with the chromatogram of oligo-dT primer alone. As shown in Figure 1, a spectrum of cDNAs arises and, as expected the bulk of the first strand cDNAs are relatively short. The second strand synthesis was accomplished using DNA polymerase I, and the appropriate components following the Stratagene protocol, but 4 µl of Fluorogreen (Amersham) was added instead of [α-^{32}P]dGTP. *Eco*RI adapters were added to both ends of the double stranded cDNA, which was then subjected to *Xho*I digestion.

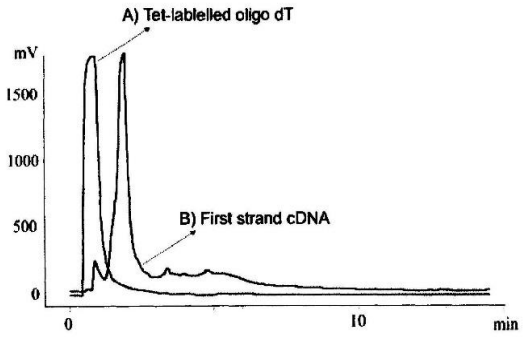

Figure 1. Chromatographic analysis of first strand cDNA synthesis.
Chromatogram A shows the result of the injection of TET-labelled oligo-dT and B shows the separation of 5 µl of the products of a first strand cDNA synthesis on a DNASep® column. The analysis was performed using a fluorescence detector with excitation and emission wavelengths set at 521 and 536 nm, respectively. The majority of products are short size single stranded DNAs that elute close to oligo-dT together with some longer products.

The cDNA was fractionated manually by gel filtration using a Sepharose CL-2B column according to the Stratagene's protocol, and a small

portion of each fraction was injected on to a DNASep® column to determine the molecular weight and yield of the fragments in each fraction as shown in Figure 2. This provides an example of the rapid analysis of cDNA synthesis products using IP RP HPLC. Other methods for analysis of cDNA size distribution including gel electrophoresis and autoradiography or digoxygenin labelling of second-strand synthesis reaction followed by blotting (Sambrook and Russell, 2001, Roeder, 1998) take considerably longer.

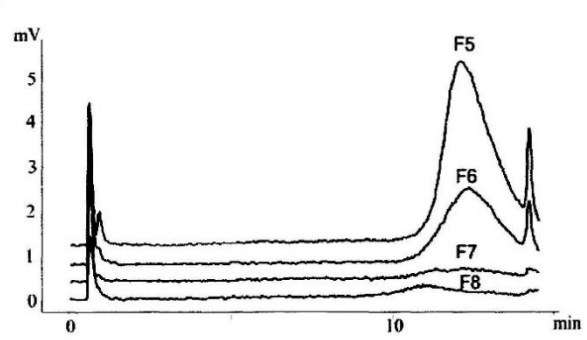

Figure 2. Rapid analysis of cDNA fractionation using IP RP HPLC. The double stranded cDNA was fractionated using a drip column (a standard gel filtration technique), according to Stratagene's manual and was subsequently analysed on the WAVE® system. 10 µl from 100 µl of each collected fraction was injected on to the DNASep® column and the chromatograms are related to fractions 5 to 8 (F5-F8) as indicated. Since Fluorogreen was incorporated into the second strand synthesis reaction the products were analysed using a fluorescence detector with excitation and emission wavelengths set at 494 and 525 nm, respectively. cDNAs greater than 500 bps elute after 12 minutes using a DNASep® column: most of the cDNAs are eluted in fractions 5 and 6.

In a separate experiment, the synthetic, double stranded cDNA was injected on to the DNASep® column (Figure 3), fractionated and collected. Those fractions containing larger fragments were selected and were used for the construction of a cDNA library which contained a larger than normal range of insert sizes as was also demonstrated before (Matin and Hornby, 2000; data not shown).

The generation of complete and full-length cDNA libraries is essential for functional assays of specific gene sequences. In this regard, the application of non-radioactive IP RP HPLC facilitates rapid quality control of cDNA synthesis reactions. This approach combines the advantages of conventional cDNA library synthesis protocols while eliminating most of their drawbacks.

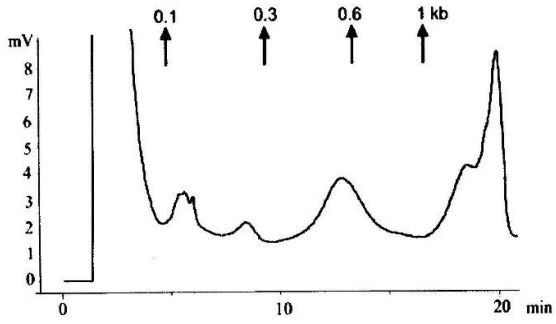

Figure 3. Analysis of second strand cDNA synthesis by IP RP HPLC. The double stranded cDNA (14 µl) was injected on to the DNASep® column and the DNA eluted after 18 min was fractionated and used in the construction of cDNA libraries enriched for larger inserts. The arrows above the chromatogram show the relative retention times for molecular weight markers under the same experimental conditions.

Other novel protocols including SMART-PCR and suppression subtractive hybridization (SSH)-PCR describe potentially less sensitive yet relatively easy and cost-effective alternatives for amplifying cDNA from sub-microgram levels of RNA (Hillmann et al., 2009). However, non-radioactive IP RP HPLC eliminates the use of radioactivity and therefore makes it a safe alternative to existing protocols.

In summary, non-radioactive IP RP HPLC is an easy to perform, safe, reliable and quantitative method which also provides a potential for RNA fractionation (2) prior to cDNA synthesis in order to further improve the quality of synthetic cDNA libraries enriched for “long” mRNAs.

References

Bashirdes, S. and Lovett, M. (2001) cDNA detection and analysis. Current Opinion in Chemical Biology 5: 15–20.

Breuzovska, K., Dimitrovska, A., Kitanovski, Z., Petrusevska, J., Ribarska, J.T. and Jolevska, S.T. (2010) Development of an ion-pair reversed-phase HPLC method with indirect UV detection for determination of phosphates and phosphites as impurities in sodium risedronate. Journal of AOAC International 93: 1113-1120.

Delmotte, N., Lasaosa, M., Tholey, A., Heinzle, E. and Huber, C.G. (2007) Two-dimensional reversed-phase x ion-pair reversed-phase HPLC: an alternative approach to high-resolution peptide separation for shotgun proteome analysis. Journal of Proteome Research 6: 4363-4373.

Doris, P.A., Oefner, P.J., Chilton, B.S. and

Hayward-Lester, A. (1998) Quantitative analysis of gene expression by ion-pair high-performance liquid chromatography. Journal of Chromatography A 806: 47-60.

Gubler, U. and Hoffman, B.J. (1983) A simple and very efficient method for generating cDNA libraries. Gene 25: 263-269.

Harbers, M. (2008) The current status of cDNA cloning. Genomics 91: 232-242.

Hillmann, A., Dunne, E. and Kenny, D. (2009) cDNA amplification by SMART-PCR and suppression subtractive hybridization (SSH)-PCR. Methods in Molecular Biology 496: 223-43.

Kiefer, P., Delmotte, N. and Vorholt, J.A. (2011) Nanoscale ion-pair reversed-phase HPLC-MS for sensitive metabolome analysis. Analytical Chemistry 83(3):850-5

Kimmel, A.R. and Berger, S.L. (1987) Preparation of cDNA and the generation of cDNA libraries: overview. Methods in Enzymology 152: 307-316.

Kyriakidesa, D. and Panderi, I. (2007) Development and validation of a reversed-phase ion-pair high-performance liquid chromatographic method for the determination of risedronate in pharmaceutical preparations. Analytica Chimica Acta 584: 153-159.

Matin, M.M. and Hornby, D.P. (2000) A positive selection vector combining tetracycline resistance that eliminates the need for bacterial plating. Analytical Biochemistry 278: 46-51.

Nakajima, K., Kitazume, S., Angata, T., Fujinawa, R., Ohtsubo, K., Miyoshi, E. and Taniguchi, N. (2010) Simultaneous determination of nucleotide sugars with ion-pair reversed-phase HPLC. Glycobiology 20: 865-871.

Okayama, H. and Berg. P. (1982) High-efficiency cloning of full-length cDNA. Molecular and Cellular Biology 2: 161-170.

Peng, S.X. and Dansereau, S.M. (2001) Ion-exchange liquid chromatographic analysis of bisphosphonates by on-line post-column photochemical reaction and spectrophotometric detection. Journal of Chromatography A 914: 105-110.

Roeder, T. (1998) Solid-phase cDNA library construction, a versatile approach. Nucleic Acids Research 26: 3451-3452.

Sambrook, J. and Russell, D. (2001) Molecular Cloning: A laboratory Manual. (3rd ed.), Cold Spring Harbor Laboratory Press, Cold Spring Harbor, NY.

Wei, X., Dai, G., Liu, Z., Cheng, H., Xie, Z., Marcucci, G., and Chan, K.K. (2006) Metabolism of GTI-2040, a phosphorothioate oligonucleotide antisense, using ion-pair reversed phase high performance liquid chromatography (HPLC) coupled with electrospray ion-trap mass spectrometry. AAPS Journal 8: E743-755.

Ying, S.Y. (2004) Complementary DNA Libraries. Molecular Biotechnology 27: 245-252.

Zhang, L. (2010) Analysis of risedronate and related substances by ion-pair reversed-phase high-performance liquid chromatography with evaporative light-scattering detection. Analytical Sciences 26: 325-329.

Journal of Cell and Molecular Research (2020) 11 (2), 59-65 DOI: 10.22067/jcmr.v11i2.84974

Research Article

Production of Silver Nanoparticles by Marigold Extract

Zohreh Sohrabi Nezhad, Hassan Marashi , Nasrin Moshtaghi *

Biotechnology and Plant Breeding Department, Ferdowsi University of Mashhad, Mashhad, Iran

Received 6 January 2020 Accepted 13 February 2020

Abstract

Silver nanoparticles are widely used in manufacturing of different products considering their unique physical and chemical properties. Also they have been noticed in medical diagnosis and treatment because of their antibacterial properties. Physical and chemical methods of producing nanoparticles, are expensive and are not safe enough as toxic substances may remain in the final preparations. To solve this problem, biological production of nanoparticles is considered as an efficient alternative method. In present study, synthesis of silver nanoparticles via seeds, petals, roots, and hairy root extracts of *Calendula officinalis* were performed. These nanoparticles were characterized by means of spectrophotometer, particle size analyzer and transmission electron microscope. Nanoparticles which were synthesized by hairy root extract showed the highest absorption at 430 nm (1/6 a.u) and the smallest size (5/3 nm), in comparison to other examined particles. Results confirmed the better performance of hairy root extracts in the synthesis of silver nanoparticles.

***Keywords*:** *Calendula officinalis*, Marigold, Hairy roots, Silver nanoparticles

Introduction

Metal nanoparticles, similar to mass metals, show special and various electrical, magnetic, catalytic and light properties. These properties cause the widespread applications of nanoparticles in biomedical engineering, chemical, optical, electronic and life sciences. At present, various types of metal nanoparticles are produced by copper, titanium, magnesium, gold, and silver alloys and applied in a wide range of applications from preparation of equipment and tools for optical, catalytic and electronic industries to treat some cancers (Naveen et al., 2010). Among metal nanoparticles, silver nanoparticles play more prominent role because of their catalytic and antibacterial properties (Garrick and Pinches, 2006). Moreover, proper particle size and distribution are among special properties of silver nanoparticles. Chemical and physical methods for synthesis of colloidal silver nanoparticles, including laser-based production, chemical reduction, photochemical reduction and laser emitters-based production are still in progress and reform. They are often encountered with problems such as low stability of nanoparticles, controlling crystal growth and aggregation of particles by a little change in the temperature and/or pH (Bhainsa and Souza, 2006). The antibacterial potential of nanoparticles is used in a large number of commercial products such as clothing, appliances, textile and weaving industries, water treatment, preparation of antimicrobial agents, and sunscreen lotions (Naveen et al., 2010).

Main reasons for the synthesis of silver nanoparticles via biological systems are their safe, simple, durable (Devina et al., 2010), eco-friendly, cost-effective and nontoxic properties (Thangaraju et al., 2012). Moreover, synthesis steps could be carried out at room temperature, without the need for providing high pressure or production of any toxic byproducts (Marchiol, 2012). David and Moldovan (2020) reported a green synthesis method for obtaining silver nanoparticles using *Viburnum opulus* fruit extracts. Their results confirmed the production of spherical and uniform-sized silver nanoparticles (AgNPs) with an average diameter of 16 nm.

Retrieval of nanoparticles form plant tissues is a tedious and expensive procedure, which needs the application of enzymes for degradation of plant cellulose tissue (Hu and Easterly, 2009). Therefore, the application of plant extracts, as substitutes of solid tissues, for small- or large-scale preparation of various metal nanoparticles is easier. For the first time, the extracts of leaves, stems, and roots of Cranesbills were applied for extracellular production

*Corresponding author's e-mail address:
moshtaghi@um.ac.ir

of gold nanoparticles. Shankar et al. (2003) reported the biological reduction of gold ions to gold nanoparticles using geranium leaf extract. Also, they were produced triangular and spherical gold nanoparticles, by lemon juice (Shankar et al., 2004). Gold nanoparticles were synthesized from the reaction of Neem extract with $HAuCl_4$ (Chloroauric acid) in a period of two hours. The formation of nanoparticles was approved by UV-Vis-IR spectroscopy analysis and observation of color changes. It seems that nanoparticles which were produced by this method, in addition to spherical structures, also tend to have thin flat structures. These flat particles which were mainly in the form of triangular and to a lesser extent in hexagonal shape, had 50-100 nm size (Shankar et al., 2004). Silver nanoparticles can be also prepared from Aloe Vera extract. Developed nanoparticles had spherical shape and were in 15/5 nm size (Chandran et al., 2006). Leela and Vivekanandan (2008) synthesized silver nanoparticles using leaf extracts of *Helianthus annuus* and *Basella alba*. They showed that *Helianthus* has a comparably stronger potential for fast reduction of silver ions. They also reported that Poly-L and freaking loop water-soluble components, are primarily responsible for the decline and stabilization of silver nanoparticles. Other studies, have been shown that various parameters including plant source, organic compounds of leaves' extracts, AgNO3 concentration, temperature and the presence of pigments are effective in the development of nanoparticles (Leela and Vivekanandan, 2008). Bar et al, (2009) made silver nanoparticles using *Jatropha curcas*, as a reducing agent. These nanoparticles were identified by high-resolution transmission electron microscopy (HRTEM), X-ray diffraction and UV-Vis spectroscopy. As it was confirmed by HRTEM imaging, particles with 10 to 20 nm size ranges are usually stabilized by the cyclic peptides. Zargar et al, (2011) synthesized silver nanoparticles using methanol extract of *Vitex negundo* as a reducing and stabilizing agent, and investigated their antimicrobial properties. Changing solution's color from yellowish green to dark brown was considered as the determinant of nanoparticles formation. Spectrum UV-Vis experiments, indicated broadband SPR in two peaks of 442 and 447 nm.

Gnana Jobitha et al, (2012) were produced silver nanoparticles using Elettaria cardamomum and investigated their antimicrobial properties. Formation of silver nanoparticles was confirmed by pale yellow to dark brown color changes and the presence of a unique peak in the range of 460 nm, which was detected by UV spectrophotometer. Also, antibacterial properties of these nanoparticles against pathogenic bacteria including *Bacillus subtilis* and *Klebsiella planticola* were reported. Shafaghat in 2014 used methanol extract of Viburnum lantana leaves for biosynthesis of silver nanoparticles and assessed their biological activity against gram-positive and gram-negative bacteria. Results indicated the strong antimicrobial effects of silver nanoparticles by rapid reduction of Ag^+ ions to Ag^0 as the mechanism of action.

Marigold extract has been used previously for the synthesis of silver nanoparticles. Marigold with scientific name *Calendula officinalis* belongs to the Asteraceae family. This medicinal plant is cultivated throughout the temperate and sunny regions of the world and could be localized easily. Chidambaram et al, (2014) synthesized silver nanoparticles using petal extracts of marigold. Baghizadeh et al, (2015) were applied calendula seed extracts for silver nanoparticle synthesis. Rodino et al, (2019) have been produced silver nanoparticles via green synthesis, using vegetal extracts of pot marigold flowers (Calendula officinalis), and investigated their application for healthy storage of fruits.

Materials and Methods

Plant extracts preparation steps

The silver nitrate was purchased from the Merck Company (Germany) and Marigold seeds were purchased from Isfahan Pakan seed Company. Marigold seeds were planted in the pots while they were kept in the greenhouse until flowering time. Sterile seedlings, were applied for preparation of Marigold hairy roots, which were then grown in a liquid $^1/_2$ B5 medium to collect hairy root extracts. In addition, roots, petals, and seeds of Marigold were used for preparation of aqueous extracts. 10 grams of roots, petals, seeds and hairy roots were washed by deionized water. Then the samples were dried, powdered, and boiled in 100 ml of deionized water for 10 minutes before filtration by Whatman paper (No. 1). Final preparations, were kept in the refrigerator for downstream applications.

Synthesis and purification of silver nanoparticles

The aqueous extracts, with two different volumes (5 and 10 ml) were poured into 100 ml Erlenmeyer flasks and brought to the volume of 100 ml by the addition of Silver nitrate solution (1×10^{-3} M), for converting the Ag^+ ions to Ag^0 ones. They were kept at room temperature for 24 hours.

Then, silver nanoparticle solutions were centrifuged at 13,000 rpm for 15 minutes (Sigma 14-1, Germany). The upper solution was poured out in

each case and the silver nanoparticles which were precipitated at the bottom of the tube, mixed with deionized water and centrifuged again. This procedure was repeated for three times to increase the purity of nanoparticles. Then, the best samples were selected based on their appearance properties, such as intensity of darkness and applied for further experiments.

Characterization of silver nanoparticles

The revival of pure Ag^+ ions was evaluated through UV-Vis spectroscopy. The UV-Vis spectrum analyses were performed using Array Photonix Ar 2015 spectrophotometer in the range of 300-350 nm wavelengths. In order to determine the size distribution of synthesized nanoparticles, Particle Size Analyzer (Vasco, France) was applied. To do this, samples were diluted (10 folds) with distilled water prior to analyses. Also, for more precise determination of particle sizes and morphological study of nanoparticles, transmission electron microscopy (Leo 912AB) was carried out at a voltage of 120 kV. TEM samples were prepared on carbon coated copper grids by dropping AgNPs colloidal solutions and the following drying steps under vacuum.

Results and Discussion

At first, plant extracts were pale yellow or green but following the addition of silver nitrate solution, their color changed to dark brown in 24 hours. As demonstrated in figure 1, this color changes were apparently visible (Figure 1).

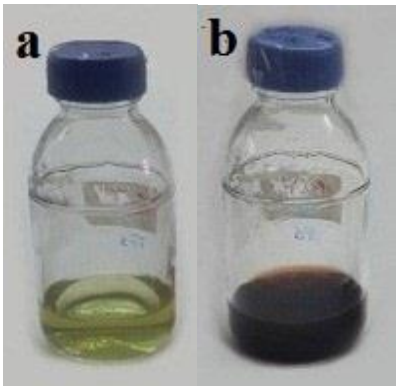

Figure 1. Color differences between (a) Marigold extract solutions and (b) Marigold extracts in the presence of silver nitrate solutions.

Plant extracts, which were kept in the absence of silver nitrate solution and didn't show any color changes, were considered as controls. The establishment of dark brown color after mixing the extracts with silver ions was a clear indicator of the metal ions reduction and the formation of silver nanoparticles in the environment. The addition of plant extracts to silver nitrate solution at a ratio of 10 to 100 was the best and produced relatively darker nanoparticle solutions.

In general, if color changes are associated with the formation of sediments, so they will show the formation of large particles; but, when color changes happened without any sedimentation, it could be concluded that synthesized nanoparticles have a very small particle size distribution. During our experiments no sedimentation was observed in nanoparticle solutions of marigold extracts.

Formation and stability of silver nanoparticles

To confirm the formation and proper stability of silver nanoparticles, their absorption spectrum was read after 24 hours in the range of 300-350 nm using a spectrophotometer (Unico Gene Company, USA). Results of UV-Vis analyses (Figure 2) showed that the aqueous extracts of various plant organs of Marigold, were produced different concentrations of silver nanoparticles. The highest absorbance at 430 nm was 1.6 a.u (Absorbance unit) and recorded for the nanoparticles which were synthesized using hairy root extracts, while, the lowest was obtained for nanoparticles synthesized by seed extracts (0.8 a.u). Absorptions of 1.5 a.u and 1.17 a.u were respectively observed at 430 nm for nanoparticles synthesized by petal and root extracts. Marchiol et al, (2014) used extracts of different organs (leaves, stems and roots) of various plants including *Brassica juncea*, *Festuca rubra* and *Medicago sativa* for synthesis of silver nanoparticles. Extracts of different plant organs indicated different performances during synthesis of nanoparticles. In *Brassica juncea* and *Festuca rubra*, root extracts showed a better performance, while, in *Medicago sativa*, leaf extracts were the best. In the present study the potential of various organ extracts of marigold (leaves, petals, seeds, roots and hairy roots) for production of silver nanoparticles were assessed comparatively, and the priority of hairy root extracts were confirmed.

The results of particle size analyses were shown in Figure 3. Results indicated that nanoparticles which were synthesized using hairy root and root extracts had the smallest size, respectively. The size of smallest and largest nanoparticles synthesized were equal to 5.4 and 22.4 nm in hairy root extracts, 14.8 and 61.7 nm in root extracts, 16.2 and 67.6 nm in petal extracts, and 29.5 and 67.6 nm for seed extracts. As demonstrated in Figure 3 (C, D), nanoparticles synthesized by hairy root and root extracts of marigold had the smallest size.

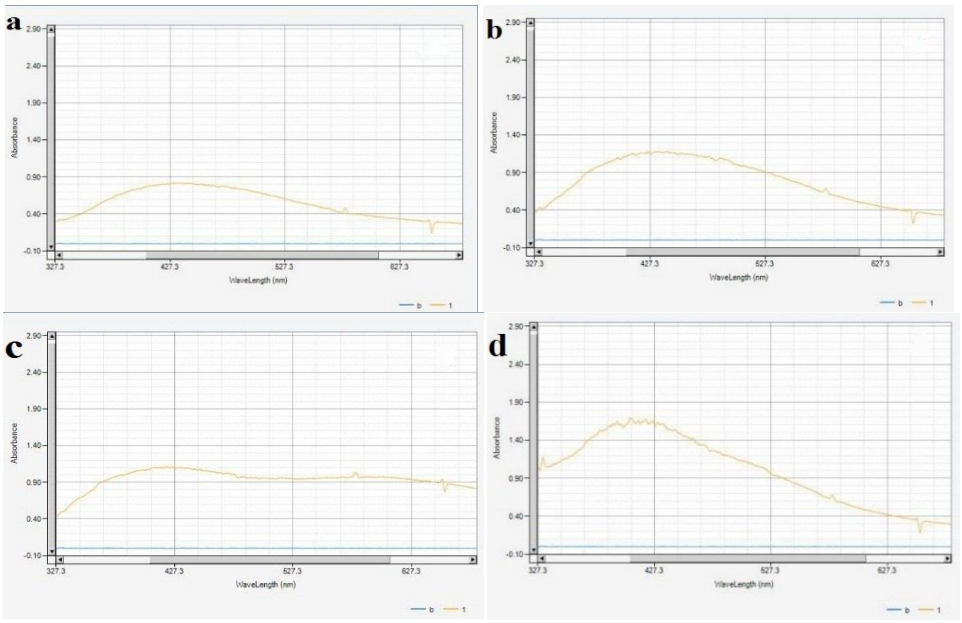

Figure 2. The results of UV-Vis analyses of silver nanoparticles synthesized by seed (a), petal (b), root and (c), hairy root (d) extracts of Marigold.

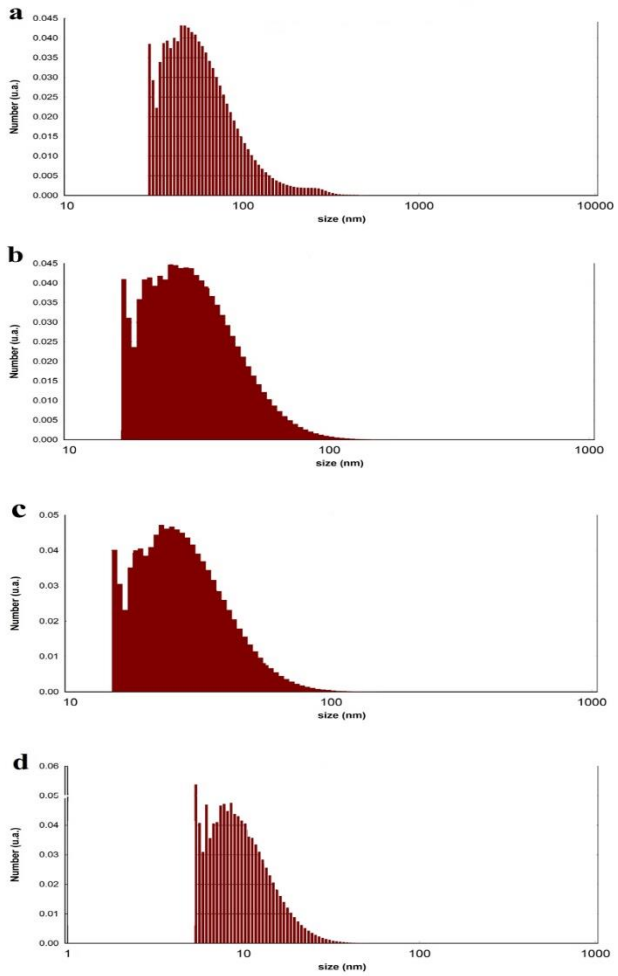

Figure 3. The results of nanoparticle size analyses obtained based on dynamic light scattering experiments (Cumulants mode) for silver nanoparticles synthesized by seed (a) petal (b) root (c) and hairy root (d) extracts of *Calendula officinalis.*

For more certainty and also to determine the morphological features of silver nanoparticles, they were investigated via transmission electron microscope.

The size of silver nanoparticles can be very different. This depends on materials applied to reduce silver ions, silver nitrate concentration, temperature conditions, and so on. In 2011, Darroudi et al, from Putra Malaysia University reported green synthesis and characterization of silver nanoparticles.

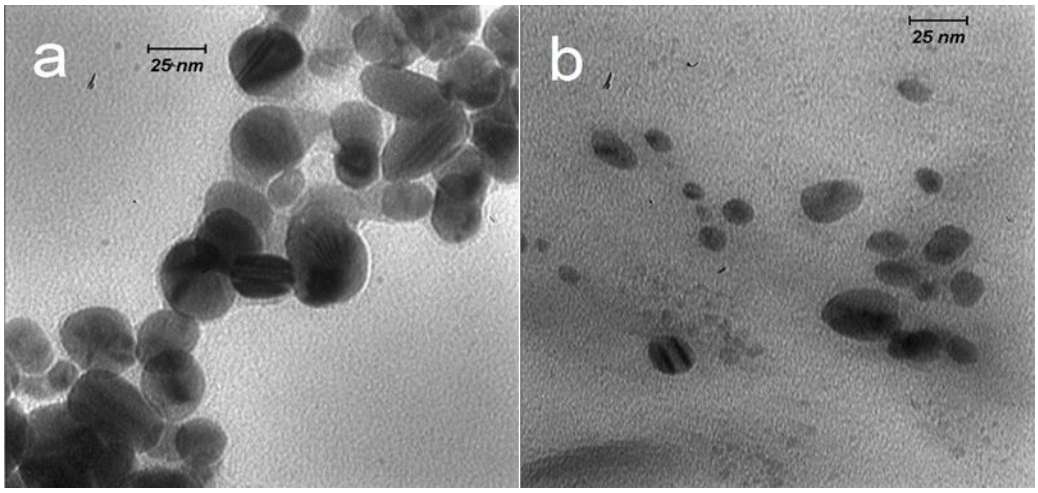

Figure 4. Images obtained via transmission electron microscopy (TEM) for silver nanoparticles with spherical appearance, which were synthesized using root (a) and hairy root (b) extracts of *Calendula officinalis*, scale bar: 25 nm.

They showed that by increasing the temperature, smaller silver nanoparticles are produced. Also, silver nanoparticles which were obtained in gelatin solution were smaller than the ones prepared in sugar containing gelatin solution. In another study, *Catharanthus roseus* was applied for synthesis of nanoparticles and their properties were determined by spectrophotometer UV-VIS, SEM and X-Ray analyses. They reported the preparation of nanoparticles with a diameter between 48 and 67 nm.

This method was introduced as eyewitness to produce nanoparticles with added value for commercial and industrial applications (Mukunthan et al., 2011). Padalia et al. (2015) produced silver nanoparticles by *Calendula officinalis* extract. The size of the synthesized nanoparticles was between 10-90 nm and they had spherical, hexagonal, and irregular shapes. Chidambaram et al. (2014) prepared silver nanoparticles from petal extracts of *Calendula officinalis* with 2-20 nm size ranges. Baghizadeh et al. (2015), reported the synthesis of silver nanoparticles form marigold seed extracts with spherical shape and diameter of 5 to 25 nm. Most of the nanoparticles produced in this study were located between 5 to 10 nm, considering their size distribution. It seems that the size and shape of synthesized silver nanoparticles, vastly, depend on the used materials and synthesis conditions. TEM confirmed the desired spherical appearance for silver nanoparticles which were synthesized in present study (Figure 4).

Conclusion

During last decades, silver nanoparticles have been attracted worldwide attention due to their unique physical and chemical properties. Considering disadvantages of physical and chemical methods of nanoparticle synthesis, green synthesis technologies were suggested as efficient alternatives. Different plant organs could be examined to achieve best results. Results from the present study, for the first time, confirmed that hairy root extracts of marigold had a better performance for production of desirable silver nanoparticles in comparison to other organs extracts.

Acknowledgment

The authors wish to thank Central Laboratory of Ferdowsi University of Mashhad for their help for performing part of the experiments.

Conflict of Interest

The authors report no conflicts of interest.

References

Baghizadeh A., Ranjbar S., Gupta VK., Asif M., Pourseyedi S., Karimi M. and Mohammadinejad R. (2015) Green synthesis of silver nanoparticles using seed extract of *Calendula officinalis* in liquid phase. Journal of Molecular Liquids 207: 159-163.

Bar H., Bhui DK., Sahoo G., Sarkar P. and Misra A. (2009) Green synthesis of silver nanoparticles using latex of *Jatropha curcas*. Colloids and Surfaces A: Physicochemical and Engineering Aspects 339: 134-139.

Bhainsa K.C. and Souza S.F.D. (2006) Extracellular biosynthesis of silver nanoparticles using the fungus *Aspergillus fumigatus*. Colloids and Surfaces B: Biointerfaces 47(2):160-164.

Chandran S.P., Chaudhary M., Pasricha R., Ahmad A. and Sastry M. (2006) Synthesis of gold nanotriangles and silver nanoparticles using Aloe Vera plant extract. Biotechnology Progress 22:577–583.

Chidambaram K., Saritha R., Maheswari. and Syedmuzammil M. (2014) Efficacy of green synthesis of Silver nanoparticles using flowers of *Calendula Officinalis*. Chemical Science Transactions 3(2): 773-777.

Darroudi M., Bin Ahmad M, Abdullah M. and Ibrahim N. (2011) Green synthesis and characterization Gelatin-based and suger-redused silver nanoparticles. International Journal of Nanomedicine 1(6): 569-574.

David L. and Moldovan B. (2020) Green Synthesis of Biogenic Silver Nanoparticles for Efficient Catalytic Removal of Harmful Organic Dyes. Nanomaterials 10(2): 202-217.

Devina Merin D., Prakash S. and Valentine Bhimba B. (2010) Antibacterial screening of silver nanoparticles synthesized by marine micro algae. Asian Pacific Journal of Tropical Medicine 3(10):797-799.

Gericke M. and Pinches A. (2006) Biological synthesis of metal nanoparticles. Hydrometallurgy 83:132-136.

Ghaffari-Moghaddam M. and Hadi-Dabanlou R. (2014) Plant mediated green synthesis and antibacterial activity of silver nanoparticles using Crataegus douglasii fruit extract. Journal of Industrial and Engineering Chemistry 20(2):739-744.

Gnana Jobitha G., Annadurai G. and Kannan Ch. (2012) Green synthesis of nanoparticle using *Elettaria Cardamom* and assessment of its antimicrobial activity. International Journal of PharmaScience and research 3: 323-330.

Hu M. and Easterly C. (2009) A novel them al electero chemical synthesis method for production of stable colloids of “naked” metal (Ag) nanocrystals. Materials Science and Engineering 29:726-736.

Leela A. and Vivekanandan M. (2007) Tapping the unexploited plant resources for the synthesis of silver nanoparticles. African Journal of Biotechnology 7: 3162-3165.

Marchiol L. (2012) Synthesis of Metal nanoparticles in living plants. Italian Journal of Agronomy 7(3): 122-128.

Marchiol L., Mattiello A., Poscic F., Giordano C. and Musetti R. (2014) In vivo synthesis of nanomaterials in plants: location of silver nanoparticles and plant metabolism. Nanoscale Research Letters 9: 101-112.

Mukunthan KS., Elumalai EK., Trupti N Patel. and V Ramachandra Murty. (2011) Catharanthus roseus: a natural source for the synthesis of silver nanoparticle. Asian Pacific of Tropical Biomedicine 270-274.

Naveen K.S., Kumar G., L K. and Rao K.V B. (2010) Extracellular biosynthesis of silver nanoparticles using the filamentous fungus Penicillium sp. Archives of Applied Science Research 2(6): 161-167.

Padalia H., Moteriya P. and Chanda S. (2015) Green synthesis of silver nanoparticles from marigold flower and its synergistic antimicrobial potential. Arabian Journal of Chemistry 8:732-741.

Rodino S., Butu M. and Butu A. (2019) Application of biogenic silver nanoparticles for berries preservation. Digest Journal of Nanomaterials and Biostructures 14:601-606.

Shafaghat A. (2014) Synthesis and characterization of silver nanoparticles by photosynthesis method and their biological activity. Synthesis and reactivity in inorganic Metal-Organic and Nano-Metal Chemistry 45:381-387.

Shankar A., Ahmad R., Pasricha R. and Murali S. (2003) Bio reduction of chloroaurate ions by geranium leaves and its endophytic fungus yields gold nanoparticles of different shapes. Journal of Materials Chemistry 13:1822-1826.

Shankar S., Rai A., Ahmad A. and Sastry M. (2004) Rapid synthesis of Au,Ag and bimetallic Au core-Ag

shell nanoparticle using Neem (*Azadirachta indica*) leaf broth. Journal of Colloid and Interface Science 275(2):496-502.

Shankar S., Rai A., Ankamwar B., Singh A., Ahmad A. and Sastry M. (2004) Biological synthesis of triangular gold nanoprisms. Nature Materials 3(7): 482-488.

Thangaraju N., Venkatalakshmi R.P. and Chinnasamy A. (2012) Synthesis of silver nanoparticles and the antibacterial anticancer activities of the crude extract of *Sargassum polycystum* C. Agardh. Nano Biomedical Engineering 4(2): 89-94.

Zargar M., Abdul Hamid A., Abu Bakar F., Nor Shamsudin M., Shameli K., Jahanshiri F and Farahani F. (2011) Green synthesis and antibacterial effect of silver nanoparticles using *Vitex negundo* L. Journal of Molecules 16: 6667-6676.

Journal of Cell and Molecular Research (2020) 11 (2), 66-81 DOI: 10.22067/jcmr.v11i2.84965

Research Article

In silico Analysis of Determinant Factors in Microbial Protease Thermostability

Parisa Farrokh [1,2*], Fatemeh Salimi[1]

[1]*Department of Cellular and Molecular Biology, School of Biology, Damghan University, Damghan, Iran*
[2] *Institute of Biological Sciences, Damghan University, Damghan, Iran*

Received 7 January 2020 Accepted 16 February 2020

Abstract

Thermostable proteases are one of the pivotal enzymatic groups which play fundamental roles in biotechnology-related industries. The identification of bacterial thermostable enzymes through screening programs is a time and cost consuming process. So, extensive bioinformatics and experimental studies have been conducted to reveal thermo stabilizing factors. The current study was aimed to evaluate distinctive indicators among 33 thermostable and 10 mesostable proteolytic enzymes. The frequency of individual amino acids, aliphatic indexes, melting temperatures, isoelectric points, as well as, the frequency of AXXXA and GXXXG motifs were determined and compared among these enzymes. In addition, types of proteolytic enzymes and their active sites were assigned. Moreover, the frequency of alpha helixes, polar surface regions, and packing volumes of these enzymes with the known structures were characterized. Results showed that the frequency of Ala and AXXXA motifs were significantly higher in thermostable proteolytic enzymes, while they possess lower contents of Met, His, Lys and Leu in comparison to mesostable enzymes (P<0.05). According to statistical analysis, thermostable proteolytic enzymes indicated meaningful lower packing volumes than mesostable enzymes (P<0.05). Findings of the current study in addition to more detailed investigations on the thermostability mechanisms of various protein families are essential for designing more efficient industrial enzymes with functional properties at high temperatures.

***Keywords*:** Bioinformatics analysis, Protein engineering, Proteolytic enzyme, Thermostability

Introduction

The application of biocatalysts in various industries is safer than using chemical compounds and has environmental advantages (Razzaq et al., 2019). Proteases, as one of the main industrial enzymes, are responsible for around 60% of the world enzyme market (Raveendran et al., 2018). Proteolytic enzymes constitute a very large and complex group of hydrolases. Despite the high diversity of proteases' functions and structures, they were simple classified to exo- or endo-proteases according to their site of cleavage (Souza et al., 2015). In addition, exo-peptidases can be further categorized into amino- and carboxy-peptidases (Souza et al., 2015). Proteolytic enzymes also can be grouped based on residues in their catalytic active sites into serine proteases (Patel, 2017), aspartic proteases, asparagine proteases, cysteine proteases (Dadshahi et al., 2016), metalloproteases (Abebe et al., 2014), glutamic proteases, threonine proteases or proteases with mixed or unknown catalytic mechanisms (Rawlings et al., 2007; Rawlings et al., 2017).

Proteases are widely produced by all organisms, including plants, animals, fungi, bacteria, and archaea. Microbial-derived proteases have been applied for commercial purposes due to easier large-scale production (Wang et al., 2008; Haddar et al., 2010). Microbial proteases are deemed vital elements in a wide range of processes including nutritional, pharmaceutical, environmental, detergent, textile, leather, and livestock industries (Homaei et al., 2010; Homaei and Etemadipour, 2015; Barzkar et al., 2018). However, the primary limitation to the application of microbial proteases is their instability under high temperature and pH conditions (Iqbalsyah, et al., 2019). Hence, thermostable and/or thermophilic proteases which possess high abilities to preserve their activities under harsh conditions of industrial processes are more applicable in the field of biotechnology (Wakarchuk et al., 1994).

Thermostable and thermophilic enzymes are normally derived from thermophilic and mesophilic organisms. Most of the thermostable and/or thermophilic proteases are not only stable at high temperatures but also preserve their catalytic activities in the presence of detergents and other

* Corresponding author's e-mail address: p.farrokh@du.ac.ir

denaturing chemicals, such as urea, guanidine-HCl, Dithiothreitol, 2-mercaptoethanol, and chaotropic agents. The application of thermostable and/or thermophilic proteases in the industrial processes have some advantages, including higher reaction rates, enhanced substrate solubility, and decreased solution viscosities. In addition, their large scale production is less susceptible to contamination since there are fewer microorganisms which can grow at high temperatures. However, screening of thermophilic microorganisms for finding thermophilic proteases is a tedious, costly, and time-consuming strategy. In this regard, engineering mesostable enzymes to develop thermostable enzymes is considered as a valuable strategy (Kumar, 2002; Li and Li, 2009: Tavano et al., 2018).

To determine factors which are responsible for thermal stability of proteins several approaches can be applied. Among which, we mention *i)* bioinformatic comparison of the protein structure for thermophilic proteins versus their mesophilic homologues, *ii)* computational studies on a dataset of thermophilic and mesophilic proteins to compare their various features, *iii)* mutational-based studies, and *iv)* comparing whole genome sequences of thermophilic species with their mesophilic homologues (Sadeghi et al., 2006).

In point of structural view, thermostable proteins have higher numbers of ionic interactions, salt bridges, disulfide, and hydrogen bonds (Sadeghi et al., 2006). They have increased packing density (Sadeghi et al., 2006), higher contents of helical structures (Sadeghi et al., 2006), less short surface loops (Sadeghi et al., 2006), decreased surface area to volume ratios (Das and Gerstein, 2000; Tekaia et al., 2002), and decreased internal cavities (Pellegrini et al., 1999). At the level of amino acid sequences, thermophilic proteins have a higher frequency of hydrophobic (Razvi and Scholtz, 2006) and charged amino acids, higher relative content of Arg, Glu (Pack et al., 2013), lower occurrence of bulky polar residues, decreased contents of uncharged polar residues (Ser, Thr, Asn, and Gln) (Haney et al., 1999), and increased contents of aromatic residues (Chakravorty et al., 2011).

Therefore, further investigations about the thermostability encountered mechanisms are essential for theoretical description of protein folding and stability and also, for designing efficient thermostable industrial enzymes. Since thermostable microbial proteases have a key contributory role in the market of industrial enzyme, and whereas there are no shared particular sequences or structural patterns among heat-stable proteases, focusing on this group of enzymes is worthwhile. Here, we selected 43 thermostable/thermophilic and mesophilic proteases which their characteristics had been previously determined in experimental studies. This study, innovatively investigated the consistency of well-known thermostability parameters among thermostable proteolytic enzymes.

Materials and Methods

Sequence collection of microbial proteases

Thirty-three bacterial thermostable proteolytic enzymes, which their optimum temperature and/or thermal stability had been reported in experimental studies were selected from UniProt proteomic server (Consortium 2018). Moreover, ten well-identified mesostable proteolytic enzymes' sequences were also collected from UniProt to compare with thermostable ones. In this regard, amino acid sequences of these enzymes were retrieved in FASTA format.

Investigation the thermostability properties of different proteases

The amino acid composition, aliphatic index, and isoelectric point of each proteolytic enzyme were determined through the ProtParam tool (web.expasy.org/protparam/). Melting temperatures (Tm) and net charges of the enzymes at pH 7 were calculated using Tm Predictor (tm.life.nthu.edu.tw/) and PepCalc (pepcalc.com), respectively. Frequency of AXXXA and GXXXG motifs in the sequences were assigned through manual searching and counting.

Determination of the types of proteolytic enzymes and their active sites

The types of the proteases were determined based on their conserved domain composition using CD-search tool (Marchler-Bauer et al., 2016). The active sites of proteolytic enzymes with protease activity were identified through the literature review (Yamagata and Ichishima, 1995; Wu et al., 2004; Pombejra et al., 2018). To determine the active sites of enzymes with peptidase activity, the MEROPS database (Rawlings et al., 2017) in addition to literature review (Medrano et al., 1998; Goldstein et al., 2005; Bjelke et al., 2006; Ohara-Nemoto et al., 2014; Reddi et al., 2014) were applied.

Multiple sequence alignments

In order to determine the possible differences of conserved motifs and residues in the sequences of mesostable and thermostable proteases, multiple

sequence alignments were performed in IBIVU server using PRALINE software (Simossis and Heringa, 2005). Since the investigated amino acid sequences have significantly different lengths (285-1364 amino acid residues), matrix PAM 250 with gap opening 10 and gap extension 1 were used for alignments.

Structural analyses

Among 43 selected proteolytic enzymes, nine enzymes had a tertiary structure in the Protein Data Bank (PDB) (Bank, 2000) which four and five of them are mesostable and thermostable/thermophilic proteolytic enzymes, respectively. Structural analysis of these enzymes was performed using VADAR (Volume, Area, Dihedral Angle Reporter) software version 1.8 which can be accessed at http://redpoll. pharmacy.ualberta.ca/vadar/ (Willard et al., 2003). Furthermore, frequency of alpha helixes, polar surface regions, and packing ratios in these structures were determined. One of these structures (PDB ID: 5J44, which was related to Q8VSL2 sequence) with more than 2000 residues, was not investigable using VADAR software.

Statistical analyses

Homogeneity of variance and normal distribution of data including frequency of each twenty amino acids, AXXXA and GXXXG motifs, the mean of pI (isoelectric point), aliphatic indexes, Tm, net charges in pH 7, melting temperatures in both thermophilic/thermostable and mesostable enzymes groups were evaluated using Levene and Shapiro Wilk tests in SPSS version 23, respectively. To compare the mean of each variable in two investigated subsets (thermophilic/thermostable and mesostable proteolytic enzymes), independent *t*-test and Mann-Whitney test were applied for data with or without normal distribution, respectively. Finally, chi-square test was carried out to evaluate the possible differences in melting temperatures of proteolytic enzymes in these two groups.

Results

Source and properties of investigated sequences

All selected enzymes have bacterial origin except Q2QC89, which has been derived from an archaeon (*Thermococcus* sp.).

Proteolytic enzymes in the current study with an optimum temperature of 50°C or higher and/or thermal stability in the mentioned temperatures were considered as thermostable enzymes, and the others were placed in the mesostable group. Some properties of the proteolytic enzymes which were obtained from literature are summarized in table 1.

Distinctive features of thermophilic/thermostable proteolytic enzymes

Some characteristics of the enzymes which are related to the thermostability were summarized in table 2. The Tm Predictor categorizes proteins based on their melting temperatures in three ranges; >65°C, <55°C and 55-65°C. Statistical analysis showed that there were no significant differences in melting temperatures of thermophilic/thermostable and mesophilic proteolytic enzymes ($P>0.05$).

In addition, statistical analysis confirmed normal distributions of data related to frequency of AXXXA motifs, and amino acids except Ala, Arg, Cys, Gln, His, Leu, Phe ($P>0.05$), while isoelectric points, net charges, aliphatic indexes, and GXXXG motifs did not show normal distributions ($P<0.05$). In case of pI, aliphatic index and net charge parameters, thermostable and mesostable enzymes were similar; however, the frequency of AXXXA motif was significantly higher in thermophilic/thermostable proteolytic enzymes when compared to mesostable ones ($P<0.05$).

The percentages of amino acids present in proteolytic enzymes are presented in Figure 1. According to the *t*-test and Mann Whitney results, there was a significant difference in frequencies of Met, Ala, Leu, Lys and His between thermostable proteolytic enzymes and mesostable ones. Although, thermophilic/thermostable enzymes had higher percentages of Ala (9.2% *vs.* 8.59% in the other group) and lower percentages of Met (2.01%), Leu (7.16%), Lys (5.06%) and His (2.32%) in comparison to mesostable proteins. The frequency of the above-mentioned residues in the mesostable enzymes were as follows: Met (2.68%), Leu (8.22%), Lys (5.84%), and His (2.61%) (Figure 1). Moreover, to compare each of the twenty amino acids, the analysis of the hydrophobic, aromatic, polar charged, and polar uncharged amino acid groups was performed; but, the subsets of the residues did not show any significant differences between thermostable and mesostable enzymes.

Types of proteolytic enzymes and their active sites

Whereas the types of some proteolytic enzymes were not precisely determined in the previous studies, the retrieved sequences were classified according to their conserved domains. It was confirmed that 25 and 18 of investigated enzymes could be grouped as proteases and peptidases,

respectively (Table 2). Two types of catalytic triads within conserved sequences were observed among the proteases, which are including Asp, His, and Ser or His, His, and Glu. However, peptidases due to their variability had different active sites, and one of them (UniProt ID: G5DCB7) belongs to the peptidase family with unknown catalytic mechanism based on the MEROPS database (Table 2).

Table 1. Investigated microbial proteolytic enzymes and some of their properties obtained from literature.

UniProt ID	Source of microorganisms	Optimum temperature	Thermal stability	Optimum pH	pH stability range	References
Thermostable/thermophilic enzymes						
P06874	*Bacillus stearothermophilus*	*ND*	65ºC	7	*ND*	(Fujii et al. 1983)
P43133	*Bacillus stearothermophilus*	*ND*	65ºC	*ND*	6.5-7.5	(Kubo and Imanaka 1988)
P23341	*Thermus aquaticus* YT-1	75-80ºC	*ND*	*ND*	*ND*	(Motoshima et al. 1990)
P39899	*Bacillus subtilis*	ND	65ºC	6.6	*ND*	(Tran et al. 1991)
P23384	*Bacillus caldolyticus*	77ºC	*ND*	7	*ND*	(Van den Burg et al. 1991)
P42663	*Thermus aquaticus* YT-l	80ºC	*ND*	8	*ND*	(S.-H. Lee et al. 1992)
P41363	*Bacillus* sp. no. AH-101	*ND*	30-70ºC	ND	12-13	(Takami et al. 1992)
P0CH29	*Bacillus megaterium* ATCC 1458 1	58ºC	*ND*	6.4-7.2	*ND*	(KÜHN and FORTNAGEL 1993)
Q45670	*Bacillus* sp. strain AK.1	75ºC	*ND*	8.5	*ND*	(Maciver et al. 1994)
Q45621	*Bacillus* sp. NKS-21	50ºC	*ND*	*ND*	6-11	(Yamagata and Ichishima 1995)
P80146	*Thermus* sp. strain Rt41A	*ND*	70ºC	8	*ND*	(Munro et al. 1995)
P04189	*Bacillus subtilis*	*ND*	50ºC	8	*ND*	(Kamal et al. 1995)
Q43880	*Bacillus sp.*	82ºC	*ND*	*ND*	*ND*	(Vecerek and Kyslik 1995)
Q99405	*Bacillus* sp. KSM-K16	55ºC	*ND*	10	*ND*	(Kobayashi et al. 1995)
Q56365	*Thermoactinomyces* sp. E79	85ºC	*ND*	11	5-12	(J.-K. Lee et al. 1996)
Q59223	*Bacillus* sp. strain EAI	*ND*	85-95ºC	6.5	6-7.5	(Saul et al. 1996)
P74937	*Thermoactinomyces* sp. HS682	65ºC	*ND*	11	6-12	(Tsuchiya et al. 1997)
O33599	*Staphylococcus aureus*	*ND*	100ºC	*ND*	5-8	(Ramadurai et al. 1999)

Q93JY4	*Prevotella albensis* M384	*ND*	60ºC	*ND*	7-8	(Walker et al. 2003)
Q6W4N2	*Bacillus* sp. WF146	58ºC	*ND*	8	*ND*	(Wu et al. 2004)
Q84FM9	*Fervidobacterium islandicum*	80ºC	*ND*	8	*ND*	(Gödde et al. 2005)
Q2QC89	*Thermococcus* sp.NA1	*ND*	70-80ºC	6.5	*ND*	(H. S. Lee et al. 2006)
Q8G6Z9	*Bifidobacterium longum*	50ºC	40-60ºC	8	4-8	(Seo et al. 2007)
E0XH65	*Bacillus* sp. B001	60ºC	20-90ºC	10	5-12	(Deng et al. 2010)
G8HV17	*Bacillus circulans* MTCC 7906	60ºC	*ND*	9	*ND*	(Kaur et al. 2012)
G5DCB7	*Geobacillus thermoleovorans* DSM 15325	50ºC	*ND*	7.4	*ND*	(Jasilionis et al. 2012)
J9XWB6	*Serratia* sp. ZF03	*ND*	50-55ºC	8	8-10	(Salarizadeh et al. 2014)
H2BKX5	*Myroides profundi* D25	60ºC	*ND*	8.5	*ND*	(Ran et al. 2014)
W5RWH8	*Geobacillus thermoleovorans* DSM 15325	40ºC	50-60ºC	7.3	5-8	(Jasilionis and Kuisiene 2015)
A0A0C4XY83	*Streptomyces* sp.M30	75ºC	*ND*	9	6-11	(Xin et al. 2015)
H6WCS0	*Dichelobacter nodosus*	35ºC	15–65ºC	7	4-10	(Wani et al. 2016)
Q3HTI0	*Bacillus cereus* PMW8	60ºC	40-70ºC	9	*ND*	(Esakkiraj et al. 2016)
Q45300	*Bacillus licheniformis*	60ºC	*ND*	10	*ND*	(Ramakrishnan et al. 2017)
Mesostable enzymes						
P46544	*Lactobacillus delbrueckii* subsp. *bulgaricus* CNRZ 397	37ºC	*ND*	*ND*	*ND*	(Atlan et al. 1994)
P94870	*Lactobacillus helveticus* CNRZ32	*ND*	32-37ºC	4.5	*ND*	(Fenster et al. 1997)
O07121	*Lactococcus lactis* MG1363	37ºC	*ND*	*ND*	*ND*	(Hellendoorn et al. 1997)
Q8VSL2	*Shigella flexneri*	37ºC	*ND*	7.5	*ND*	(Benjelloun-Touimi et al. 1998)
Q7MUW6	*Porphyromonas gingivalis*	*ND*	25-37ºC	ND	6-8	(Banbula et al. 1999)
Q9L4G1	*Lactobacillus helveticus*	*ND*	25-37ºC	7.5	6-8	(Savijoki and Palva 2000)
O82882	*Escherichia coli* O157:H7	37-42ºC	*ND*	6.5-7	*ND*	(Grys et al. 2006)
Q29ZA8	*Bacillus intermedius*	37ºC	*ND*	8	*ND*	(Sharipova et al. 2008)

P9WK19	*Mycobacterium tuberculosis* H37Rv	37ºC	*ND*	7.5	*ND*	(Zhang et al. 2009)
B2RIT0	*Porphyromonas gingivalis*	37ºC	*ND*	6	*ND*	(Ohara-Nemoto et al. 2014)

ND: Not Determined

Table 2. *In silico* characterization of investigated proteolytic enzymes.

UniProt ID	Types of proteases	Active sites	pI	Aliphatic Index	Tm	Net charge in pH	Number of AXXXA motifs	Number of GXXXG motifs
P06874	Zn-dependent metalloprotease	H374, H378, E398	5.68	76.72	<55	-8.9	8	2
P43133	Zn-dependent metalloprotease	H377, H381, E401	5.82	76.46	55-65	-6.9	6	3
P23341	Aminopeptidase T	Y352	5.31	89.49	>65	-13.9	7	2
P39899	Zn-dependent metalloprotease	H369, H373, E393	5.43	73.10	55-65	-17.3	6	4
P23384	Zn-dependent metalloprotease	H370, H374, E394	5.64	75.33	<55	-8.2	8	4
P42663	Carboxypeptidase	E277	5.53	83.76	55-65	-13.6	6	6
P41363	Serine protease	D124, H154, S307	6.56	90.80	>65	-1	4	1
P0CH29	Zn-dependent metalloprotease	H388, H392, E412	8.39	70.64	55-65	4	6	5
Q45670	Thermitase-like proteins	D160, H193, S347	4.68	82.97	>65	-17.5	7	1
Q45621	Serine protease	D49, H86, S250	4.83	90.50	55-65	-17.5	3	1
P80146	Proteinase K-like proteins	D171, H204, S356	6.16	90.98	>65	-2.6	5	2
P04189	Serine protease	D138, H170, S327	9.04	81.23	>65	5.8	5	3

Q43880	Zn-dependent metalloprotease	H372, H376, E396	5.47	73.97	<55	-10.1	7	3
Q99405	Serine protease	D143, H173, S326	4.67	91.18	>65	-19.2	5	1
Q56365	Serine protease	D143, H176, S330	6.04	78.57	>65	-3.3	8	1
Q59223	Thermitase-like proteins	H372, H376, E396	5.39	74.51	55-65	-11.1	7	3
P74937	Zn-dependent metalloprotease	D49, H86, S249	4.92	87.13	>65	-15.6	3	0
O33599	Metallopeptidase	H291	6.16	38.10	55-65	-4.6	2	2
Q93JY4	Dipeptidyl peptidase IV	Y511, S600, D674, H706	7.56	70.77	55-65	2.1	5	2
Q6W4N2	Serine protease	D149, H185, S363	5.28	81.41	>65	-8.5	7	3
Q84FM9	Serine protease	D210, H248, S424	5.45	93.84	>65	-9.6	3	4
Q2QC89	Zn-dependent carboxypeptidase	E297	5.61	84.97	>65	-11.7	2	2
Q8G6Z9	Dipeptidase	C3	4.46	71.07	55-65	-47	2	0
E0XH65	Serine protease	D138, H168, S321	4.0	84.08	>65	-40.5	3	1
G8HV17	Serine protease	D155, H187, S384	5.14	79.41	55-65	-14.7	3	2
G5DCB7	Collagenase-like protease	Unknown	5.39	88.06	>65	-13.4	4	1
J9XWB6	Serralysin	E175	4.63	64.18	>65	-23.8	3	4
H2BKX5	Kp43 proteases	D129, H177, S378	5.85	79.68	55-65	-8	7	2
W5RWH8	Oligo peptidase F	E401	8.90	87.28	>65	9.2	9	3
A0A0C4XY83	Proteinase K-like proteins	D156, H187, S339	4.25	80.33	>65	-21.4	7	3
H6WCS0	Serine protease	D156, H220, S392	6.25	78.92	55-65	-4	5	3

Q3HTI0	Zn-dependent metalloprotease	H143, H147, E167	5.18	65.65	55-65	-8.3	6	2
Q45300	Serine protease	D137, H168, S325	8.94	84.70	>65	4.8	4	2
P46544	Proline iminopeptidase	S107, D246, D273	5.09	87.69	>65	-12.4	3	2
P94870	Aminopeptidases	Q64, C70, H362, N383	5.21	75.46	>65	-13.2	1	2
O07121	Dipeptidase	H92	4.73	79.87	>65	-33.7	4	3
Q8VSL2	Serine peptidase	H134, D162, S267	6.10	74.02	>65	-8.9	7	14
Q7MUW6	Dipeptidyl peptidase IV	Y518, S603, D678, H710	6.16	74.44	55-65	-8.2	4	6
Q9L4G1	Tripeptidase	D84, E178	4.77	73.90	>65	-29.8	1	2
O82882	Metallopeptidases	E447	6.39	74.59	55-65	-5.8	5	8
Q29ZA8	Serine protease	D138, H170, S327	8.96	80.73	>65	4.8	5	1
P9WK19	Methionine aminopeptidase	C105	5/07	87.89	55-65	-11.5	3	2
B2RIT0	Dipeptidyl aminopeptidase	S542, D627, H659	5.75	68.52	55-65	-10.7	4	4
Significant value			*NS*	*NS*	*NS*	*NS*	**	*NS*

NS, * and ** represent no significant differences, significant differences at 90% and 95% confidence intervals, respectively.

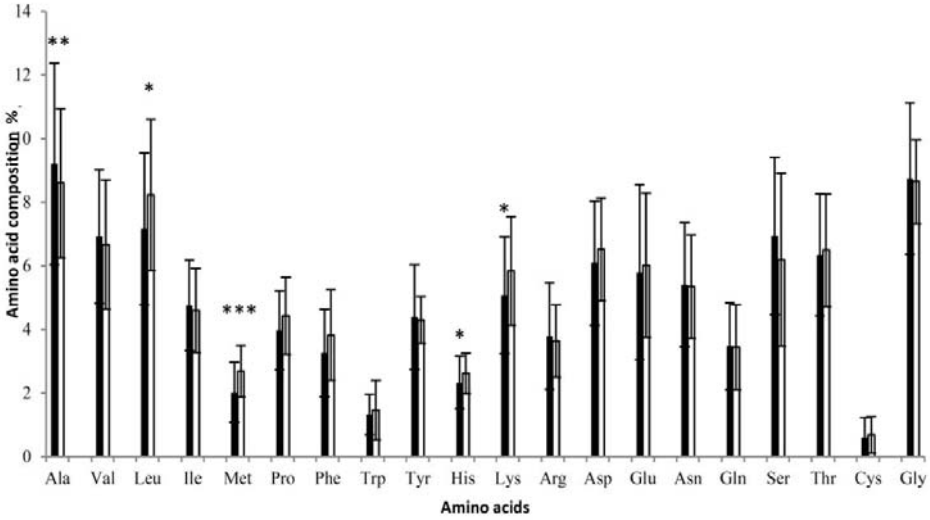

Figure 1. Frequency of different amino acids is reported for thermostable (black columns) and mesostable (white columns) groups. *, ** and *** represent significant differences at 90%, 95%, and 99% confidence intervals, respectively.

Sequence alignments

Results obtained through multiple sequence alignments indicated somewhat conserved sequences (from amino acid residues 1000 to1300) which are shown in supplementary file 1.

The structural features of thermostable/ proteolytic and mesostable enzymes

The numbers of alpha helixes, polar surface regions, and total volumes of available structures were predicted (Table 3). The statistical analyses showed that among structural characteristics, just total volumes of thermophilic/thermostable proteolytic enzymes were significantly lower than that of mesostable ones (P<0.05).

Discussion

In recent years, considerable efforts have been made to understand influential factors involved in thermal stability of thermostable or thermophilic proteins derived from mesophilic, thermophilic or

Table 3. Structural analyses of thermophilic/thermostable proteolytic enzymes and mesostable ones using VADAR software.

UniProt ID/ PDB ID	Type of enzymes	Alpha helix (%)	Polar surface Exposed)regions (polar ASA[1] (A^o) 10^{-2}	Total volume (Packing) 10^{-3} (A^o)
P43133/5WR3	**Thermophile/Thermostable**	37	4374.7	40568.7
Q45670/1DBI		28	3188.9	33870.1
P04189/1SCJ		96	3713.3	42181.7
Q99405/1MPT		78	3197.2	31663.4
O33599/1QWY		23	3810.9	29772.0
Q7MUW6/2D5L	**Mesostable**	96	6132.5	92421.4
O82882/3UJZ		56	6581.3	82474.0
P9WK19/1Y1N		71	2086.1	36599.7
Significant value		*NS*	*NS*	**

NS, and ** represent no significant difference and significant difference at 95% confidence interval, respectively.
[1] Accessible surface area.

hyper-thermophilic organisms. Thermophilic proteins preserve their native structures and consequently their activities under harsh environmental conditions, while, their mesostable homologs already denature. Comprehensive knowledge about factors involved in thermostability can be applied as a promising approach in developing thermostable enzymes through protein engineering. Most of the studies which have been worked on the thermal stability of proteins did not generally focus on a family or a limited group of proteins (Kumar et al., 2000; Liang et al., 2005; Sadeghi et al., 2006; Gromiha and Suresh, 2008). It seems that it is a reason for inconsistent results.

One of the fundamental features which profoundly affected structural, functional and biological properties of proteins is their amino acid composition. Analysis of amino acid composition and frequency can provide beneficial data about the importance of each amino acid in thermal stability of proteins. This feature can be different from one protein to another one in each organism or it can be taxon-specific (Zhou et al., 2008).

The current study showed that thermophilic or thermostable enzymes possess a higher frequency of Ala compared to mesostable ones. This residue is an appropriate helix former (Chakravorty et al., 2011) and through hydrophobic interactions provides conformational stability in the inner parts of proteins (Creighton, 1993). This feature leads to better packing, higher rigidity, hydrophobicity, and consequently more thermostability of proteins (Chakravarty and Varadarajan, 2000). This finding is analogous with previously published studies (Argos et al., 1979; Chakravarty and Varadarajan, 2000; Pack and Yoo, 2004). The percentage of Leu, another nonpolar residue, was lower in thermostable proteases than the mesostable ones. In case of Leu reported frequencies are not similar in various studies. Taylor and Vaisman detected higher percentages of Leu in thermophilic proteins (Taylor and Vaisman, 2010); while, Chakravarty and Varadaragan observed an opposite trend (Chakravarty and Varadarajan, 2000).

The present study indicated that thermophilic or thermostable proteases possess lower frequencies of thermolabile Met residue. This finding is in consistent with a previous finding (Kumar et al., 2000; Xu et al., 2003). The frequency of the other thermolabile amino acids, including Asn, Gln, and free Cys, in spite of their deamination or oxidation at high temperatures (Tomazic and Klibanov, 1988; Russell et al., 1994; Catanzano et al., 1997; Kumar et al., 2000; Xu et al., 2003), did not show indictable differences among the sequences. In the research of Kumar et al., among these temperature sensitive residues, only Cys was significantly lower in thermophilic proteins (Kumar et al., 2000).

Polar charged amino acids, including Arg, Lys, His, Asp, and Glu, contribute to the electrostatic interactions and enhancement of thermostability (Dill, 1990; Creighton, 1993; Ladbury et al., 1995; Vogt et al., 1997; Kumar et al., 2000). Although, in the current study, no significant differences were observed in the frequencies of Arg, Asp, and Glu between thermostable and mesostable proteases. Furthermore, lesser contents of Lys and His observed in thermostable proteins compared to mesostable ones. There are inconsistent reports about Lys frequency. Taylor and Vaisman found the lower percentages of Lys in thermophilic proteins (Taylor and Vaisman, 2010), while Cambillau and Claverie reported a higher percentages of Lys in hyperthermophiles (Cambillau and Claverie, 2000). Lower frequency of His in thermophilic proteins also reported in previous studies (Chakravarty and Varadarajan, 2000; Pack and Yoo, 2004; Sadeghi et al., 2006).

The aliphatic index, which is calculated based on the presence of amino acids with aliphatic side chains (Zhou et al., 2008), and melting temperature (Kumar et al., 2000) are two parameters which have positive effects on protein thermostability. However, in the present comparison, no significant differences were found between mesostable and thermostable groups for these criteria. Panja et al. showed that thermophilic proteins had a negative net charge at neutral pH and a slight acidic pI (Panja et al., 2015); while, thermostable and thermophilic proteolytic enzymes did not show any differences at the significant level of 0.05 in their study. Therefore, it seems that these factors are not determining agents for thermostability of proteases.

The AXXXA motif through helical interactions creates more stability in protein structures (Kleiger et al., 2002; Chakravorty et al., 2011). Higher frequency of AXXXA motif and poly Ala residues were also revealed through sequence analysis of the thermostable *Bacillus* lipases (Chakravorty et al., 2011). However, thermostable sequences in this study in spite of having significant higher Ala residues and AXXXA motifs did not have a higher percentages of alpha helixes in comparison with mesostable ones. If more PDB structures were available for the studied proteases, these contradictory findings might not occur. Since, limited structures of selected proteases and peptidases were available, the comprehensive

structural analyses were not possible. The exposed polar surfaces have been proposed as an effective factor for thermo stabilization of lipases (Chakravorty et al., 2011); however, our results were opposite to this expectation. Only packing volumes of the structures were significantly higher in thermostable enzymes than mesostable ones.

Investigating the thermostable and mesostable sequences through multiple sequence alignments is beneficial for finding short consensus sequences to design degenerate primers (Morya et al., 2012). Furthermore, these alignments will provide better insights for substitution of amino acids in protein engineering studies. Here, no considerable distinction was observed among the active sites or consensus motifs of thermostable and meostable enzymes.

Conclusion

In conclusion, according to the present study, thermostability of proteolytic enzymes not only can be attributed to the higher percentages of Ala, and fewer frequencies of His, Lys and Met, but also can be due to the presence of higher contents of AXXXA motifs and more packing structures in comparison to mesostable proteases. Without a doubt, the results of comparative studies between thermophilic proteins and their mesostable counterparts will revealed some thermo stabilizing factors. However, these results could not be accepted as general modes governing protein thermostability, because they completely depend on studied protein families. In addition, it is so difficult to relate any single factor as the main reason which is responsible for enhancement of thermal stability (Szilágyi and Závodszky, 2000). Therefore, extensive bioinformatic-based studies should be carried out on various thermostable and mesostable protein groups. Furthermore, the contradictory results should be taken into account to reach a reliable data and to enhance the thermal stability of mesostable proteins with desirable properties during protein designing or re-engineering processes.

Conflicts of interest

The authors declare that they have no conflict of interest.

References

Abebe B., Abrham S., Genet A., Hiwot G., Paulos K. and Melese A. (2014) Isolation, optimization and characterization of protease producing bacteria from soil and water in Gondar town, North West Ethiopia. International Journal of Bacteriology, Virology and Immunology 1:20-24.

Argos P., Rossmann M. G., Grau U. M., Zuber H., Frank G. and Tratschin J. D. (1979) Thermal stability and protein structure. Biochemistry 18:25, 5698-5703.

Atlan D., Gilbert C., Blanc B. and Portalier R. (1994) Cloning, sequencing and characterization of the pepIP gene encoding a proline iminopeptidase from *Lactobacillus delbrueckii* subsp. *bulgaricus* CNRZ 397. Microbiology 140:3, 527-535.

Banbula A., Mak P., Bugno M., Silberring J., Dubin A., Nelson D., et al. (1999) Prolyl tripeptidyl peptidase from *Porphyromonas gingivalis*. A novel enzyme with possible pathological implications for the development of periodontitis. The Journal of Biological Chemistry 274:14, 9246-9252.

Berman H. M., Westbrook j., Feng Z., Gilliland G., Bhat T. N., Weissig H., et al. (2000) The protein data bank. Nucleic Acids Research 28:235-242.

Barzkar N., Homaei A., Hemmati R. and Patel S. (2018) Thermostable marine microbial proteases for industrial applications: scopes and risks. Extremophiles 22:3, 335-346.

Benjelloun-Touimi Z., Tahar M. S., Montecucco C., Sansonetti P. J. and Parsot C. (1998) SepA, the 110 kDa protein secreted by *Shigella flexneri*: two-domain structure and proteolytic activity. Microbiology 144:7, 1815-1822.

Bjelke J. R., Christensen J., Nielsen P. F., Branner S., Kanstrup A. B., Wagtmann N., et al. (2006) Dipeptidyl peptidases 8 and 9: specificity and molecular characterization compared with dipeptidyl peptidase IV. Biochemical Journal 396:2, 391-399.

Cambillau C. and Claverie J. M. (2000) Structural and genomic correlates of hyperthermostability. Journal of Biological Chemistry 275:42, 32383-32386.

Catanzano F., Barone G., Graziano G. and Capasso S. (1997) Thermodynamic analysis of the effect of

selective monodeamidation at asparagine 67 in ribonuclease A. Protein Science 6:8, 1682-1693.

Chakravarty S. and Varadarajan R. (2000) Elucidation of determinants of protein stability through genome sequence analysis. FEBS Letters 470:1, 65-69.

Chakravorty D., Parameswaran S., Dubey V. K. and Patra S. (2011) In silico characterization of thermostable lipases. Extremophiles 15:1, 89-103.

Consortium U. (2018) UniProt: a worldwide hub of protein knowledge. Nucleic Acids Research 47:D1, D506-D515.

Creighton T. E. (1993) Proteins: structures and molecular properties. Second ed. W. H. Freeman and Co. New York, 80-100 pp.

Dadshahi Z., Homaei A., Zeinali F., Sajedi R. H. and Khajeh K. (2016) Extraction and purification of a highly thermostable alkaline caseinolytic protease from wastes *Penaeus vannamei* suitable for food and detergent industries. Food Chemistry 202: 110-115.

Das R. and Gerstein M. (2000) The stability of thermophilic proteins: a study based on comprehensive genome comparison. Functional and Integrative Genomics 1:1, 76-88.

Deng A., Wu J., Zhang Y., Zhang G. and Wen T. (2010) Purification and characterization of a surfactant-stable high-alkaline protease from *Bacillus* sp. B001. Bioresource Technology 101:18, 7100-7106.

Dill K. A. (1990) Dominant forces in protein folding. Biochemistry 29:31, 7133-7155.

Esakkiraj P., Meleppat B., Lakra A. K., Ayyanna R. and Arul V. (2016) Cloning, expression, characterization and application of protease produced by *Bacillus cereus* PMW8. RSC Advances 6:45, 38611-38616.

Fenster K. M., Parkin K. L. and Steele J. L. (1997) Characterization of a thiol-dependent endopeptidase from *Lactobacillus helveticus* CNRZ32. Journal of Bacteriology 179:8, 2529-2533.

Fujii M., Takagi M., Imanaka T. and Aiba S. (1983) Molecular cloning of a thermostable neutral protease gene from *Bacillus stearothermophilus* in a vector plasmid and its expression in *Bacillus stearothermophilus* and *Bacillus subtilis*. Journal of Bacteriology 154:2, 831-837.

Gödde C., Sahm K., Brouns S. J., Kluskens L. D., van der Oost J., de Vos W. M., et al. (2005) Cloning and expression of islandisin, a new thermostable subtilisin from *Fervidobacterium islandicum*, in *Escherichia coli*. Applied and Environmental Microbiology 71:7, 3951-3958.

Goldstein J., Kordula T., Moon J., Mayo J. and Travis J. (2005) Characterization of an extracellular dipeptidase from *Streptococcus gordonii* FSS2. Infection and Immunity 73:2, 1256-1259.

Gromiha M. M. and Suresh M. X. (2008) Discrimination of mesophilic and thermophilic proteins using machine learning algorithms. Proteins 70:4, 1274-1279.

Grys T. E., Walters L. L. and Welch R. A. (2006) Characterization of the StcE protease activity of *Escherichia coli* O157: H7. Journal of Bacteriology 188:13, 4646-4653.

Haddar A., Fakhfakh-Zouari N., Hmidet N., Frikha F., Nasri M. and Kamoun A. S. (2010) Low-cost fermentation medium for alkaline protease production by *Bacillus mojavensis* A21 using hulled grain of wheat and sardinella peptone. Journal of Bioscience and Bioengineering 110:3, 288-294.

Haney P. J., Badger J. H., Buldak G. L., Reich C. I., Woese C. R. and Olsen G. J. (1999) Thermal adaptation analyzed by comparison of protein sequences from mesophilic and extremely thermophilic *Methanococcus* species. Proceedings of the National Academy of Sciences 96:7, 3578-3583.

Hellendoorn M. A., Franke-Fayard B. M., Mierau I., Venema G. and Kok J. (1997) Cloning and analysis of the pepV dipeptidase gene of *Lactococcus lactis* MG1363. Journal of Bacteriology 179:11, 3410-3415.

Homaei A. and Etemadipour R. (2015) Improving the activity and stability of actinidin by immobilization on gold nanorods. International Journal of Biological Macromolecules 72:1176-1181.

Homaei A. A., Sajedi R. H., Sariri R., Seyfzadeh S. and Stevanato R. (2010) Cysteine enhances activity and stability of immobilized papain. Amino Acids 38:3, 937-942.

Iqbalsyah T. M., Malahayati, Atikah, and Febriani. (2019) Purification and partial characterization of a thermo-halostable protease produced by *Geobacillus* sp. strain PLS A isolated from undersea fumaroles. Journal of Taibah University for Science 13:1, 850-857.

Jasilionis A., Kaupinis A., Ger M., Valius M., Chitavichius D. and Kuisiene N. (2012) Gene expression and activity analysis of the first thermophilic U32 peptidase. Central European Journal of Biology *7*:4, 587-595.

Jasilionis A. and Kuisiene N. (2015) Characterization of a novel thermostable oligopeptidase from *Geobacillus thermoleovorans* DSM 15325. Journal of Microbiology and Biotechnology 25:7, 1070-1083.

Kamal M., Höög J. O., Kaiser R., Shafqat J., Razzaki T., Zaidi Z. H., et al. (1995) Isolation, characterization and structure of subtilisin from a thermostable *Bacillus subtilis* isolate. FEBS Letters 374:3, 363-366.

Kaur I., Kocher G. S. and Gupta V. (2012) Molecular cloning and nucleotide sequence of the gene for an alkaline protease from *Bacillus circulans* MTCC 7906. Indian Journal of Microbiology 52:4, 630-637.

Kleiger G., Grothe R., Mallick P. and Eisenberg D. (2002) GXXXG and AXXXA: common α-helical interaction motifs in proteins, particularly in extremophiles. Biochemistry 41:19, 5990-5997.

Kobayashi T., Hakamada Y., Adachi S., Hitomi J., Yoshimatsu T., Koike K., et al. (1995) Purification and properties of an alkaline protease from alkalophilic *Bacillus* sp. KSM-K16. Applied Microbiology and Biotechnology 43:3, 473-481.

Kubo M. and Imanaka T. (1988) Cloning and nucleotide sequence of the highly thermostable neutral protease gene from *Bacillus stearothermophilus*. Microbiology 134:7, 1883-1892.

Kühn S. and Fortnagel P. (1993) Molecular cloning and nucleotide sequence of the gene encoding a calcium-dependent exoproteinase from *Bacillus megaterium* ATCC 14581. Microbiology 139:1, 39-47.

Kumar C. (2002) Purification and characterization of a thermostable alkaline protease from alkalophilic *Bacillus pumilus*. Letters in Applied Microbiology. 34:1, 13-17.

Kumar S., Tsai C. J. and Nussinov R. (2000) Factors enhancing protein thermostability. Protein Engineering 13:3, 179-191.

Ladbury J. E., Wynn R., Thomson J. A. and Sturtevant J. M. (1995) Substitution of charged residues into the hydrophobic core of *Escherichia coli* thioredoxin results in a change in heat capacity of the native protein. Biochemistry 34:7, 2148-2152.

Lee H. S., Kim Y. J., Bae S. S., Jeon J. H., Lim J. K., Kang S. G., et al. (2006) Overexpression and characterization of a carboxypeptidase from the hyperthermophilic archaeon *Thermococcus* sp. NA1. Bioscience, Biotechnology, and Biochemistry 70:5, 1140-1147.

Lee J. K., Kim Y. O., Kim H. K., Park Y. S. and Oh T. K. (1996) Purification and characterization of a thermostable alkaline protease from *Thermoactinomyces* sp. E79 and the DNA sequence of the encoding gene. Bioscience, Biotechnology, and Biochemistry 60:5, 840-846.

Lee S. H., Minagawa E., Taguchi H., Matsuzawa H., Ohta T., Kaminogawa S., et al. (1992) Purification and characterization of a thermostable carboxypeptidase (carboxypeptidase Taq) from *Thermus aquaticus* YT-1. Bioscience, Biotechnology, and Biochemistry 56:11, 1839-1844.

Li A. N. and Li D. C. (2009) Cloning, expression and characterization of the serine protease gene from *Chaetomium thermophilum*. Journal of Applied Microbiology 106:2, 369-380.

Liang H. K., Huang C. M., Ko M. T. and Hwang J. K. (2005) Amino acid coupling patterns in thermophilic proteins. Proteins 59:1, 58-63.

Maciver B., McHale R. H., Saul D. J. and Bergquist P. L. (1994) Cloning and sequencing of a serine

proteinase gene from a thermophilic *Bacillus* species and its expression in *Escherichia coli*. Applied and Environmental Microbiology 60:11, 3981-3988.

Marchler-Bauer A., Bo Y., Han L., He J., Lanczycki C. J., Lu S., et al. (2016) CDD/SPARCLE: functional classification of proteins via subfamily domain architectures. Nucleic Acids Research 45:D1, D200-D203.

Medrano F., Alonso J., Garcia J., Romero A., Bode W. and Gomis-Ruth F. (1998) Structure of proline iminopeptidase from *Xanthomonas campestris* pv. citri: a prototype for the prolyl oligopeptidase family. The EMBO Journal 17:1, 1-9.

Morya V. K., Yadav S., Kim E. K. and Yadav D. (2012) In silico characterization of alkaline proteases from different species of *Aspergillus*. Applied Biochemistry and Biotechnology 166:1, 243-257.

Motoshima H., Azuma N., Kaminogawa S., Ono M., Minagawa E., Matsuzawa H., et al. (1990) Molecular cloning and nucleotide sequence of the aminopeptidase T gene of *Thermus aquaticus* YT-1 and its high-level expression in *Escherichia coli*. Agricultural and biological chemistry 54:9, 2385-2392.

Munro G. K., McHale R. H., Saul D. J., Reeves R. A. and Bergquist P. L. (1995) A gene encoding a thermophilic alkaline serine proteinase from *Thermus* sp. strain Rt41A and its expression in *Escherichia coli*. Microbiology 141:7, 1731-1738.

Ohara-Nemoto Y., Rouf S. M., Naito M., Yanase A., Tetsuo F., Ono T., et al. (2014) Identification and characterization of prokaryotic dipeptidyl-peptidase 5 from *Porphyromonas gingivalis*. The Journal of Biological Chemistry 289:9, 5436-5448.

Pack S. P., Kang T. J. and Yoo Y. J. (2013) Protein thermostabilizing factors: high relative occurrence of amino acids, residual properties, and secondary structure type in different residual state. Applied Biochemistry and Biotechnology 171:5, 1212-1226.

Pack S. P. and Yoo Y. J. (2004) Protein thermostability: structure-based difference of amino acid between thermophilic and mesophilic proteins. Journal of Biotechnology 111:3, 269-277.

Panja A. S., Bandopadhyay, B. and Maiti, S. (2015) Protein thermostability is owing to their preferences to non-polar smaller volume amino acids, variations in residual physico-chemical properties and more salt-bridges. PLoS ONE 10:7, e0131495.

Patel S. (2017) A critical review on serine protease: key immune manipulator and pathology mediator. Allergologia et Immunopathologia 45:6, 579-591.

Pellegrini M., Marcotte E. M., Thompson M. J., Eisenberg D. and Yeates T. O. (1999) Assigning protein functions by comparative genome analysis: protein phylogenetic profiles. Proceedings of the National Academy of Sciences 96:8, 4285-4288.

Pombejra S. N., Jamklang M., Uhrig J. P., Vu K. and Gelli A. (2018) The structure-function analysis of the Mpr1 metalloprotease determinants of activity during migration of fungal cells across the blood-brain barrier. PLoS ONE 13:8, e0203020.

Ramadurai L., Lockwood K. J., Lockwood J., Nadakavukaren M. J. and Jayaswal R. K. (1999) Characterization of a chromosomally encoded glycylglycine endopeptidase of *Staphylococcus aureus*. Microbiology 145:4, 801-808.

Ramakrishnan V., Thambidurai Y., Rajasekharan S. K. and Mohanvel S. K. (2017) Partial characterization and cloning of protease from *Bacillus*. Asian Journal of Pharmaceutical and Clinical Research 10:10, 187-191.

Ran L. Y., Su H. N., Zhou M. Y., Wang L., Chen X. L., Xie B. B., et al. (2014) Characterization of a novel subtilisin-like protease myroicolsin from deep sea bacterium *Myroides profundi* D25 and molecular insight into its collagenolytic mechanism. The Journal of Biological Chemistry 289:9, 6041-6053.

Raveendran S., Parameswaran B., Beevi Ummalyma S., Abraham A., Kuruvilla Mathew A., Madhavan A., et al. (2018) Applications of microbial enzymes in food industry. Food Technology and Biotechnology 56:1, 16-30.

Rawlings N. D., Barrett A. J., Thomas P. D., Huang X., Bateman A. and Finn R.D. (2017) The MEROPS database of proteolytic enzymes, their substrates and inhibitors in 2017 and a comparison with peptidases in the PANTHER database. Nucleic Acids Research 46:D1, D624-D632.

Rawlings N. D., Morton F. R., Kok C. Y., Kong J. and Barrett A. J. (2007) MEROPS: the peptidase database. Nucleic Acids Research 36:suppl_1, D320-D325.

Razvi A. and Scholtz J. M. (2006) Lessons in stability from thermophilic proteins. Protein Science 15:7, 1569-1578.

Razzaq A., Shamsi S., Ali A., Ali Q., Sajjad M., Malik A. and Ashraf M. (2019) Microbial proteases applications. Frontiers in Bioengineering and Biotechnology 7:110.

Reddi R., Arya T., Kishor C., Gumpena R., Ganji R. J., Bhukya S., et al. (2014) Selective targeting of the conserved active site cysteine of *Mycobacterium tuberculosis* methionine aminopeptidase with electrophilic reagents. The FEBS Journal 281:18, 4240-4248.

Russell R. J., Hough D. W., Danson M. J. and Taylor G. L. (1994) The crystal structure of citrate synthase from the thermophilic archaeon, *Thermoplasma acidophilum*. Structure 2:12, 1157-1167.

Sadeghi M., Naderi-Manesh H., Zarrabi M. and Ranjbar B. (2006) Effective factors in thermostability of thermophilic proteins. Biophysical Chemistry 119:3, 256-270.

Salarizadeh N., Hasannia S., Akbari Noghabi K. and Hassan Sajedi R. (2014) Purification and characterization of 50 kDa extracellular metalloprotease from *Serratia* sp. ZF03. Iranian Journal of Biotechnology12:3, 18-27.

Saul D. J., Williams L. C., Toogood H. S., Daniel R. M. and Bergquist P. L. (1996) Sequence of the gene encoding a highly thermostable neutral proteinase from *Bacillus* sp. strain EA1: expression in *Escherichia coli* and characterisation. Biochimica et Biophysica Acta 1308:1, 74-80.

Savijoki K. and Palva A. (2000) Purification and molecular characterization of a tripeptidase (PepT) from *Lactobacillus helveticus*. Applied and Environmental Microbiology 66:2, 794-800.

Seo J. M., Ji G. E., Cho S. H., Park M. S. and Lee H. J. (2007) Characterization of a *Bifidobacterium longum* BORI dipeptidase belonging to the U34 family. Applied and Environmental Microbiology 73:17, 5598-5606.

Sharipova M., Balaban N., Kayumov A., Kirillova Y., Mardanova A., Gabdrakhmanova L., et al. (2008) The expression of the serine proteinase gene of *Bacillus intermedius* in *Bacillus subtilis*. Microbiological Research 163:1, 39-50.

Simossis V. A. and Heringa J. (2005) PRALINE: a multiple sequence alignment toolbox that integrates homology-extended and secondary structure information. Nucleic Acids Research 33:suppl_2, W289-W294.

Souza P. M. D., Bittencourt, M. L. D. A., Caprara, C. C., Freitas, M. D., Almeida, R. P. C. D., Silveira, D., et al. (2015) A biotechnology perspective of fungal proteases. Brazilian Journal of Microbiology 46:2, 337-346.

Szilágyi A. and Závodszky P. (2000) Structural differences between mesophilic, moderately thermophilic and extremely thermophilic protein subunits: results of a comprehensive survey. Structure 8:5, 493-504.

Takami H., Kobayashi T., Aono R. and Horikoshi K. (1992) Molecular cloning, nucleotide sequence and expression of the structural gene for a thermostable alkaline protease from *Bacillus* sp. no. AH-101. Applied Microbiology and Biotechnology 38:1, 101-108.

Tavano O. L., Berenguer-Murcia A., Secundo F. and Fernandez-Lafuente R. (2018) Biotechnological applications of proteases in food technology. Comprehensive Reviews in Food Science and Food Safety 17:2, 412-436.

Taylor T. J. and Vaisman I. I. (2010) Discrimination of thermophilic and mesophilic proteins. BMC Structural Biology10:1, S5.

Tekaia F., Yeramian E. and Dujon B. (2002) Amino acid composition of genomes, lifestyles of organisms, and evolutionary trends: a global picture with correspondence analysis. Gene 297:1-2, 51-60.

Tomazic S. J. and Klibanov A. M. (1988) Mechanisms of irreversible thermal inactivation of *Bacillus* alpha-amylases. Journal of Biological Chemistry 263:7, 3086-3091.

Tran L., Wu X. and Wong S. (1991) Cloning and expression of a novel protease gene encoding an extracellular neutral protease from *Bacillus subtilis*. Journal of Bacteriology 173:20, 6364-6372.

Tsuchiya K., Ikeda I., Tsuchiya T. and Kimura T. (1997) Cloning and expression of an intracellular alkaline protease gene from alkalophilic *Thermoactinomyces* sp. HS682. Bioscience, Biotechnology, and Biochemistry 61:2, 298-303.

Van den Burg B., Enequist H., Van der Haar M., Eijsink V., Stulp B. and Venema G. (1991) A highly thermostable neutral protease from *Bacillus caldolyticus*: cloning and expression of the gene in *Bacillus subtilis* and characterization of the gene product. Journal of Bacteriology 173:13, 4107-4115.

Vecerek B. and Kyslik P. (1995) Cloning and sequencing of the neutral protease-encoding gene from a thermophilic strain of *Bacillus* sp. Gene 158:1, 147-148.

Vogt G., Woell S. and Argos P. (1997) Protein thermal stability, hydrogen bonds, and ion pairs. Journal of Molecular Biology 269:4, 631-643.

Wakarchuk W. W., Sung W. L., Campbell R. L., Cunningham A., Watson D. C. and Yaguchi M. (1994) Thermostabilization of the *Bacillus circulans* xylanase by the introduction of disulfide bonds. Protein Engineering, Design and Selection 7:11, 1379-1386.

Walker N. D., McEwan N. R. and Wallace R. J. (2003) Cloning and functional expression of dipeptidyl peptidase IV from the ruminal bacterium *Prevotella albensis* M384T. Microbiology 149:8, 2227-2234.

Wang S. L., Wang C. Y. and Huang T. Y. (2008) Microbial reclamation of squid pen for the production of a novel extracellular serine protease by *Lactobacillus paracasei* subsp *paracasei* TKU012. Bioresource Technology 99:9, 3411-3417.

Wani A. H., Sharma M., Salwan R., Singh G., Chahota R. and Verma S. (2016) Cloning, expression, and functional characterization of serine protease Aprv2 from virulent isolate *Dichelobacter nodosus* of Indian origin. Applied Biochemistry and Biotechnology 180:3, 576-587.

Willard L., Ranjan A., Zhang H., Monzavi H., Boyko R. F., Sykes B. D., et al. (2003) VADAR: a web server for quantitative evaluation of protein structure quality. Nucleic Acids Research 31:13, 3316-3319.

Wu J., Bian Y., Tang B., Chen X., Shen P. and Peng Z. (2004) Cloning and analysis of WF146 protease, a novel thermophilic subtilisin-like protease with four inserted surface loops. FEMS Microbiology Letters 230:2, 251-258.

Xin Y., Sun Z., Chen Q., Wang J., Wang Y., Luogong L., et al. (2015) Purification and characterization of a novel extracellular thermostable alkaline protease from *Streptomyces* sp. M30. Journal of Microbiology and Biotechnology 25:11, 1944-1953.

Xu Z., Liu Y., Yang Y., Jiang W., Arnold E. and Ding J. (2003) Crystal structure of D-hydantoinase from *Burkholderia pickettii* at a resolution of 2.7 Angstroms: insights into the molecular basis of enzyme thermostability. Journal of Bacteriology 185:14, 4038-4049.

Yamagata Y. and Ichishima E. (1995) A new alkaline serine protease from alkalophilic *Bacillus* sp.: cloning, sequencing, and characterization of an intracellular protease. Current Microbiology 30:6, 357-366.

Zhang X., Chen S., Hu Z., Zhang L. and Wang H. (2009) Expression and characterization of two functional methionine aminopeptidases from *Mycobacterium tuberculosis* H37Rv. Current Microbiology 59:5, 520-525.

Zhou X. X., Wang Y. B., Pan Y. J. and Li W. F. (2008) Differences in amino acids composition and coupling patterns between mesophilic and thermophilic proteins. Amino Acids 34:1, 25-33.

Supplementary Materials:

Supplementary file 1

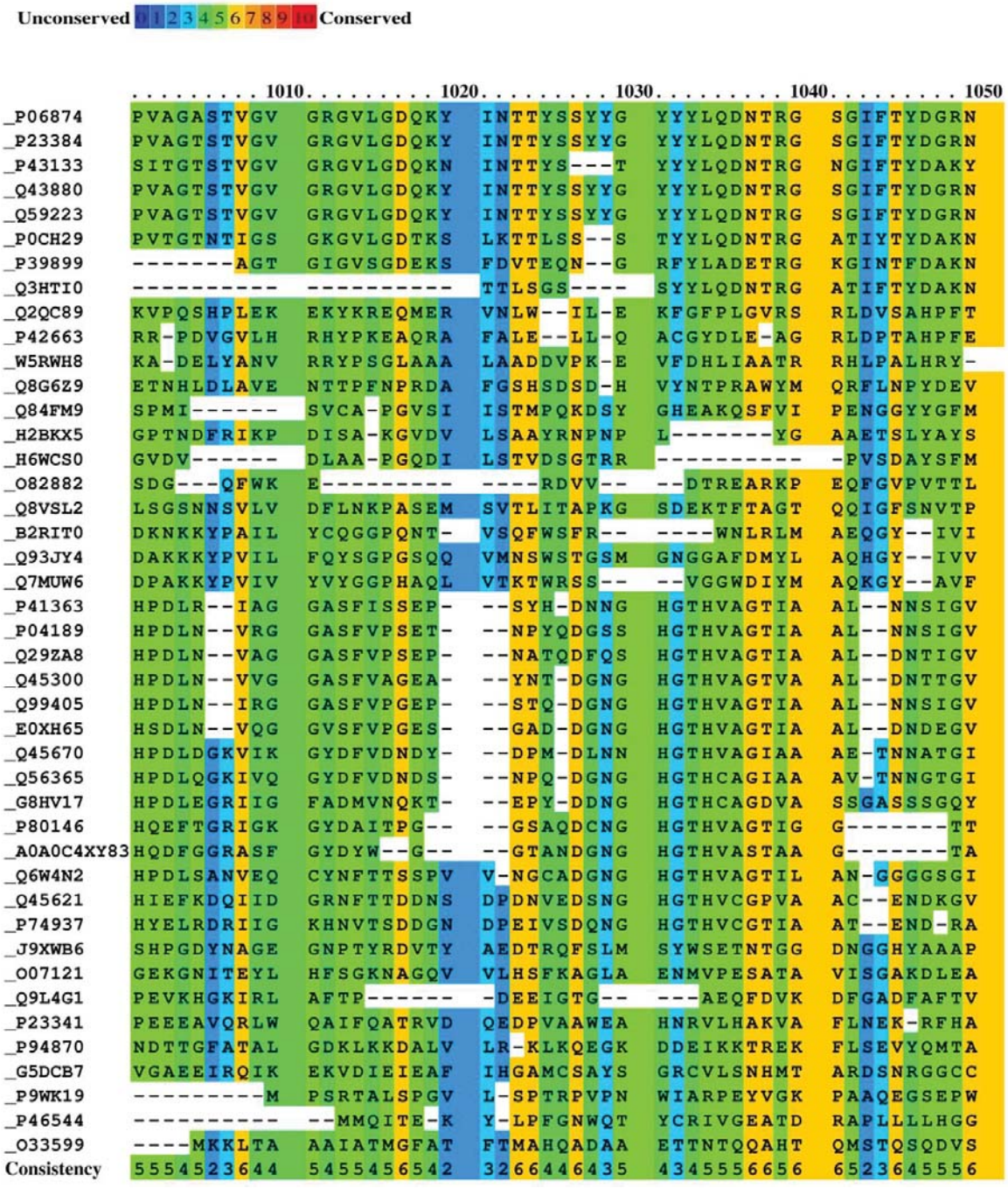

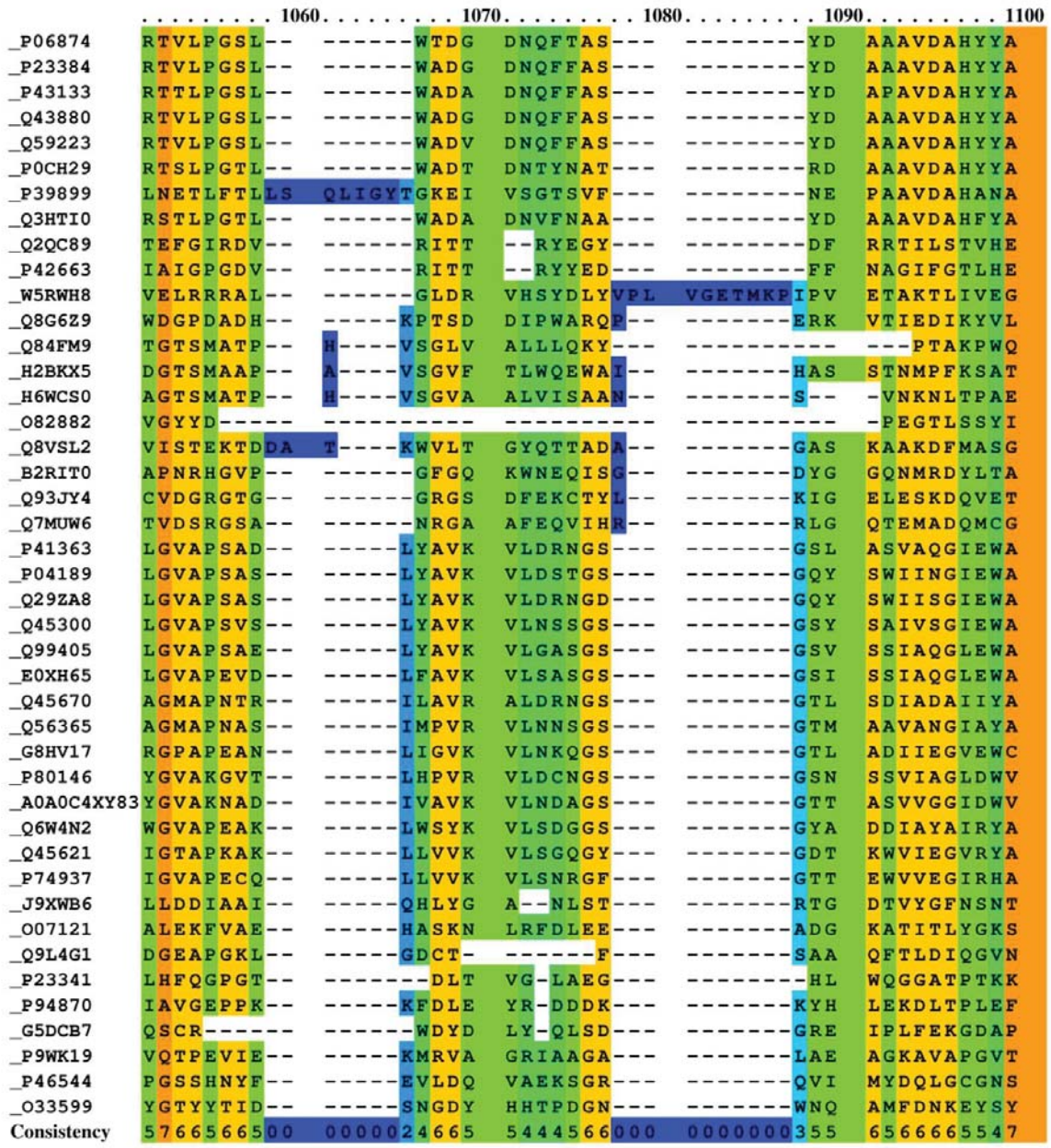
1060
1070
1080
1090
1100
_P06874 RTVLPGSL-- ------WTDG DNQFTAS--- --------YD AAAVDAHYYA
_P23384 RTVLPGSL-- ------WADG DNQFFAS--- --------YD AAAVDAHYYA
_P43133 RTTLPGSL-- ------WADA DNQFFAS--- --------YD APAVDAHYYA
_Q43880 RTVLPGSL-- ------WADG DNQFFAS--- --------YD AAAVDAHYYA
_Q59223 RTVLPGSL-- ------WADV DNQFFAS--- --------YD AAAVDAHYYA
_P0CH29 RTSLPGTL-- ------WADT DNTYNAT--- --------RD AAAVDAHYYA
_P39899 LNETLFTLLS QLIGYTGKEI VSGTSVF--- --------NE PAAVDAHANA
_Q3HTI0 RSTLPGTL-- ------WADA DNVFNAA--- --------YD AAAVDAHFYA
_Q2QC89 TEFGIRDV-- ------RITT --RYEGY--- --------DF RRTILSTVHE
_P42663 IAIGPGDV-- ------RITT --RYYED--- --------FF NAGIFGTLHE
_W5RWH8 VELRRRAL-- ------GLDR VHSYDLYVPL VGETMKPIPV ETAKTLIVEG
_Q8G6Z9 WDGPDADH-- -----KPTSD DIPWARQP-- -------ERK VTIEDIKYVL
_Q84FM9 TGTSMATP-- H----VSGLV ALLLQKY--- ---------- ---PTAKPWQ
_H2BKX5 DGTSMAAP-- A----VSGVF TLWQEWAI-- -------HAS STNMPFKSAT
_H6WCS0 AGTSMATP-- H----VSGVA ALVISAAN-- -------S-- -VNKNLTPAE
_O82882 VGYYD----- ---------- ---------- ---------- -PEGTLSSYI
_Q8VSL2 VISTEKTDDA T----KWVLT GYQTTADA-- -------GAS KAAKDFMASG
_B2RIT0 APNRHGVP-- ------GFGQ KWNEQISG-- -------DYG GQNMRDYLTA
_Q93JY4 CVDGRGTG-- ------GRGS DFEKCTYL-- -------KIG ELESKDQVET
_Q7MUW6 TVDSRGSA-- ------NRGA AFEQVIHR-- -------RLG QTEMADQMCG
_P41363 LGVAPSAD-- -----LYAVK VLDRNGS--- -------GSL ASVAQGIEWA
_P04189 LGVAPSAS-- -----LYAVK VLDSTGS--- -------GQY SWIINGIEWA
_Q29ZA8 LGVAPSAS-- -----LYAVK VLDRNGD--- -------GQY SWIISGIEWA
_Q45300 LGVAPSVS-- -----LYAVK VLNSSGS--- -------GSY SAIVSGIEWA
_Q99405 LGVAPSAE-- -----LYAVK VLGASGS--- -------GSV SSIAQGLEWA
_E0XH65 LGVAPEVD-- -----LFAVK VLSASGS--- -------GSI SSIAQGLEWA
_Q45670 AGMAPNTR-- -----ILAVR ALDRNGS--- -------GTL SDIADAIIYA
_Q56365 AGMAPNAS-- -----IMPVR VLNNSGS--- -------GTM AAVANGIAYA
_G8HV17 RGPAPEAN-- -----LIGVK VLNKQGS--- -------GTL ADIIEGVEWC
_P80146 YGVAKGVT-- -----LHPVR VLDCNGS--- -------GSN SSVIAGLDWV
_A0A0C4XY83 YGVAKNAD-- -----IVAVK VLNDAGS--- -------GTT ASVVGGIDWV
_Q6W4N2 WGVAPEAK-- -----LWSYK VLSDGGS--- -------GYA DDIAYAIRYA
_Q45621 IGTAPKAK-- -----LLVVK VLSGQGY--- -------GDT KWVIEGVRYA
_P74937 IGVAPECQ-- -----LLVVK VLSNRGF--- -------GTT EWVVEGIRHA
_J9XWB6 LLDDIAAI-- -----QHLYG A--NLST--- -------RTG DTVYGFNSNT
_O07121 ALEKFVAE-- -----HASKN LRFDLEE--- -------ADG KATITLYGKS
_Q9L4G1 DGEAPGKL-- -----GDCT- ------F--- -------SAA QFTLDIQGVN
_P23341 LHFQGPGT-- -------DLT VG-LAEG--- --------HL WQGGATPTKK
_P94870 IAVGEPPK-- -----KFDLE YR-DDDK--- -------KYH LEKDLTPLEF
_G5DCB7 QSCR------ ------WDYD LY-QLSD--- -------GRE IPLFEKGDAP
_P9WK19 VQTPEVIE-- -----KMRVA GRIAAGA--- -------LAE AGKAVAPGVT
_P46544 PGSSHNYF-- -----EVLDQ VAEKSGR--- -------QVI MYDQLGCGNS
_O33599 YGTYYTID-- -----SNGDY HHTPDGN--- -------WNQ AMFDNKEYSY
Consistency 5766566500 0000024665 5444566000 0000000355 6566665547

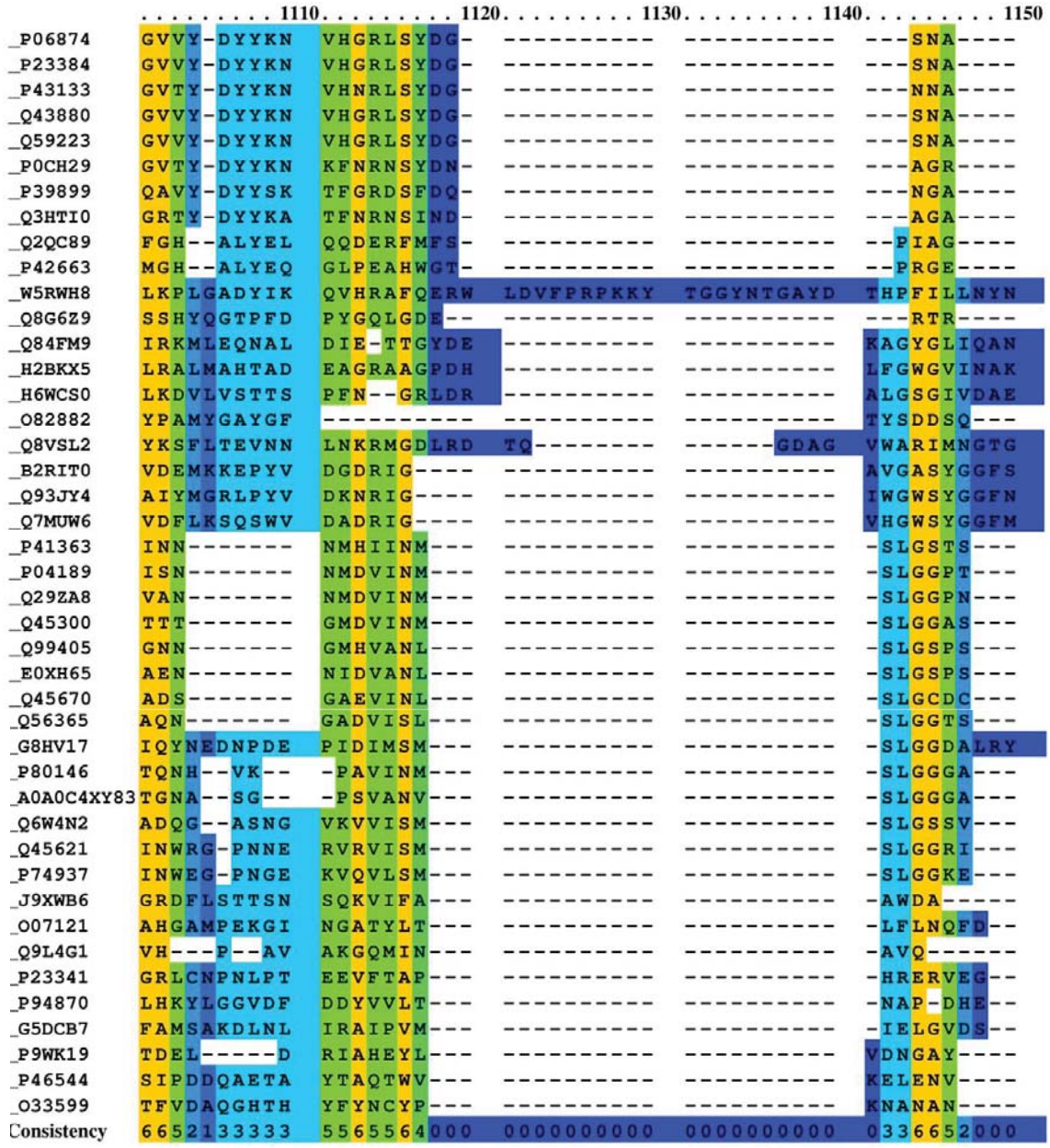
1110
1120
1130
1140
1150
_P06874 GVVY-DYYKN VHGRLSYDG- ---SNA----
_P23384 GVVY-DYYKN VHGRLSYDG- ---SNA----
_P43133 GVTY-DYYKN VHNRLSYDG- ---NNA----
_Q43880 GVVY-DYYKN VHGRLSYDG- ---SNA----
_Q59223 GVVY-DYYKN VHGRLSYDG- ---SNA----
_P0CH29 GVTY-DYYKN KFNRNSYDN- ---AGR----
_P39899 QAVY-DYYSK TFGRDSFDQ- ---NGA----
_Q3HTI0 GRTY-DYYKA TFNRNSIND- ---AGA----
_Q2QC89 FGH--ALYEL QQDERFMFS- --PIAG----
_P42663 MGH--ALYEQ GLPEAHWGT- --PRGE----
_W5RWH8 LKPLGADYIK QVHRAFQERW LDVFPRPKKY TGGYNTGAYD THPFILLNYN
_Q8G6Z9 SSHYQGTPFD PYGQLGDE-- ---RTR----
_Q84FM9 IRKMLEQNAL DIE-TTGYDE KAGYGLIQAN
_H2BKX5 LRALMAHTAD EAGRAAGPDH LFGWGVINAK
_H6WCS0 LKDVLVSTTS PFN--GRLDR ALGSGIVDAE
_O82882 YPAMYGAYGF TYSDDSQ---
_Q8VSL2 YKSFLTEVNN LNKRMGDLRD TQ------GDAG VWARIMNGTG
_B2RIT0 VDEMKKEPYV DGDRIG---- AVGASYGGFS
_Q93JY4 AIYMGRLPYV DKNRIG---- IWGWSYGGFN
_Q7MUW6 VDFLKSQSWV DADRIG---- VHGWSYGGFM
_P41363 INN------- NMHIINM--- -SLGSTS---
_P04189 ISN------- NMDVINM--- -SLGGPT---
_Q29ZA8 VAN------- NMDVINM--- -SLGGPN---
_Q45300 TTT------- GMDVINM--- -SLGGAS---
_Q99405 GNN------- GMHVANL--- -SLGSPS---
_E0XH65 AEN------- NIDVANL--- -SLGSPS---
_Q45670 ADS------- GAEVINL--- -SLGCDC---
_Q56365 AQN------- GADVISL--- -SLGGTS---
_G8HV17 IQYNEDNPDE PIDIMSM--- -SLGGDALRY
_P80146 TQNH--VK-- -PAVINM--- -SLGGGA---
_A0A0C4XY83 TGNA--SG-- -PSVANV--- -SLGGGA---
_Q6W4N2 ADQG--ASNG VKVVISM--- -SLGSSV---
_Q45621 INWRG-PNNE RVRVISM--- -SLGGRI---
_P74937 INWEG-PNGE KVQVLSM--- -SLGGKE---
_J9XWB6 GRDFLSTTSN SQKVIFA--- -AWDA-----
_O07121 AHGAMPEKGI NGATYLT--- -LFLNQFD--
_Q9L4G1 VH---P--AV AKGQMIN--- -AVQ------
_P23341 GRLCNPNLPT EEVFTAP--- -HRERVEG--
_P94870 LHKYLGGVDF DDYVVLT--- -NAP-DHE--
_G5DCB7 FAMSAKDLNL IRAIPVM--- -IELGVDS--
_P9WK19 TDEL-----D RIAHEYL--- VDNGAY----
_P46544 SIPDDQAETA YTAQTWV--- KELENV----
_O33599 TFVDAQGHTH YFYNCYP--- KNANAN----
Consistency 6652133333 5565564000 0000000000 0000000000 0336652000

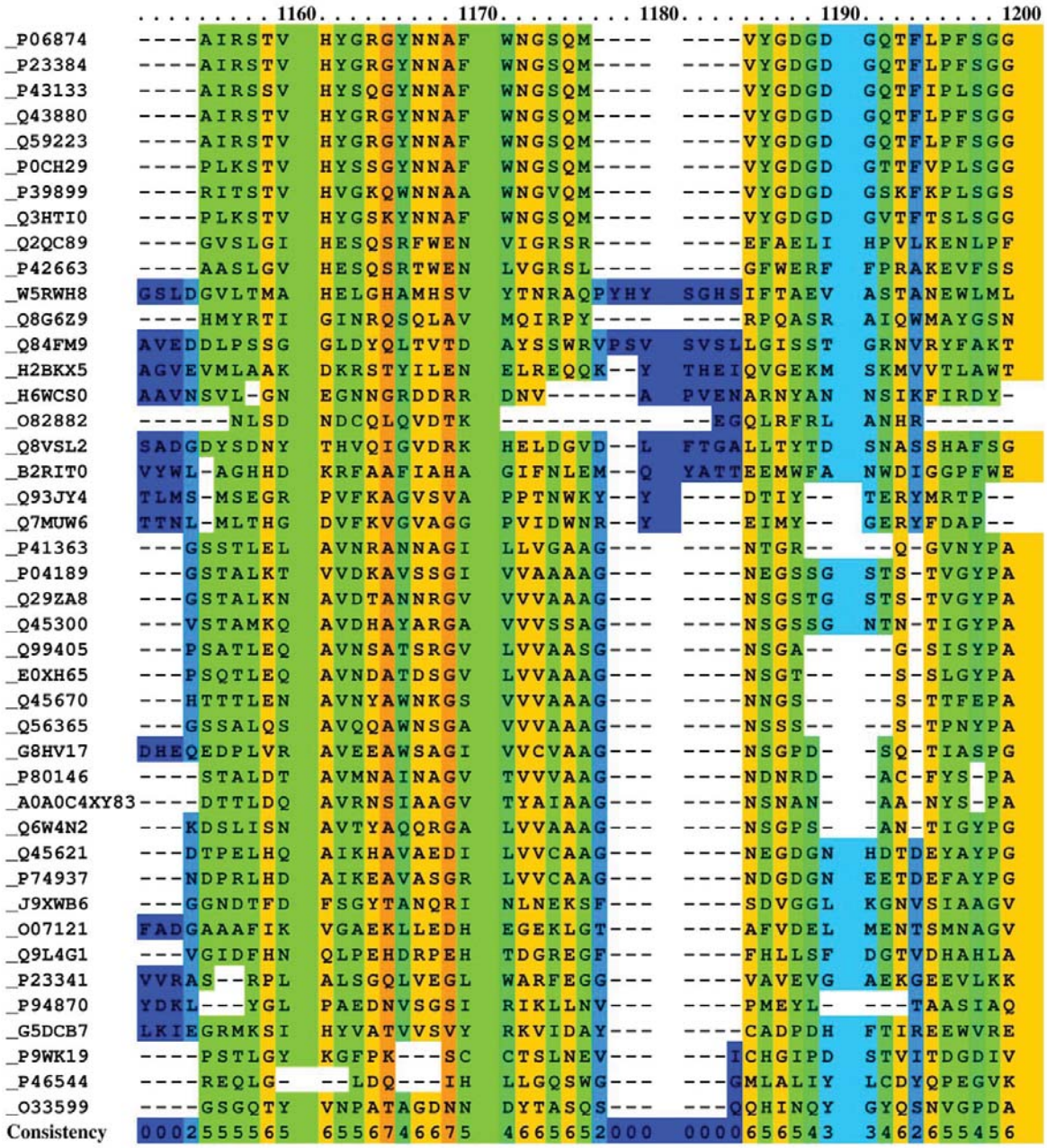
1160
1170
1180
1190
1200
_P06874 ----AIRSTV HYGRGYNNAF WNGSQM---- ----VYGDGD GQTFLPFSGG
_P23384 ----AIRSTV HYGRGYNNAF WNGSQM---- ----VYGDGD GQTFLPFSGG
_P43133 ----AIRSSV HYSQGYNNAF WNGSQM---- ----VYGDGD GQTFIPLSGG
_Q43880 ----AIRSTV HYGRGYNNAF WNGSQM---- ----VYGDGD GQTFLPFSGG
_Q59223 ----AIRSTV HYGRGYNNAF WNGSQM---- ----VYGDGD GQTFLPFSGG
_P0CH29 ----PLKSTV HYSSGYNNAF WNGSQM---- ----VYGDGD GTTFVPLSGG
_P39899 ----RITSTV HVGKQWNNAA WNGVQM---- ----VYGDGD GSKFKPLSGS
_Q3HTI0 ----PLKSTV HYGSKYNNAF WNGSQM---- ----VYGDGD GVTFTSLSGG
_Q2QC89 ----GVSLGI HESQSRFWEN VIGRSR---- ----EFAELI HPVLKENLPF
_P42663 ----AASLGV HESQSRTWEN LVGRSL---- ----GFWERF FPRAKEVFSS
_W5RWH8 GSLDGVLTMA HELGHAMHSV YTNRAQPYHY SGHSIFTAEV ASTANEWLML
_Q8G6Z9 ----HMYRTI GINRQSQLAV MQIRPY---- ----RPQASR AIQWMAYGSN
_Q84FM9 AVEDDLPSSG GLDYQLTVTD AYSSWRVPSV SVSLLGISST GRNVRYFAKT
_H2BKX5 AGVEVMLAAK DKRSTYILEN ELREQQK--Y THEIQVGEKM SKMVVTLAWT
_H6WCS0 AAVNSVL-GN EGNNGRDDRR DNV------A PVENARNYAN NSIKFIRDY-
_O82882 ------NLSD NDCQLQVDTK ---------- --EGQLRFRL ANHR------
_Q8VSL2 SADGDYSDNY THVQIGVDRK HELDGVD--L FTGALLTYTD SNASSHAFSG
_B2RIT0 VYWL-AGHHD KRFAAFIAHA GIFNLEM--Q YATTEEMWFA NWDIGGPFWE
_Q93JY4 TLMS-MSEGR PVFKAGVSVA PPTNWKY--Y ----DTIY-- TERYMRTP--
_Q7MUW6 TTNL-MLTHG DVFKVGVAGG PVIDWNR--Y ----EIMY-- GERYFDAP--
_P41363 ---GSSTLEL AVNRANNAGI LLVGAAG--- ----NTGR-- --Q-GVNYPA
_P04189 ---GSTALKT VVDKAVSSGI VVAAAAG--- ----NEGSSG STS-TVGYPA
_Q29ZA8 ---GSTALKN AVDTANNRGV VVVAAAG--- ----NSGSTG STS-TVGYPA
_Q45300 ---VSTAMKQ AVDHAYARGA VVVSSAG--- ----NSGSSG NTN-TIGYPA
_Q99405 ---PSATLEQ AVNSATSRGV LVVAASG--- ----NSGA-- --G-SISYPA
_E0XH65 ---PSQTLEQ AVNDATDSGV LVVAAAG--- ----NSGT-- --S-SLGYPA
_Q45670 ---HTTTLEN AVNYAWNKGS VVVAAAG--- ----NNGS-- --S-TTFEPA
_Q56365 ---GSSALQS AVQQAWNSGA VVVAAAG--- ----NSSS-- --S-TPNYPA
_G8HV17 DHEQEDPLVR AVEEAWSAGI VVCVAAG--- ----NSGPD- -SQ-TIASPG
_P80146 ----STALDT AVMNAINAGV TVVVAAG--- ----NDNRD- -AC-FYS-PA
_A0A0C4XY83 ----DTTLDQ AVRNSIAAGV TYAIAAG--- ----NSNAN- -AA-NYS-PA
_Q6W4N2 ---KDSLISN AVTYAQQRGA LVVAAAG--- ----NSGPS- -AN-TIGYPG
_Q45621 ---DTPELHQ AIKHAVAEDI LVVCAAG--- ----NEGDGN HDTDEYAYPG
_P74937 ---NDPRLHD AIKEAVASGR LVVCAAG--- ----NDGDGN EETDEFAYPG
_J9XWB6 ---GGNDTFD FSGYTANQRI NLNEKSF--- ----SDVGGL KGNVSIAAGV
_O07121 FADGAAAFIK VGAEKLLEDH EGEKLGT--- ----AFVDEL MENTSMNAGV
_Q9L4G1 ---VGIDFHN QLPEHDRPEH TDGREGF--- ----FHLLSF DGTVDHAHLA
_P23341 VVRAS--RPL ALSGQLVEGL WARFEGG--- ----VAVEVG AEKGEEVLKK
_P94870 YDKL---YGL PAEDNVSGSI RIKLLNV--- ----PMEYL- ---TAASIAQ
_G5DCB7 LKIEGRMKSI HYVATVVSVY RKVIDAY--- ----CADPDH FTIREEWVRE
_P9WK19 ----PSTLGY KGFPK---SC CTSLNEV--- ---ICHGIPD STVITDGDIV
_P46544 ----REQLG- --LDQ---IH LLGQSWG--- ---GMLALIY LCDYQPEGVK
_O33599 ----GSGQTY VNPATAGDNN DYTASQS--- ---QQHINQY GYQSNVGPDA
Consistency 0002555565 6556746675 4665652000 0000656543 3462655456

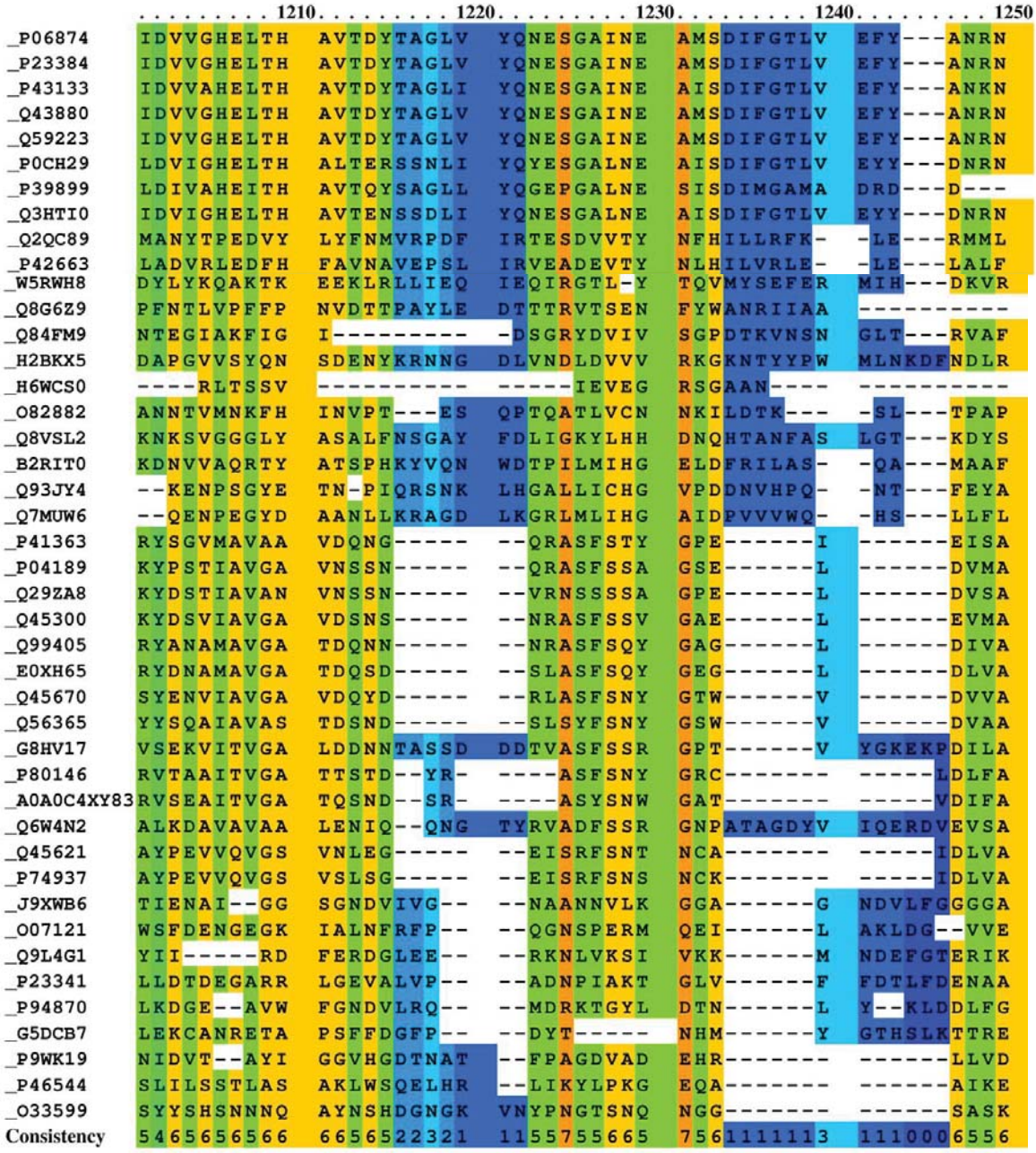
1210
1220
1230
1240
1250
_P06874 IDVVGHELTH AVTDYTAGLV YQNESGAINE AMSDIFGTLV EFY---ANRN
_P23384 IDVVGHELTH AVTDYTAGLV YQNESGAINE AMSDIFGTLV EFY---ANRN
_P43133 IDVVAHELTH AVTDYTAGLI YQNESGAINE AISDIFGTLV EFY---ANKN
_Q43880 IDVVGHELTH AVTDYTAGLV YQNESGAINE AMSDIFGTLV EFY---ANRN
_Q59223 IDVVGHELTH AVTDYTAGLV YQNESGAINE AMSDIFGTLV EFY---ANRN
_P0CH29 LDVIGHELTH ALTERSSNLI YQYESGALNE AISDIFGTLV EYY---DNRN
_P39899 LDIVAHEITH AVTQYSAGLL YQGEPGALNE SISDIMGAMA DRD---D---
_Q3HTI0 IDVIGHELTH AVTENSSDLI YQNESGALNE AISDIFGTLV EYY---DNRN
_Q2QC89 MANYTPEDVY LYFNMVRPDF IRTESDVVTY NFHILLRFK- -LE---RMML
_P42663 LADVRLEDFH FAVNAVEPSL IRVEADEVTY NLHILVRLE- -LE---LALF
_W5RWH8 DYLYKQAKTK EEKLRLLIEQ IEQIRGTL-Y TQVMYSEFER MIH---DKVR
_Q8G6Z9 PFNTLVPFFP NVDTTPAYLE DTTTRVTSEN FYWANRIIAA ----------
_Q84FM9 NTEGIAKFIG I--------- -DSGRYDVIV SGPDTKVNSN GLT---RVAF
_H2BKX5 DAPGVVSYQN SDENYKRNNG DLVNDLDVVV RKGKNTYYPW MLNKDFNDLR
_H6WCS0 ----RLTSSV ---------- -----IEVEG RSGAAN---- ----------
_O82882 ANNTVMNKFH INVPT---ES QPTQATLVCN NKILDTK--- -SL---TPAP
_Q8VSL2 KNKSVGGGLY ASALFNSGAY FDLIGKYLHH DNQHTANFAS LGT---KDYS
_B2RIT0 KDNVVAQRTY ATSPHKYVQN WDTPILMIHG ELDFRILAS- -QA---MAAF
_Q93JY4 --KENPSGYE TN-PIQRSNK LHGALLICHG VPDDNVHPQ- -NT---FEYA
_Q7MUW6 --QENPEGYD AANLLKRAGD LKGRLMLIHG AIDPVVVWQ- -HS---LLFL
_P41363 RYSGVMAVAA VDQNG----- --QRASFSTY GPE------I ------EISA
_P04189 KYPSTIAVGA VNSSN----- --QRASFSSA GSE------L ------DVMA
_Q29ZA8 KYDSTIAVAN VNSSN----- --VRNSSSSA GPE------L ------DVSA
_Q45300 KYDSVIAVGA VDSNS----- --NRASFSSV GAE------L ------EVMA
_Q99405 RYANAMAVGA TDQNN----- --NRASFSQY GAG------L ------DIVA
_E0XH65 RYDNAMAVGA TDQSD----- --SLASFSQY GEG------L ------DLVA
_Q45670 SYENVIAVGA VDQYD----- --RLASFSNY GTW------V ------DVVA
_Q56365 YYSQAIAVAS TDSND----- --SLSYFSNY GSW------V ------DVAA
_G8HV17 VSEKVITVGA LDDNNTASSD DDTVASFSSR GPT------V YGKEKPDILA
_P80146 RVTAAITVGA TTSTD--YR- ----ASFSNY GRC------- -----LDLFA
_A0A0C4XY83 RVSEAITVGA TQSND--SR- ----ASYSNW GAT------- -----VDIFA
_Q6W4N2 ALKDAVAVAA LENIQ--QNG TYRVADFSSR GNPATAGDYV IQERDVEVSA
_Q45621 AYPEVVQVGS VNLEG----- --EISRFSNT NCA------- -----IDLVA
_P74937 AYPEVVQVGS VSLSG----- --EISRFSNS NCK------- -----IDLVA
_J9XWB6 TIENAI--GG SGNDVIVG-- --NAANNVLK GGA------G NDVLFGGGGA
_O07121 WSFDENGEGK IALNFRFP-- --QGNSPERM QEI------L AKLDG--VVE
_Q9L4G1 YII-----RD FERDGLEE-- --RKNLVKSI VKK------M NDEFGTERIK
_P23341 LLDTDEGARR LGEVALVP-- --ADNPIAKT GLV------F FDTLFDENAA
_P94870 LKDGE--AVW FGNDVLRQ-- --MDRKTGYL DTN------L Y--KLDDLFG
_G5DCB7 LEKCANRETA PSFFDGFP-- --DYT----- NHM------Y GTHSLKTTRE
_P9WK19 NIDVT--AYI GGVHGDTNAT --FPAGDVAD EHR------- ------LLVD
_P46544 SLILSSTLAS AKLWSQELHR --LIKYLPKG EQA------- ------AIKE
_O33599 SYYSHSNNNQ AYNSHDGNGK VNYPNGTSNQ NGG------- ------SASK
Consistency 5465656566 6656522321 1155755665 7561111113 1110006556

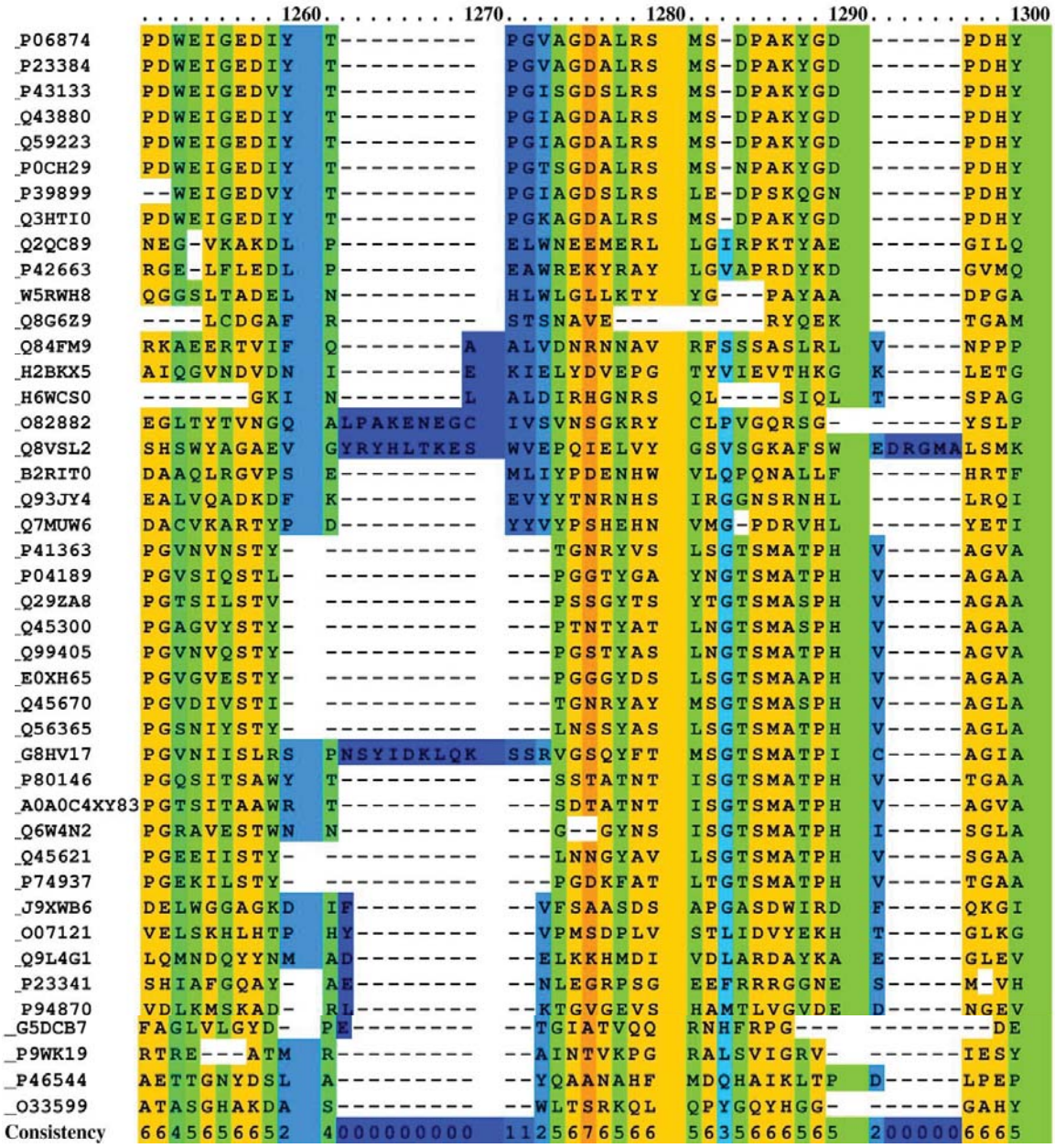

Multiple sequence alignment of the thermostable proteolytic enzymes. More conserved parts of the alignment have been presented from amino acid residues from 1000 to 1300

Journal of Cell and Molecular Research (2020) 11 (2), 82-89 DOI: 10.22067/jcmr.v11i2.85426

Research Article

Evaluation of IFN-γ and T-bet Expression Levels as Possible Molecular Markers of Schizophrenia

Roghaye Lorestani[1], Sohrab Boozarpour[1*], Sakineh Alijanpour[1], Leila Ahangar[2]

[1]*Department of Biology, Faculty of Basic Sciences, Gonbad kavous University, Gonbad kavous, Golestan, Iran*
[2]*Department of Plant Production, Collage of Agriculture Science and Natural Resource, Gonbad kavous University, Gonbad kavous, Golestan, Iran*

Received 12 February 2020 Accepted 2 March 2020

Abstract

Schizophrenia is an irritating mental disorder that affects around 1% of the world's population. The immune system contributes to the onset of the disease, particularly through production and secretion of some cytokines. In patients with schizophrenia, the balance of Th1 to Th2 ratio is often altered. In the present study, we investigated these changes by measuring the gene expression levels of IFN-γ and T-bet as Th1 indicators, as well as IL-4 and GATA-3 as representatives for Th2. Blood samples of schizophrenic patients (n=25) and healthy individuals (n=10) were obtained. Total RNA was extracted from leukocytes and cDNA synthesis was performed based on provided protocols. Real-time PCR technique was utilized for the assessment of gene expression levels. Results indicated a significant increase in the expression of IFN-γ and its transcription factor, T-bet, while IL-4 gene expression was reduced significantly. The expression level of GATA-3 gene revealed no meaningful changes. Altogether, results confirmed the relative shift of Th1 to Th2 status in the patient with schizophrenia and re-emphasize the importance of the inflammatory events in the incidence of the disease. Moreover, a new index was introduced based on the IFN-γ and T-bet genes expression, which can determine healthy condition with total accuracy of 79%.

***Keywords*:** Molecular marker, Schizophrenia, Th1, Th2, IFN-γ, T-bet

Introduction

Schizophrenia is a disturbance in the executive and sensory functions of the central nervous system (Ajami et al., 2014), which affects about one percent of the world's population (Rajasekaran et al., 2016). The onset of the disease usually occurs in late adolescence or early adulthood with a wide range of symptoms, including hallucinations, delusions, affective disorders and cognitive impairments (Srinivasan et al., 2016).

A substantial genetic contribution was demonstrated for familial cases of schizophrenia (Ayalew et al., 2012). Previous investigations were reported 41 to 65 percent risk of schizophrenia for monozygotic twins who have an affected brother or sister and 28 percent risk of disease for children with affected parents (Cardno and Gottesman, 2000). It has been illustrated that schizophrenia is a very complex genetic disorder and various genes are involved in its pathogenesis (Kumar et al., 2019). Some immune system disorders, such as infections and autoimmune inflammatory diseases could be considered as other risk factors (Benros and Mortensen, 2020; Benros et al., 2011; Eaton et al., 2006), which explain the impact of immune system imbalance on the pathology of the disease. Furthermore, it was evidenced that different types of cytokines play significant roles in the stimulation, production, and secretion of neurodegenerative modulators (Chang and Bistrian, 1998; Sonti et al., 1996). In various psychiatric disorders such as schizophrenia, changes in the balance of cytokine regulations can disrupt the balance of T-helper 1 (Th1) to T-helper 2 (Th2) cells (Macedo, 2019; Potvin et al., 2008).

Some cytokines play a role in the differentiation of T helper cells from $CD4^+$T cells. Interferon gamma (IFN-γ) is the major cytokine that mediates the differentiation of $CD4^+$T cells into Th1 ones (Lazarevic et al., 2013); and, simultaneously, prevents their differentiation into Th2 cells. In contrast, IL-4 promotes the differentiation of naive $CD4^+$T cells into Th2 cells (Dai et al., 2009; Myles et al., 2017). So, IFN-γ and IL-4 are Th1 and Th2

*Corresponding author's e-mail address: so.boozarpour@gmail.com

specific cytokines, respectively (Annunziato et al., 1999; Katsikis et al., 1995). While, they are not suitable candidates for assessment of Th2 to Th1 ratio, since some other cells also produce and release them (Chakir et al., 2003).

T-bet is one of the main regulatory transcription factors which mediates the differentiation of $CD4^+$T cells to Th1 subset (Tullius et al., 2014). Also, it is a direct inhibitor of the GATA-3 gene expression (Kanhere et al., 2012). In turn, GATA-3 stimulates the differentiation of naïve $CD4^+$T cells into Th2 cells and prevents the differentiation of these cells to Th1 clones through the inhibition of STAT4 and T-bet. Considering the fact that T-bet and GATA-3 act as upstream factors for IFN-γ and IL-4 cytokine production, respectively (Wang et al., 2010), their expression levels were also investigated for accurate measurement of Th1 to Th2 ratio in schizophrenic patients.

Materials and Methods

Blood sample collection and RNA isolation

A total of 25 blood samples were obtained from 20 male and 5 female patients, diagnosed for schizophrenia according to the clinical interview, in the ages of 22 to 57. 10 healthy samples were also taken as controls. EDTA[1] was applied to prevent clotting of the samples. Leukocytes were obtained following the rupturing of red blood cells (RBCs). Therefore, 10 ml RBC lysis buffer (pH= 7.5) was added to 5 ml blood, after centrifuge at 5000 rpm for 20 min, pellet was isolated. For purifying leukocytes, the washing procedure was repeated twice. Total RNA extraction was carried out for leukocytes via Tripure reagent (Roche, Germany) according to standard protocols provided by the manufacturers. Then, quantitative and qualitative features of RNA samples were evaluated using nanodrop device, Picodrop. Also, the integrity of RNA samples was evaluated by agarose gel electrophoresis. In the following step, DNase I treatment (Sinaclon, Iran) performed based on the manufacturer's instructions, to ensure the elimination of genomic DNA.

Synthesis of cDNA and quantitative real-time PCR

A mixture of oligo (dT) and random hexamers was utilized for the synthesis of cDNA by the application of PrimScript™ RT reagent kit (TAKARA, Japan). Samples were diluted 25 folds before further applications. For assessment of IFN-γ, IL-4, T-bet and GATA-3 genes expression, specific primers were designed using GeneRunner and Primer-BLAST online software (Table 1). Gene expression experiments were performed via the Step One Plus Real-time PCR ™ device and Premix Ex Taq™ II SYBR reagent (TAKARA, Japan). The final volume of each reaction was 15 µl containing 7.2 µl of SYBR Premix Taq II (2X) (TAKARA, Japan), 0.3 µl ROX (50X), 3 pmol of each primer and 2 µl (diluted) of desired cDNA sample. DNA amplification performed using the following program: initial denaturation for 30 s, followed by 40 PCR cycles consisting of 95°C for 5 s, annealing and extension at 60°C for 30 s.

Statistical analyses

Relative gene expression levels were calculated through $2^{-\Delta Ct}$ (formula 1) (Schmittgen and Livak, 2008). Finally, data analysis was performed by Excel and R, using logistic regression.

Formula 1:

ΔCt Healthy= mean (Ct target-Ct control)

ΔCt Patient=mean (Ct target-Ct control)

Ratio= $2^{-\Delta Ct}$ Patient/ $2^{-\Delta Ct}$ Healthy

Considering the relationship of IFN-γ and T-bet gene expressions, Index 1 was introduced for different ratios of gene expression; and their differences were evaluated for patients versus healthy subjects.

$$\text{Index 1} = \frac{\text{IFN}\gamma + \text{Tbet}}{\text{IFN}\gamma - \text{Tbet}}$$

The strength and ability of the index were evaluated using logistic regression. The frequency of predicted classes versus observed ones was evaluated for model performance evaluations in the separation of dependent variable classes.

To predict the status of different individuals based on the model, predicted values were classified based on the default value of critical probability, which is equal to 0.5. The logistic regression model was evaluated based on different criteria including classification accuracy, classification specificity, classification sensitivity, and performance. Furthermore, the predictive power of the model was evaluated using the criterion of the area below ROC (Receiver Operating Characteristic) Curve (Hosmer et al., 2013; Metz, 1978).

[1] Ethylene diamine tetraacetic acid

Table 1. Sequences and characteristics of primer pairs which were applied for Real-time PCR experiments

Product length	Sequence	Accession number NCBI	Genes
136 bp	F:5'-GAATTGGAAAGAGGAGAGTGACAGA-3'	NG_015840.1	*IFN-γ*
	R:5'- GACATTCATGTCTTCCTTGATGGTC-3'		
130 bp	F:5'-GCTGCCTCCAAGAACACAACTG-3'	NG_023252.1	*IL-4*
	R:5'- TGTGCCTGTGGAACTGCTGTG -3'		
141 bp	F:5'- GACGGCGGATGTTCCCATT-3'	NG_012166.1	*T-bet*
	R:5'- TGTGCCTGTGGAACTGCTGTG -3'		
136 bp	F:5'- TCATTAAGCCCAAGCGAAGG -3'	NG_015859.1	*GATA3*
	R:5'-GTCCCCATTGGCATTCCTC-3'		
123 bp	F:5'- GTGAACCATGAGAAGTATGACAAC-3'	NG_007073.2	*GAPDH*
	R:5'- CATGAGTCCTTCCACGATACC-3'		

The criteria of the model performance were reliable while they were calculating based on new data which were not used in the fitted model. In the present study, the "leave-one-out" method was applied for validation of the regression model.

Results

Ratio of optical absorbance of RNA samples at 260/280 wavelengths was about 1.9 and agarose gel electrophoresis showed the integrity of RNAs with desirable quality. Comparative gene expression analysis between patient and healthy individuals represented increment in IFN-γ (*p*-value = 0.068) and T-bet (*p*-value = 0.007) expression levels. While, no significant changes observed in GATA-3 (*p*-value > 0.05) expression. The expression of IL-4 was not evidenced here.

Index 1, which shows combined effects of IFN-γ and T-bet genes in the frame of a numerical ratio, was significantly different between healthy and disease conditions, when it was evaluated based on the Mann-Whitney test (*p*-value = 0.015). Descriptive statistics of index 1 are presented in table 2.

Table 2. Descriptive statistics of index 1

	Mean	Min	Max
Healthy	1	-1.3	6.2
Schizophrenic cases	-2.8	-27	2

In the present study, IFN-γ, T-bet and index1 were introduced as independent variables which entered into the logistic regression model. Parameter estimates, odd ratios and statistical significance of regression coefficients are presented in table 3.

The regression equation is:

$$\mathrm{Log}\left(\frac{\mathrm{p}}{1-\mathrm{p}}\right) = 1.363 + 3.311(\mathrm{IFN}\gamma) - 0.68(\mathrm{Tbet}) - 0.832(\mathrm{index})$$

According to table 3, IFN-γ, T-bet and index 1 explain a significant amount of variations in the probability of healthy status. Although, IFN-γ gene and intercept were not significant according to Wald test, these variables were significant based on likelihood ratio test (*p*-value = 0.02) and the corresponding model with these variables showed a lower AIC (Akaike information criterion) than the reduced model.

Table 3. Parameter estimates, odd ratios and statistical significance of regression coefficients

Variables in model	Coefficient	Standard deviation	Odds ratio	*p*-value
Intercept	1.363	0.764	3.908	0.065
IFN-γ	3.311	2.311	27.417	0.068
T-bet	-0.68	0.383	0.506	0.007
Index1	-0.832	0.372	0.435	0.001

It was estimated that for every one-unit increase in the introduced index, the odds ratio is reduced to 0.43.

Table 4. Logistic regression model evaluation using leave-one-out validation method.

Accuracy classification	Classification feature	Sensitivity classification	Area under the ROC curve	R2Nagelkerke
0.79	0.25	1	0.76	0.19

According to the classification table which was obtained from the validation test (Table 4), the overall accuracy of the model was 79%. The area under the ROC curve was 76% and the pseudo-R2 value was 19%. These are indicatives of a fairly good prediction of the fitted model. Therefore, the introduced index in the present study, not only indicates a statistically significant difference at the confidence level of 5% (Mann-Whitney test) but also, it has a good classification capability for the diagnosis of patients with schizophrenia.

Discussion

Inflammatory events of the central and peripheral nervous systems are important determinants of various stages of schizophrenia (Khandaker et al., 2015). Perhaps, it can render acceptable molecular markers through deep monitoring of the immune system's performances in schizophrenic patients.

The immune system plays a significant function in the incidence, pathogenesis and treatment of mental illnesses (Rosenblat, 2019; Tomasik et al., 2016), in a cytokine-mediated manner (Chang and Bistrian, 1998; Sonti et al., 1996). The association of immune encountered genes' polymorphisms, especially for *IFN-γ*, *TNF-α*, *IL-4* and *IL-10* genes with the incidence of schizophrenia has been reported (Noto et al., 2015; Na and Kim, 2007). Also, modifications in the expression levels of several immune-related genes have been reported in schizophrenic patients (Chan et al., 2011; He et al., 2020; Kim et al., 2004; Momtazmanesh et al., 2019; Potvin et al., 2008). According to the "equilibrium hypothesis", there is a balance in the ratio of Th1 to Th2 cells in healthy individuals (Kidd, 2003). This equilibrium lost its balanced status during various psychiatric disorders (Solek et al., 2018; Cox et al., 2015; de Witte et al., 2014). It was demonstrated that in schizophrenic patients, serum expression levels of *IFN-γ* and *IL-4*, as an indicator of Th1 to Th2 ratio, increased in comparison to control cases (Kim et al., 2004). Moreover, the higher activity of Th1 cells is associated with the reduced activity and less production of IL-4 and IL-10, as the representatives of Th2 cells' activity (Mansur et al., 2012).

In the present study, the gene expression profile of schizophrenic patients regarding their cytokine balance was investigated. So, IFN-γ and IL-4 were selected as the main cytokines of Th1 and Th2 cells, respectively. The expression of *T-bet* and *GATA-3* transcription factors were also evaluated. Results indicated a significant increase in the activity of Th1 cells in comparison to Th2 population, which means that in patients with schizophrenia, inflammatory events are increased prominently (Kelsven et al., 2020). Several factors, such as severe infection, autoimmune disorders and high smoking rates can lead to genetic changes, especially in case of schizophrenia, which clarifies more than ever the function of inflammatory events in this disease (Shi et al., 2009; Stolz et al., 2019). Likewise, the therapeutic effects of anti-inflammatory drugs and genetic, biochemical and immunological findings indicate the important role of inflammation in schizophrenia (Muller et al., 2015; Upthegrove and Khandaker, 2020).

An important step in providing appropriate treatment strategies is to identify molecular biomarkers that can be applied for early detection or prediction of schizophrenia (Liu et al., 2017; Trovao et al., 2019; Vatankhah et al., 2019). Although the use of post-mortem brain biopsies provides an opportunity for direct work on patient's neurons, this is not an ideal method, for reasons such as reduced mRNA integrity, and consequently reduced credibility and usefulness of biomarkers (Modai and Shomron, 2016). On the other hand, neurological-based assessments are costly (Kahn and Sommer, 2015). Thus, in recent years, the search for blood sample-based biomarkers of schizophrenia has been considered as a valid alternative (Bahn and Chan, 2015; He et al., 2019; Tasic et al., 2019). These biomarkers were classified into different categories and were discovered through various approaches (Lai et al., 2016). Although a variety of blood markers were examined and introduced, more than 70% of these markers for schizophrenia are playing a role during inflammatory responses (Chan et al., 2011). It should be noted that only a small number of previous studies have been identified the sensitivity and specificity of their introduced markers (Al Awam et al., 2015; Sun et al., 2015; Li et al., 2012).

The significance of the present study is its ability for prediction of the disease condition using a logistic regression based on the measurement of candidate cytokines. Although our index is weak to identify normal individuals, which may be due to the small sample size and some other factors that affect the immune system. It could be promising to introduce a novel indicator for screening of schizophrenic patients with high accuracy. However, we are aware that there should be certainly more additional tests for better confirmation of the results. Nevertheless, it is the first study of its kind in Iran.

Acknowledgements
We would like to express our sincere appreciation to Dr. Shaaban Ghalandarayeshi (Gonbad Kavous University), for carrying out statistical analyses and introducing indices.

Conflict of Interest
The authors report no conflicts of interest in this work.

References

Ajami A., Abedian F., Hosseini S. H., Akbarian E., Alizadeh-Navaei R. and Taghipour M. (2014) Serum TNF-α, IL-10 and IL-2 in Schizophrenic Patients Before and After Treatment with Risperidone and Clozapine. Iranian Journal of Immunology 11:200-209.

Al Awam K., Haussleiter I. S., Dudley E., Donev R., Brune M., Juckel G. and Thome J. (2015) Multiplatform metabolome and proteome profiling identifies serum metabolite and protein signatures as prospective biomarkers for schizophrenia. Journal of Neural Transmission (Vienna) 122 Suppl 1:S111-122.

Annunziato F., Cosmi L., Galli G., Beltrame C., Romagnani P., Manetti R., Romagnani S. and Maggi E. (1999) Assessment of chemokine receptor expression by human Th1 and Th2 cells in vitro and in vivo. Journal of Leukocyte Biology 65:691-699.

Ayalew M., Le-Niculescu H., Levey D. F., Jain N., Changala B., Patel S. D., Winiger E., Breier A., Shekhar A., Amdur R., Koller D., Nurnberger J. I., Corvin A., Geyer M., Tsuang M. T., Salomon D., Schork N. J., Fanous A. H., O'Donovan M. C. and Niculescu A. B. (2012) Convergent functional genomics of schizophrenia: from comprehensive understanding to genetic risk prediction. Molecular Psychiatry 17:887-905.

Bahn S. and Chan M. K. (2015) What Can We Learn About Depression from Gene Expression in Peripheral Tissues? Biological Psychiatry 77:207-209.

Benros M. E. and Mortensen P. B. (2020) Role of Infection, Autoimmunity, Atopic Disorders, and the Immune System in Schizophrenia: Evidence from Epidemiological and Genetic Studies. Current Topics in Behavioral Neurosciences 44:141-159.

Benros M. E., Nielsen P. R., Nordentoft M., Eaton W. W., Dalton S. O. and Mortensen P. B. (2011) Autoimmune diseases and severe infections as risk factors for schizophrenia: a 30-year population-based register study. American Journal of Psychiatry 168:1303-1310.

Cardno A. G. and Gottesman, II. (2000) Twin studies of schizophrenia: from bow-and-arrow concordances to star wars Mx and functional genomics. American Journal of Medical Genetics 97:12-17.

Chakir H., Wang H., Lefebvre D. E., Webb J. and Scott F. W. (2003) T-bet/GATA-3 ratio as a measure of the Th1/Th2 cytokine profile in mixed cell populations: predominant role of GATA-3. Journal of Immunological Methods 278:157-169.

Chan M. K., Guest P. C., Levin Y., Umrania Y., Schwarz E., Bahn S. and Rahmoune H. (2011) Converging evidence of blood-based biomarkers for schizophrenia: an update. International Review of Neurobiology 101:95-144.

Chang H. R. and Bistrian B. (1998) The role of cytokines in the catabolic consequences of infection and injury. Journal of Parenteral and Enteral Nutrition 22:156-166.

Cox D., Chan M. K. and Bahn S. (2015) The potential of immune biomarkers to advance personalized medicine approaches for schizophrenia. Journal of Nervous and Mental Disease 203:393-399.

Dai J., Megjugorac N. J., Gallagher G. E., Yu R. Y. and Gallagher G. (2009) IFN-lambda1 (IL-29) inhibits GATA3 expression and suppresses Th2

responses in human naive and memory T cells. Blood 113:5829-5838.

de Witte L., Tomasik J., Schwarz E., Guest P. C., Rahmoune H., Kahn R. S. and Bahn S. (2014) Cytokine alterations in first-episode schizophrenia patients before and after antipsychotic treatment. Schizophrenia Research 154:23-29.

Eaton W. W., Byrne M., Ewald H., Mors O., Chen C. Y., Agerbo E. and Mortensen P. B. (2006) Association of schizophrenia and autoimmune diseases: linkage of Danish national registers. American Journal of Psychiatry 163:521-528.

He K., Guo C., Guo M., Tong S., Zhang Q., Sun H., He L. and Shi Y. (2019) Identification of serum microRNAs as diagnostic biomarkers for schizophrenia. Hereditas 156:23.

He X., Ma Q., Fan Y., Zhao B., Wang W., Zhu F., Ma X. and Zhou L. (2020) The Role of Cytokines in Predicting the Efficacy of Acute Stage Treatment in Patients with Schizophrenia. Neuropsychiatric Disease and Treatment 16:191-199.

Hosmer D. W., Lemeshow S. and Sturdivant R. X. 2013. Applied logistic regression. Wiley, Hoboken, New Jersey. xvi, 500 pages pp.

Kahn R. S. and Sommer I. E. (2015) The neurobiology and treatment of first-episode schizophrenia. Molecular Psychiatry 20:84-97.

Kanhere A., Hertweck A., Bhatia U., Gökmen M. R., Perucha E., Jackson I., Lord G. M. and Jenner R. G. (2012) T-bet and GATA3 orchestrate Th1 and Th2 differentiation through lineage-specific targeting of distal regulatory elements. Nature Communications 3:1268.

Katsikis P. D., Cohen S. B., Londei M. and Feldmann M. (1995) Are CD4+ Th1 cells pro-inflammatory or anti-inflammatory? The ratio of IL-10 to IFN-gamma or IL-2 determines their function. International Immunology 7:1287-1294.

Kelsven S., de la Fuente-Sandoval C., Achim C. L., Reyes-Madrigal F., Mirzakhanian H., Domingues I. and Cadenhead K. (2020) Immuno-inflammatory changes across phases of early psychosis: The impact of antipsychotic medication and stage of illness. Schizophrenia Research.

Khandaker G. M., Cousins L., Deakin J., Lennox B. R., Yolken R. and Jones P. B. (2015) Inflammation and immunity in schizophrenia: implications for pathophysiology and treatment. Lancet Psychiatry 2:258-270.

Kidd P. (2003) Th1/Th2 balance: the hypothesis, its limitations, and implications for health and disease. Alternative Medicine Review 8:223-246.

Kim Y. K., Myint A. M., Lee B. H., Han C. S., Lee H. J., Kim D. J. and Leonard B. E. (2004) Th1, Th2 and Th3 cytokine alteration in schizophrenia. Progress in Neuro-Psychopharmacology & Biological Psychiatry 28:1129-1134.

Kumar A., Pareek V., Singh H. N., Faiq M. A., Narayan R. K., Raza K. and Kumar P. (2019) Altered Expression of a Unique Set of Genes Reveals Complex Etiology of Schizophrenia. Frontiers in Psychiatry 10:906.

Lai C. Y., Scarr E., Udawela M., Everall I., Chen W. J. and Dean B. (2016) Biomarkers in schizophrenia: A focus on blood based diagnostics and theranostics. World Journal of Psychiatry 6:102-117.

Lazarevic V., Glimcher L. H. and Lord G. M. (2013) T-bet: a bridge between innate and adaptive immunity. Nature Reviews Immunology 13:777-789.

Li Y., Zhou K., Zhang Z., Sun L., Yang J., Zhang M., Ji B., Tang K., Wei Z., He G., Gao L., Yang L., Wang P., Yang P., Feng G., He L. and Wan C. (2012) Label-free quantitative proteomic analysis reveals dysfunction of complement pathway in peripheral blood of schizophrenia patients: evidence for the immune hypothesis of schizophrenia. Molecular BioSystems 8:2664-2671.

Liu S., Zhang F., Shugart Y. Y., Yang L., Li X., Liu Z., Sun N., Yang C., Guo X., Shi J., Wang L., Cheng L., Zhang K., Yang T. and Xu Y. (2017) The early growth response protein 1-miR-30a-5p-neurogenic differentiation factor 1 axis as a novel biomarker for schizophrenia diagnosis and treatment monitoring. Translational Psychiatry 7:e998.

Macedo D. (2019) 37. NEUROIMMUNE DYSFUNCTION IN SCHIZOPHRENIA: FROM

BIOMARKERS TO DRUG REPURPOSING. Schizophrenia Bulletin 45:S147-S147.

Mansur R. B., Zugman A., Asevedo E. M., da Cunha G. R., Bressan R. A. and Brietzke E. (2012) Cytokines in schizophrenia: possible role of anti-inflammatory medications in clinical and preclinical stages. Psychiatry and Clinical Neurosciences 66:247-260.

Metz C. E. (1978) Basic principles of ROC analysis. Seminars in Nuclear Medicine 8:283-298.

Modai S. and Shomron N. (2016) Molecular Risk Factors for Schizophrenia. Trends in Molecular Medicine 22:242-253.

Momtazmanesh S., Zare-Shahabadi A. and Rezaei N. (2019) Cytokine Alterations in Schizophrenia: An Updated Review. Frontiers in Psychiatry 10:892.

Muller N., Weidinger E., Leitner B. and Schwarz M. J. (2015) The role of inflammation in schizophrenia. Frontiers in Neuroscience 9:372.

Myles A., Gearhart P. J. and Cancro M. P. (2017) Signals that drive T-bet expression in B cells. Cellular Immunology 321:3-7.

Na K. S. and Kim Y. K. (2007) Monocytic, Th1 and th2 cytokine alterations in the pathophysiology of schizophrenia. Neuropsychobiology 56:55-63.

Nagelkerke N. J. D. (1991) A Note on a General Definition of the Coefficient of Determination. Biometrika 78:691-692.

Noto C., Maes M., Ota V. K., Teixeira A. L., Bressan R. A., Gadelha A. and Brietzke E. (2015) High predictive value of immune-inflammatory biomarkers for schizophrenia diagnosis and association with treatment resistance. World Journal of Biological Psychiatry 16:422-429.

Potvin S., Stip E., Sepehry A. A., Gendron A., Bah R. and Kouassi E. (2008) Inflammatory cytokine alterations in schizophrenia: a systematic quantitative review. Biological Psychiatry 63:801-808.

Rajasekaran A., Shivakumar V., Kalmady S. V., Narayanaswamy J. C., Subbana M., Venugopal D., Amaresha A. C., Venkatasubramanian G. and Debnath M. (2016) The impact of IL10 polymorphisms and sHLA-G levels on the risk of schizophrenia. Asian Journal of Psychiatry 23:39-43.

Rosenblat J. D. (2019) Targeting the immune system in the treatment of bipolar disorder. Psychopharmacology (Berl) 236:2909-2921.

Schmittgen T. D. and Livak K. J. (2008) Analyzing real-time PCR data by the comparative CT method. Nature Protocols 3:1101-1108.

Shi J., Levinson D. F., Duan J., Sanders A. R., Zheng Y., Pe'er I., Dudbridge F., Holmans P. A., Whittemore A. S., Mowry B. J., Olincy A., Amin F., Cloninger C. R., Silverman J. M., Buccola N. G., Byerley W. F., Black D. W., Crowe R. R., Oksenberg J. R., Mirel D. B., Kendler K. S., Freedman R. and Gejman P. V. (2009) Common variants on chromosome 6p22.1 are associated with schizophrenia. Nature 460:753-757.

Solek C. M., Farooqi N., Verly M., Lim T. K. and Ruthazer E. S. (2018) Maternal immune activation in neurodevelopmental disorders. Developmental Dynamics 247:588-619.

Sonti G., Ilyin S. E. and Plata-Salaman C. R. (1996) Anorexia induced by cytokine interactions at pathophysiological concentrations. American Journal of Physiology 270:R1394-1402.

Srinivasan S., Bettella F., Mattingsdal M., Wang Y., Witoelar A., Schork A. J., Thompson W. K., Zuber V., Schizophrenia Working Group of the Psychiatric Genomics Consortium T. I. H. G. C., Winsvold B. S., Zwart J. A., Collier D. A., Desikan R. S., Melle I., Werge T., Dale A. M., Djurovic S. and Andreassen O. A. (2016) Genetic Markers of Human Evolution Are Enriched in Schizophrenia. Biological Psychiatry 80:284-292.

Stolz P. A., Wehring H. J., Liu F., Love R. C., Ellis M., DiPaula B. A. and Kelly D. L. (2019) Effects of Cigarette Smoking and Clozapine Treatment on 20-Year All-Cause & Cardiovascular Mortality in Schizophrenia. Psychiatric Quarterly 90:351-359.

Sun X. Y., Lu J., Zhang L., Song H. T., Zhao L., Fan H. M., Zhong A. F., Niu W., Guo Z. M., Dai Y. H., Chen C., Ding Y. F. and Zhang L. Y. (2015)

Aberrant microRNA expression in peripheral plasma and mononuclear cells as specific blood-based biomarkers in schizophrenia patients. Journal of Clinical Neuroscience 22:570-574.

Tasic L., Larcerda A. L. T., Pontes J. G. M., da Costa T., Nani J. V., Martins L. G., Santos L. A., Nunes M. F. Q., Adelino M. P. M., Pedrini M., Cordeiro Q., Bachion de Santana F., Poppi R. J., Brietzke E. and Hayashi M. A. F. (2019) Peripheral biomarkers allow differential diagnosis between schizophrenia and bipolar disorder. Journal of Psychiatric Research 119:67-75.

Tomasik J., Rahmoune H., Guest P. C. and Bahn S. (2016) Neuroimmune biomarkers in schizophrenia. Schizophrenia Research 176:3-13.

Trovao N., Prata J., VonDoellinger O., Santos S., Barbosa M. and Coelho R. (2019) Peripheral Biomarkers for First-Episode Psychosis-Opportunities from the Neuroinflammatory Hypothesis of Schizophrenia. Psychiatry Investigation 16:177-184.

Tullius S. G., Biefer H. R. C., Li S., Trachtenberg A. J., Edtinger K., Quante M., Krenzien F., Uehara H., Yang X., Kissick H. T., Kuo W. P., Ghiran I., de la Fuente M. A., Arredouani M. S., Camacho V., Tigges J. C., Toxavidis V., El Fatimy R., Smith B. D., Vasudevan A. and ElKhal A. (2014) NAD^+ protects against EAE by regulating $CD4^+$ T-cell differentiation. Nature Communications 5:5101.

Upthegrove R. and Khandaker G. M. (2020) Cytokines, Oxidative Stress and Cellular Markers of Inflammation in Schizophrenia. Current Topics in Behavioral Neurosciences 44:49-66.

Vatankhah V., Mirabzadeh A., Iranpour H., Dieji B., Norouzi M., Karimipour M., Nobakht J., Esmaeili E. and Ayazi M. (2019) Determination of Changes in Blood Biomarker Levels in Antipsychotic Polypharmacy and Aripiprazole Monotherapy in Patients With Long-term Schizophrenia. Iranian-Rehabilitation-Journal 17:369-376.

Wang T., Holland J. W., Martin S. A. M. and Secombes C. J. (2010) Sequence and expression analysis of two T helper master transcription factors, T-bet and GATA3, in rainbow trout Oncorhynchus mykiss and analysis of their expression during bacterial and parasitic infection. Fish & Shellfish Immunology 29:705-715.

Journal of Cell and Molecular Research (2020) 11 (2), 90-98 DOI: 10.22067/jcmr.v11i2.85667

Research Article

Immunosuppressive Effects of Human Chorionic Gonadotropin (hCG) on Mesenchymal Stromal Cells

Sepideh sadat Hosseini[1†], Shadi Mehrzad[1†], Halimeh Hassanzadeh[2,3], Hamid Reza Bidkhori[2], Mahdi Mirahmadi[2], Madjid Momeni-Moghaddam[1], Fatemeh Sadeghifar[*1], Moein Farshchian[*2]

[1]*Department of Biology, Faculty of science, Hakim Sabzevari University, Sabzevar, Iran*
[2]*Stem Cells and Regenerative Medicine Research Department, Academic Center for Education, Culture and Research (ACECR) - Khorasan Razavi, Mashhad, Iran*
[3]*Department of Biology, Faculty of Science, Ferdowsi University of Mashhad, Mashhad, Iran*

Received 18 February 2020 Accepted 12 March 2020

Abstract

Mesenchymal stem/stromal cells (MSCs) as one of the most important types of adult stem cells secrete a variety of immunomodulatory cytokines. However, their immunomodulatory features strongly depend on the molecular cross-talk between cells and the surrounding microenvironment. Hence, some strategies were proposed to empower their beneficial effects during cell-therapeutic procedures to avoid confusing results. Licensing the cells with chemical compounds could be considered as one of the most applicable methods for induction of anti-inflammatory status in the cells. Human chorionic gonadotropin (hCG) is a pregnancy related hormone which has been shown to be essential for the establishment of a successful pregnancy. HCG supports the implantation of fetus in the maternal endometrium, due to its immunomodulatory effects. Moreover, the regulatory role of hCG has been previously mentioned in case of some autoimmune-based diseases. In the present study, the capacity of this hormone for induction of different immune-encountered genes expression was examined in primary cultures of human adipose tissue derived mesenchymal stem cells (Ad-MSCs). In this regard, Ad-MSCs were exposed to 10 IU of hCG for 72 hours. Molecular studies via quantitative Real-time PCR (qRT-PCR) experiments were performed to detect gene expression modifications based on the application of SYBR Green as the fluorescent dye and in comparison to the *RPLP0* as the housekeeping gene. Results confirmed that hCG significantly upregulated *TSG-6*, *TGF-β1*, *IL-1β* and *IL-6* expression levels comparing with the control group, while it downregulates *COX-2* expression, and had no statistically significant effects on *IL-10* and *TDO2*. In conclusion, priming Ad-MSCs with hCG may enhance the proliferation and immunoregulatory potential of these cells, although it needs further investigations to reveal involved molecular pathways.

***Keywords*:** Mesenchymal stem cells, Human Chorionic Gonadotropin, Pregnancy, Immunomodulation, Pretreatment

Introduction

The human immune system employs a complicated network of organs, tissues, cells and molecules to defend the host against a wide range of pathogens (Netea et al., 2016). Both innate and adaptive immune responses are playing role in the recognition and eradication of infections. During innate immune responses some biologically active small molecules such as different cytokines and chemokines are secreted by activated cells. Pregnancy is a physiological exception during which the fetal allograft is well tolerated by the maternal immune system (Chaplin, 2010). Decidual stromal cells normally produce chemokine gradients, which in turns recruited maternal leukocytes.

On the other hand, trophoblastic cells can induce the differentiation of immune cells into a trophoblast-supporting phenotype (Ander et al., 2019). While the majority of the decidual leukocytes are natural killer cells (NK) with the capacity for production of a vast array of growth factors and cytokines, and decidual anti-inflammatory M2-like cells, T cell subsets are also playing functional roles (Liu et al., 2017). Although exact molecular events which are involved in the fetal tolerance have still remained unknown, it is clear that *i)* the uterus/placenta displays a distinguished immune site and that *ii)* there are multiple mechanisms for maintenance of local inflammation and hemostasis of T-cell specific responses (Pazos et al., 2012). Pregnancy is a

† Both authors contributed equally to this work.
* Corresponding authors' e-mail address:
moeinfarshchy@yahoo.com
f.sadeghifar@hsu.ac.ir

combination of pro-inflammatory and anti-inflammatory situations, depending on the stage of gestation. Hence, understanding the mechanisms which are engaged with tolerance induction and immune system modulation during gestation may provide new insights into the regulatory systems which may be disturbed during autoimmune diseases (Mor et al., 2011).

Human chorionic gonadotropin (hCG) is a specific hormone that has been demonstrated to have immunoregulatory properties and is essential for the establishment of a successful pregnancy (Schumacher et al., 2009). hCG has a necessary role in modulating the phenotype of B cells and their ability to produce IL-10 (Fettke et al., 2016). Moreover, other functions have been reported for hCG, including regulating the phenotype of macrophages in the benefit of M2-like cells, suppressing Th1 cytokine production and *in vivo* induction of T regulatory suppressive activities (Schumacher et al., 2014). It has been demonstrated that hCG potentially induces attraction of neutrophils, monocytes, and lymphocytes. Also, stimulation of monocytes with hCG increased the production of IL-8, as a leukocyte attractors (Schumacher et al., 2009, Ushigoe et al., 2000). It has been confirmed that hCG-treated decidual dendritic cells had a high capacity for induction of regulatory T cells (Schumacher et al., 2013). In addition, the application of hCG in a murine model of autoimmune diabetes could prevent disease progression (Khil et al., 2007). Finally, a great potential of hCG, as an anti-rejection agent following solid organ transplantation, has been clearly demonstrated (Theofanakis et al., 2017). The remission of several autoimmune-based diseases during pregnancy recommends the roles of hCG as an immunosuppressive agent in solid organ or allogeneic transplant settings (Koldehoff et al., 2011).

Regenerative properties of MSCs resulted in their therapeutic applications in a majority of disorders, such as orthopedic injuries (Volarevic et al., 2017). Also, it has been demonstrated that MSCs modulate the functions of immune cells, including T cells, B cells, natural killer (NK) cells, antigen-presenting cells, macrophages and neutrophils, which makes them promising candidates for cell therapies in a variety of auto-immune and inflammation-related diseases (Wang et al., 2016). It has been possible to extend the release of effective biomolecules and immune response effectors by pre-conditioning of MSCs with small molecules (Hu and Li, 2018). For example, it was shown that pre-treatment of Ad-MSCs with progesterone enhances the expression of some immunomodulatory factors such as Human Leukocyte Antigen G **(**HLA-G), Prostaglandin E2 (PGE2) and Interleukin 6 (IL-6) (Susheelamma et al., 2018). Also, treatment of Ad-MSCs with melatonin, increased the release of mitogenic factors, such as basic Fibroblast Growth Factor (b-FGF) and Hepatocyte Growth Factor (HGF); while reduced the production of harmful inflammatory cytokines like TNF-α (Han et al., 2016a). Moreover, aspirin treatment could significantly enhance the immunoregulatory properties of MSCs via up-regulation of regulatory T cells (Tregs) and down-regulation of T helper 17 (Th17) cells (Tang et al., 2014).

Taken together, considering outstanding properties of MSCs in cell-based therapeutics and pivotal immunoregulative features of hCG, we conducted this *in vitro* study to shed light on the consequences of hCG priming on immunomodulatory properties of MSCs at the molecular level.

Materials and Methods

Primary cells derivation and expansion

Freshly prepared adipose tissues obtained from subcutaneous sites were acquired from healthy individuals with informed consent. All procedures were performed under internationally accepted ethical guidelines of working with human tissues, as approved by the ACECR Biomedical Research Ethics Committee (Mashhad, Iran, Code: IR.ACECR.JDM.REC.1398.008).

Adipose tissues were washed three times with phosphate-buffered saline (PBS1X) supplemented with penicillin-streptomycin (Biosera, France) and then incubated for 1 hour at 37°C with freshly prepared 0.1% collagenase solution (Invitrogen, USA), 0.1% of BSA (Biowest, France) and 2mM $CaCl_2$ which were prepared in PBS. They were shaken vigorously for 5 to 10 seconds periodically to avoid phase dissociation. After that, fetal bovine serum (FBS) was added to the reaction as the inhibitor of collagenase activity. Digested adipose tissues were then centrifuged at room temperature (600 *g*, 10 minutes). Pellets were re-suspended in freshly prepared media and following another round of centrifugation (400 *g*, 6 minutes) they were seeded in culture vessels containing Dulbecco's Modified Eagle's Medium (DMEM, Biowest, France), supplemented by 100 mg/mL streptomycin and 100 U/mL penicillin (Invitrogen,

USA). Mesenchymal stromal cells were purified based on their plastic-adherent capacity. Cells of passage number 3 were applied for downstream applications.
The medium was exchanged every 2–3 days. Upon reaching proper confluency (85 to 90%), cells were detached via trypsin/EDTA (0.025%, initial seeding density 5000–10000 cells/cm^2).

Characterization of human adipose tissue derived mesenchymal stromal cells

To evaluate the expression levels of mesenchymal lineage-specific cell surface markers, Ad-MSCs ($2x10^5$ cells) were trypsinized following two rounds of washing with PBS 1X and were precipitated by centrifugation.

Cell pellets were then re-suspended in 100 µl of cold PBS, containing 5% FBS and stained with 2 µg/ml of PE-conjugated CD73, CD13, FITC-conjugated CD90, CD34, CD14 and HLA-DR, and APC-conjugated CD44, CD45 antibodies for 1 hour (all from Cytognos, Spain). Data were obtained via FACScalibur Cytometer equipped with 488-nm argon laser; the analysis was performed with FlowJo software (version 7.6.1).

The capacity of the cells for adipogenic differentiation was evaluated following exposing the cells with adipogenic differentiation media for a period of two weeks. Low glucose DMEM supplemented by 10% FBS was applied as the basic media. It was complemented by 200 mM indomethacin, 1 mM dexamethasone, and 10 mM *β*-glycerophosphate (all from Sigma Aldrich, Germany). The differentiation medium was changed every 3 days. The level of differentiation induction was evaluated by the application of Oil Red O staining (Sigma Aldrich, Germany) as the indicator of intracellular lipid droplets.
In addition, osteogenic differentiation of the cells was assessed qualitatively based on the cytochemical analysis (alizarin red, Sigma Aldrich, Germany). To do so, Ad-MSCs were treated with osteogenic inductive media containing 50 mM ascorbate-2- phosphate (Sigma Aldrich, Germany), 0.1 mM dexamethasone, and 10 mM *β*-glycerophosphate. Three weeks later, osteogenesis was explored based on staining procedures which reveals the calcium mineralization of extracellular matrix and alkaline phosphatase (AP) activity, respectively (Sigma Aldrich, Germany).

Treatment of MSCs with hCG

Fully characterized cultures of human Ad-MSCs with proper cell densities were treated with hCG (10 IU/ml, Homapharmed, Iran) for 72h. The concentration of hCG and incubation time was selected based on our initial screening experiments. Untreated cells were applied as controls.

MTT assay

Cell survival was determined using 3-(4, 5-dimethylthiazolyl-2)-2,5-diphenyltetrazolium bromide (MTT) assay (5 mg/ml, Sigma Aldrich, USA). Briefly, cells were seeded in 96-well plates at a density of 5000 cells per well and then MSCs were treated with various concentrations of hCG (2, 4, 6, 8, 10, 12 IU/ml). After 24 to 72 hours incubation, proper amount of MTT dye was added per well. 4 hours later, the media removed from all replicates and formazan crystals were solved in Dimethyl sulfoxide (DMSO, Sigma Aldrich, Germany). Optical densities (ODs) were read at 540 nm wavelength.

RNA extraction and RT-PCR

Cells, from different treatments, were homogenized in TriPure reagent (Roche Diagnostics, Germany) for extraction of total RNA according to the manufacturer instructions. Quantity and purity of all RNA samples were determined using the Nanodrop ND-1000 spectrophotometer (Bio-Tek, USA). The integrity of RNA samples was also evaluated by gel electrophoresis to detect 28s and 18s ribosomal RNAs.
Total RNAs were treated with 1 unit of *DNase* I (Thermo Fisher Scientific, USA), to avoid amplification of contaminating genomic DNA. cDNA was synthesized using oligo(dT) primer and *M-MuLV* reverse transcriptase (Thermo Fisher Scientific, USA) according to the manufacturer protocols.

Quantitative Real-time PCR (qRT-PCR)

The qRT-PCR was carried out using the Bio-Rad CFX-96 system (Bio-Rad, USA). Each reaction mixture contained 2 µl cDNA (0.1 diluted), 10 µl SYBR Green PCR Master Mix (Takara, Japan) and 1 µl of 10 pmol/ml mixture of forward and reverse primers in a final volume of 20 µl. Experiments were performed in duplicate. Specific primers applied for gene amplifications are listed in Table 1. The expression levels of target genes were normalized to *RPLP0*. Relative quantification of gene expression modifications was carried out based on the application of log 2-ΔΔCt formula.

Table 1. Primer sequences applied for qRT-PCR experiments.

Target Gene	Sequence	Product size (bp)
RPLP0	**F**: TGGTCATCCAGCAGGTGTTCGA **R**: ACAGACACTGGCAACATTGCGG	119
TGF-β1	**F**: GTTCAAGCAGAGTACACACAGC **R**: GTATTTCTGGTACAGCTCCACG	154
TSG-6	**F**: GCTGCTGGATGGATGGCTAAG **R**: CTCCTTTGCGTGTGGGTTGTAG	156
COX-2	**F**: CCAGAGCAGGCAGATGAAATACC **R**: ACCAGAAGGGCAGGATACAGC	168
IL-1β	**F**: CCTCTCTCACCTCTCCTACTCAC **R**: CTGCTACTTCTTGCCCCCTTTG	186
IL-6	**F**: ACTCACCTCTTCAGAACGAATTG **R**: GCAAGTCTCCTCATTGAATCCAG	196
IL-10	**F:**GAGATGCCTTCAGCAGAGTGAAGA **R:**AGGCTTGGCAACCCAGGTAAC	114
TDO2	**F:** ACCTCCGTGCTTCTCAGACAG **R:**GACCTCCTTTGCTGGCTCTATTC	151

Statistical analysis

The GraphPad Prism statistical program (version 7) was used for data analysis. The values are reported as mean of at least three independent experiments ± SD. The significance of differences among data was examined at the confidence level of 95% (p<0.05) using the T-test.

Results

Characterization of human Ad-MSCs

The authentication of Ad-MSCs was performed based on surface antigen characterization. Cells were demonstrated a spindle-like morphology (Figure 1, a-c). The expression levels for positive markers including CD73, CD90, CD13 and CD44 were equal to 99.3%, 99.9%, 98.7% and 98.2%, respectively.

Ad-MSCs indicated the expression of non-

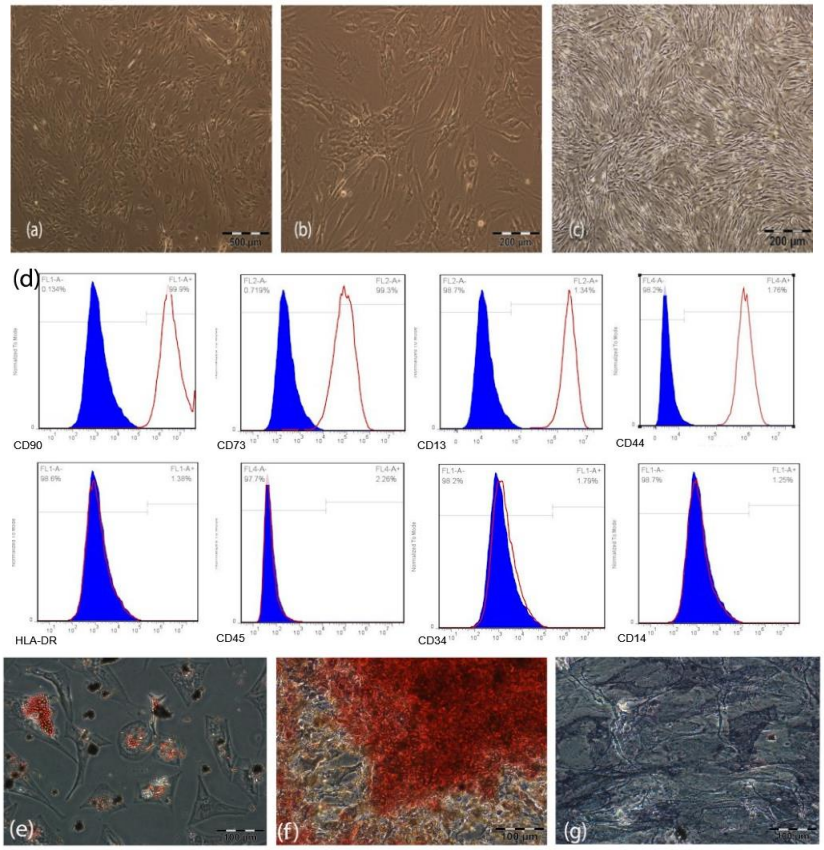

Figure 1. Characterization of Human Ad-MSCs, (a, b) Undifferentiated human Ad-MSCs represent spindle-shaped morphology (magnification 4x and 10x, respectively). (c) Morphological characteristics of MSC exposed to 10 IU/ml of hCG for 72 hours. (d) Flow cytometric analysis showed that almost all cultured Ad-MSCs expressed CD73 (99.3%), CD13 (98.7%), CD90 (99.9%), and CD44 (98.2%), whereas a small portion of the cells were expressed CD34 (1.79%), CD45 (2.26%), CD14 (1.25%) and HLA-DR (1.38%). Expressions of cell surface markers of Ad-MSCs are shown as compared with their respected isotype controls. (e) Adipogenic differentiated human Ad-MSCs were stained with Oil Red O. (f) Osteogenic differentiated human Ad-MSCs were stained with alizarin red. (g) Osteogenic differentiation as evidenced by alkaline phosphatase activity assay.

mesenchymal cell-specific markers for less than 3%: CD45 (2.26%), CD34 (1.79%), CD14 (1.25%) and HLA-DR (1.38%) (Figure 1d).

Effects of hCG on cell viability

MSCs viability assessment was performed using MTT assay. Ad-MSCs were treated with a range of hCG concentrations (2, 4, 6, 8, 10, 12 IU/ml). Although minor decrease was observed in cell viability percent following treatment with different concentrations of hCG in comparison to the control group, these changes were not statistically significant. Thus, our results demonstrated that pre-conditioning of the cells with hCG does not exert remarkable toxicity against Ad-MSCs (Figure 2).

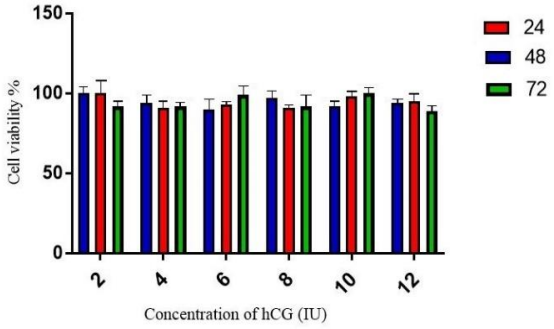

Figure 2. Cell viability (MTT) assay. Results indicated that pretreatment of Ad-MSCs with different concentrations of hCG does not affect their survival significantly.

Effects of hCG on the expression of genes involved in MSC-mediated Immuno-regulation

We evaluated the expression levels of some pro- and anti-inflammatory cytokines (TGF-*β1*, COX-2, TSG-6, IL-1β and IL-6) in hCG-stimulated Ad-MSCs, in comparison with untreated cells from passage number 3, via qRT-PCR. Results showed that hCG markedly enhanced the mRNA levels of *TGF-β*, *TSG-6*, *IL-1β* and *IL-6* and reduced the expression of *COX-2* compared with the control group (Figure 3).

Discussion

As a specific soluble factor produced by the placenta, hCG supports pregnancy by inhibiting adverse immune responses, facilitating trophoblast invasion, promoting angiogenesis and ensuring the nourishment of the fetus. It has been shown that hCG immunoregulatory properties is through binding to special LH/CG receptors expressed by immune cells (Schumacher et al., 2014). hCG exerts anti-inflammatory effects in decidual tissues through different mechanisms: 1) increasing the proportion of Tregs; 2) alleviating the proportion of macrophages and neutrophils; 3) inducing an M1→M2 macrophage polarization and also 4) increasing the percentage of decidual Th17 cells (Schumacher et al., 2009).

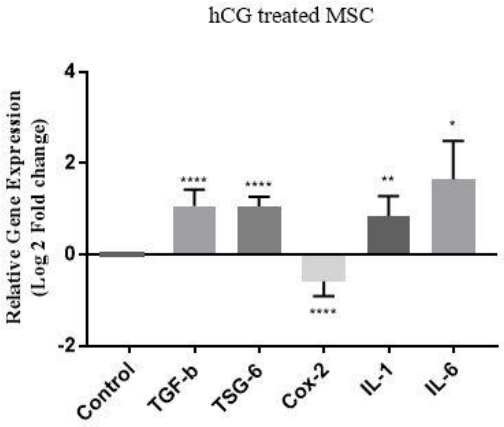

Figure 3. mRNA quantification of cytokines in Ad-MSCs treated with 10 IU hCG after 72hrs: Results showed that hCG preconditioning decreases the inflammatory properties of MSCs. Data are shown as mean ± SEM (n=3) and presented as fold change (log 2) of expressions in preconditioned versus untreated cells. One star represents $p < 0.05$, two stars represent $p < 0.01$, three stars represent $p < 0.001$ and four stars represent $p < 0.0001$.

hCG increases the secretion of macrophage inhibitory factor in human endometrial and granulosa cells. This hormone also enhances the secretion of NO, ROS, IL6, IL12p40 in bone marrow-derived macrophages (Schumacher et al., 2009). Yoshimura and colleagues found that hCG upregulates maturation markers on peripheral blood DCs, stimulates the secretion of inflammatory cytokines and increases T cells activity (Yoshimura et al., 2003).

Moreover, Poloski showed that in addition to its function as a Treg cell attractor, hCG has the potential to stimulate the conversion of non-Treg cells into Treg cells (Poloski et al., 2016). In a previous study, it has been shown that hCG inhibits the upregulation of MHC class II molecules on DCs, diminishes their T cell stimulatory capacity, and induces the secretion of IL-10 and TGF-β *in vitro* (Segerer et al., 2009, Tang et al., 2014). Other studies indicated the effects of hCG on Regulatory B cells (Breg cells). It was shown that hCG not

only increases the number of Breg cells but also enhances the production of IL-10 (Fettke et al., 2016). Another study confirmed the effects of 10 IU/ml of hCG on murine T and B cells. This concentration of hCG could activate B cells, but failed to affect T cells' functionality *in vivo* (Schumacher, 2017). It was already demonstrated that hCG is a strong attractor of neutrophils, monocytes, and lymphocytes at very low doses, and stimulation of monocytes with hCG reinforced the production of IL-8 (Schumacher et al., 2009). hCG anti-inflammatory effects makes it a proper candidate for development of inventive biomimetic strategies toward a pro-regenerative phenotype in case of tissue injuries or inflammations (Han et al., 2016b). Also, during pregnancy, hCG is responsible for the amelioration in the symptoms of rheumatoid arthritis, induction the shift of Th1 mediated cellular immunity to a pre-pregnancy Th2 immunity and increased T cell regulatory activities (Ostensen et al., 2012). In addition, other hormones such as estrogen and testosterone affect immune cells differentiation and function leading to either a pro-inflammatory or an anti-inflammatory phenotype. Testosterone regulates the immune system activities by enhancing Th1 responses, down-regulating NK cells activities and increasing the secretion of anti-inflammatory IL-10. Estrogen modulates B cell functions and switches Th1 responses to Th2 ones (Taneja, 2018).

As we mentioned before, stem cells are extensively used in regenerative medicine applications because of their considerable advantages, especially their ability to release bioactive molecules that were known to have an immunosuppressive capability (Caplan, 2007). The substantial immunosuppressive effects of MSCs are due to their ability for T cell proliferation inhibition and reprogramming of M1 macrophages to M2 cells (Regmi et al., 2019). Furthermore, inflammatory cascades are influenced by active MSCs. They take part in tissue homeostasis through the secretion of trophic factors with anti-inflammatory functions (Lange-Consiglio et al., 2016). It was proposed that various cytokines, growth factors, anti-inflammatory agents, and extracellular vesicles (EVs) are responsible for immunomodulatory features of MSCs (English et al., 2009).

This study was conducted to quantitatively analyze the expression levels of important immunoregulatory genes (including TGF-*β1*, *TSG-6*, *COX-2*, *IL-1β*, and *IL-6*) in hCG primed Ad-MSCs. The secretion of TGF-*β1* by MSCs leads to Treg generation and confining lymphocyte activation (Regmi et al., 2019). TGF-*β* and interleukin 6 (IL-6) are pleiotropic cytokines that play crucial roles in immune suppression (Basu et al., 2017). hCG-mediated production of IL-6 by DCs affected by different stimulation conditions (Wan et al., 2008). It has been shown that IL-6 is responsible for differentiation of pro-inflammatory M1 cells into the anti-inflammatory M2 macrophages (Wan et al., 2008). IL-1*β* is a central inflammatory cytokine, which could modulate the inflammatory cytokines through IL-1 receptor/ MYD88 and also could be affected by NF-κB signal transduction pathways (Hoesel and Schmid, 2013). TSG-6 is synthesized in response to pro-inflammatory mediators. It has been identified as a critical mediator of anti-inflammatory effects of human MSCs. TSG-6 attenuates inflammatory events through the inhibition of neutrophils invasion into the inflammatory sites (Dyer et al., 2016). It has been shown that IL-1*β* induces the expression of *TSG6* in multiple cell types, whereas its suppression enhances the level of inflammation. *TSG6* can reduce inflammation by the inhibition of NF-κB signaling (Mittal et al., 2016). *COX-2* is directly responsible for the induction of prostaglandin-mediated inflammation. In line with these studies, targeting *COX-2* by hCG could be proposed as a logical therapeutic strategy for management of inflammatory situations (Basu et al., 2017). TGF-*β* has serine/threonine kinases receptors that directly phosphorylate Smad2/3, and with co-stimulation of IL-1β can induce expression of IL-6 in pericytes (Rustenhoven et al., 2016, Travis and Sheppard, 2014). According to our results, we hypothesized that *IL-6* over expression is a direct or indirect consequence of to the *TGF-β* and/or *IL-1* over expression.

To our knowledge, this is the first study which reports the effects of hCG on immunoregulatory and anti-inflammatory properties of MSCs by evaluating the expression levels of some critical genes. In conclusion, hCG could enhance the anti-inflammatory ability of MSCs accompanied by increased *TGF-β*, *TSG-6*, *IL-1β*, and *IL-6* expressions and decreased *COX-2* expression. Also, it was confirmed that hCG treatment of MSCs had no significant effects on *IL-10* and *TDO2* expression levels (Data not shown). Further studies should be performed to unravel the mechanistic functions of hCG treatment on MSCs transcriptome and proteome networks.

Acknowledgments
This study was funded by ACECR-Khorasan Razavi. It was the MSc thesis of Sepideh sadat Hosseini, Hakim Sabzevari University, Sabzevar, Iran.
We are grateful to Dr. Sanjar Mosavi for his kind contribution in collecting samples.

Conflict of Interest
Authors declare that there is no conflict of interest regarding the publication of this article.

References

Ander S. E., Diamond M. S. and Coyne C. B. (2019) Immune responses at the maternal-fetal interface. Science immunology 4.

Basu A., Das A. S., Sharma M., Pathak M. P., Chattopadhyay P., Biswas K. and Mukhopadhyay R. (2017) STAT3 and NF-κB are common targets for kaempferol-mediated attenuation of COX-2 expression in IL-6-induced macrophages and carrageenan-induced mouse paw edema. Biochemistry and biophysics reports 12:54-61.

Caplan A. I. (2007) Adult mesenchymal stem cells for tissue engineering versus regenerative medicine. Journal of cellular physiology 213:341-347.

Chaplin D. D. (2010) Overview of the immune response. Journal of Allergy and Clinical Immunology 125:S3-S23.

Dyer D. P., Salanga C. L., Johns S. C., Valdambrini E., Fuster M. M., Milner C. M., Day A. J. and Handel T. M. (2016) The anti-inflammatory protein TSG-6 regulates chemokine function by inhibiting chemokine/glycosaminoglycan interactions. Journal of Biological Chemistry 291:12627-12640.

English K., Ryan J., Tobin L., Murphy M., Barry F. and Mahon B. P. (2009) Cell contact, prostaglandin E2 and transforming growth factor beta 1 play non-redundant roles in human mesenchymal stem cell induction of CD4+ CD25Highforkhead box P3+ regulatory T cells. Clinical & Experimental Immunology 156:149-160.

Fettke F., Schumacher A., Canellada A., Toledo N., Bekeredjian-Ding I., Bondt A., Wuhrer M., Costa S.-D. and Zenclussen A. C. (2016) Maternal and fetal mechanisms of B cell regulation during pregnancy: human chorionic gonadotropin stimulates B cells to produce IL-10 while alpha-fetoprotein drives them into apoptosis. Frontiers in immunology 7:495.

Han D., Huang W., Li X., Gao L., Su T., Li X., Ma S., Liu T., Li C. and Chen J. (2016a) Melatonin facilitates adipose-derived mesenchymal stem cells to repair the murine infarcted heart via the SIRT1 signaling pathway. Journal of pineal research 60:178-192.

Han J.-S., Rahaman K. A., Seo J.-E., Hasan M., Lee K.-T., Min H., Lee K. M., Park J.-H., Kim H. J. and Kim K. H. (2016b) Human chorionic gonadotropin (hCG) sub-chronic administration mediated MMP-9 activities and cytokine association deteriorate experimental autoimmune encephalomyelitis (EAE) condition in mice model. Journal of Pharmaceutical Investigation 46:685-695.

Hoesel B. and Schmid J. A. (2013) The complexity of NF-κB signaling in inflammation and cancer. Molecular cancer 12:86.

Hu C. and Li L. (2018) Preconditioning influences mesenchymal stem cell properties in vitro and in vivo. Journal of cellular and molecular medicine 22:1428-1442.

Khil L.-Y., Jun H.-S., Kwon H., Yoo J., Kim S., Notkins A. and Yoon J.-W. (2007) Human chorionic gonadotropin is an immune modulator and can prevent autoimmune diabetes in NOD mice. Diabetologia 50:2147-2155.

Koldehoff M., Katzorke T., Wisbrun N., Propping D., Wohlers S., Bielfeld P., Steckel N., Beelen D. and Elmaagacli A. (2011) Modulating impact of human chorionic gonadotropin hormone on the maturation and function of hematopoietic cells: Journal of Leukocyte Biology. Embryology–Updates and Highlights on Classic Topics 116.

Lange-Consiglio A., Perrini C., Tasquier R., Deregibus M. C., Camussi G., Pascucci L., Marini M. G., Corradetti B., Bizzaro D. and De Vita B. (2016) Equine amniotic microvesicles and their anti-inflammatory potential in a tenocyte model in vitro. Stem cells and development 25:610-621.

Liu S., Diao L., Huang C., Li Y., Zeng Y. and Kwak-Kim J. Y. (2017) The role of decidual

immune cells on human pregnancy. Journal of reproductive immunology 124:44-53.

Mittal M., Tiruppathi C., Nepal S., Zhao Y. Y., Grzych D., Soni D., Prockop D. J. and Malik A. B. (2016) TNFalpha-stimulated gene-6 (TSG6) activates macrophage phenotype transition to prevent inflammatory lung injury. Proc Natl Acad Sci U S A 113:E8151-E8158.

Mor G., Cardenas I., Abrahams V. and Guller S. (2011) Inflammation and pregnancy: the role of the immune system at the implantation site. Annals of the New York Academy of Sciences 1221:80.

Netea M. G., Joosten L. A., Li Y., Kumar V., Oosting M., Smeekens S., Jaeger M., Ter Horst R., Schirmer M. and Vlamakis H. (2016) Understanding human immune function using the resources from the Human Functional Genomics Project. Nature medicine 22:831.

Ostensen M., Villiger P. M. and Forger F. (2012) Interaction of pregnancy and autoimmune rheumatic disease. Autoimmunity Reviews 11:A437-446.

Pazos M., Sperling R. S., Moran T. M. and Kraus T. A. (2012) The influence of pregnancy on systemic immunity. Immunologic research 54:254-261.

Poloski E., Oettel A., Ehrentraut S., Luley L., Costa S.-D., Zenclussen A. C. and Schumacher A. (2016) JEG-3 trophoblast cells producing human chorionic gonadotropin promote conversion of human CD4+ FOXP3− T cells into CD4+ FOXP3+ regulatory T cells and foster T cell suppressive activity. Biology of reproduction 94: 101-111.

Regmi S., Pathak S., Kim J. O., Yong C. S. and Jeong J.-H. (2019) Mesenchymal stem cell therapy for the treatment of inflammatory diseases: challenges, opportunities, and future perspectives. European journal of cell biology 98: 5-8.

Rustenhoven J., Aalderink M., Scotter E. L., Oldfield R. L., Bergin P. S., Mee E. W., Graham E. S., Faull R. L., Curtis M. A., Park T. I. and Dragunow M. (2016) TGF-beta1 regulates human brain pericyte inflammatory processes involved in neurovasculature function. Journal of Neuroinflammation 13:37.

Schumacher A. (2017) Human chorionic gonadotropin as a pivotal endocrine immune regulator initiating and preserving fetal tolerance. International journal of molecular sciences 18:2166.

Schumacher A., Brachwitz N., Sohr S., Engeland K., Langwisch S., Dolaptchieva M., Alexander T., Taran A., Malfertheiner S. F. and Costa S.-D. (2009) Human chorionic gonadotropin attracts regulatory T cells into the fetal-maternal interface during early human pregnancy. The Journal of Immunology 182:5488-5497.

Schumacher A., Costa S.-D. and Zenclussen A. C. (2014) Endocrine factors modulating immune responses in pregnancy. Frontiers in immunology 5:196.

Schumacher A., Heinze K., Witte J., Poloski E., Linzke N., Woidacki K. and Zenclussen A. C. (2013) Human chorionic gonadotropin as a central regulator of pregnancy immune tolerance. The Journal of Immunology 190:2650-2658.

Segerer S. E., Müller N., Van Den Brandt J., Kapp M., Dietl J., Reichardt H. M., Rieger L. and Kämmerer U. (2009) Impact of female sex hormones on the maturation and function of human dendritic cells. American Journal of Reproductive Immunology 62:165-173.

Susheelamma C. J., Pillai S. M. and Nair S. A. (2018) Oestrogen, progesterone and stem cells: the discordant trio in endometriosis? Expert reviews in molecular medicine 20.

Taneja V. (2018) Sex hormones determine immune response. Frontiers in immunology 9:1931.

Tang J., Xiong J., Wu T., Tang Z., Ding G., Zhang C., Wang S. and Liu Y. (2014) Aspirin treatment improved mesenchymal stem cell immunomodulatory properties via the 15d-PGJ2/PPARγ/TGF-β1 pathway. Stem cells and development 23:2093-2103.

Theofanakis C., Drakakis P., Besharat A. and Loutradis D. (2017) Human chorionic gonadotropin: the pregnancy hormone and more. International journal of molecular sciences 18:1059.

Travis M. A. and Sheppard D. (2014) TGF-beta activation and function in immunity. Annual Review of Immunology 32:51-82.

Ushigoe K., Irahara M., Fukumochi M., Kamada M. and Aono T. (2000) Production and regulation of cytokine-induced neutrophil chemoattractant in rat ovulation. Biology of reproduction 63:121-126.

Volarevic V., Gazdic M., Markovic B. S., Jovicic N., Djonov V. and Arsenijevic N. (2017) Mesenchymal stem cell-derived factors: Immuno-modulatory effects and therapeutic potential. Biofactors 43:633-644.

Wan H., Versnel M. A., Leijten L. M., van Helden-Meeuwsen C. G., Fekkes D., Leenen P. J., Khan N. A., Benner R. and Kiekens R. C. (2008) Chorionic gonadotropin induces dendritic cells to express a tolerogenic phenotype. Journal of leukocyte biology 83:894-901.

Wang Q., Ding G. and Xu X. (2016) Immunomodulatory functions of mesenchymal stem cells and possible mechanisms. Histology and histopathology 31:949-959.

Yoshimura T., Inaba M., Sugiura K., Nakajima T., Ito T., Nakamura K., Kanzaki H. and Ikehara S. (2003) Analyses of dendritic cell subsets in pregnancy. American Journal of Reproductive Immunology 50:137-145.

Journal of Cell and Molecular Research (2020) 11 (2), 99-107 DOI: 10.22067/jcmr.v11i2.85668

Research Article

Vitamin E Pretreatment of Mesenchymal Stem Cells: The Interplay of Oxidative Stress and Inflammation

Shadi Mehrzad[1†], Sepideh sadat Hosseini[1†], Madjid Momeni-Moghaddam[1], Moein Farshchian[2], Halimeh Hassanzadeh[2,3], Mahdi Mirahmadi[2], Fatemeh Sadeghifar[1*], Hamid Reza Bidkhori[2*]

[1]*Department of Biology, Faculty of science, Hakim Sabzevari University, Sabzevar, Iran*

[2]*Stem Cells and Regenerative Medicine Research Department, Academic Center for Education, Culture and Research (ACECR)-Khorasan Razavi, Mashhad, Iran*

[3]*Department of Biology, Faculty of Sciences, Ferdowsi University of Mashhad, Mashhad, Iran*

Received 18 February 2020 Accepted 12 March 2020

Abstract

Oxidative stress occurs as a result of breaking down the balance between oxidants (e.g., reactive oxygen species (ROS)) and antioxidants in cells. Several studies have shown that there is a close relationship between oxidative stress and inflammation at the sites of injury. Mesenchymal stem cells (MSCs) are exposed to endogenous and exogenous oxidants generated during their *ex vivo* expansion or following *in vivo* transplantation. *α*-tocopherol (vitamin E) is a fat-soluble compound known for its anti-oxidant and anti-inflammatory properties. In many studies, the immunomodulatory effects of vitamin E have been observed *in vivo*. This study aimed to determine whether pretreatment of MSCs with antioxidants like vitamin E, will enhance the anti-inflammatory and immunomodulatory properties of these cells. For this purpose, adipose-derived MSCs (ASCs) were treated with vitamin E (600 µM) for 48 h. Quantitative PCR (qPCR) experiments were performed to evaluate the expression of genes related to inflammation (*IL-1β, IL-6, IL-17, IL-10*) or immunomodulation (*TSG-6, COX-2, TDO2, TGF-β1*). Results indicated that vitamin E significantly increased the expression of *COX-2*, *TSG-6*, and *IL-1β* genes at the mRNA level compared with the control group, while it significantly decreased *IL-6* and *TGF-β* expressions. No effect was observed for *IL-17*, *IL-10*, and *TDO2* genes. These results suggest that *in vitro* preconditioning of ASCs with vitamin E may allow the cells to improve their anti-inflammatory and immunoregulatory capacities. Vitamin E pretreatment could lead to the improvement of their therapeutic abilities in conditions that are influenced by oxidative stress.

***Keywords*:** Mesenchymal Stem Cells, Vitamin E, Immunomodulation, Oxidative stress, Preconditioning

Introduction

Reactive oxygen species (ROS), which are generated during cellular metabolisms (Schieber and Chandel, 2014), are neutralized by antioxidants to gain a balance between oxidants and anti-oxidizing agents. Oxidative stress occurs as a result of excessive levels of ROS or low levels of antioxidants (Barrows et al., 2019). Oxidative stress as a pathophysiological condition is closely related to inflammation. ROS can initiate intracellular signal transductions and mediates the activation of various transcription factors (e.g., Nuclear factor kappa-light-chain-enhancer of activated B cells (NF-κB)) (Yuan et al., 2019). These transcription factors, in turn, raise the expression of pro-inflammatory genes and induce chronic inflammatory status (Biswas, 2016). Concurrently, inflammatory cells promote oxidative stress by releasing numerous reactive species at the sites of inflammation (Droge, 2002).

Antioxidant therapy seems to be a beneficial strategy to prevent or improve inflammatory diseases caused by oxidative stress. Nevertheless, some clinical studies were not promising (Kelly et al., 2008; Mahmood et al., 2018; Mishra et al., 2003). *α*-tocopherol (vitamin E) is the most effective lipid-soluble antioxidant that protects polyunsaturated fatty acids (PUFAs) of biological membranes (Azzi, 2007) and, is critical in the regulation of the immune response (Lee and Han, 2018).

† Both authors contributed equally to this work.

*Corresponding authors' e-mail address:
bidkhori@acecr.ac.ir
f.sadeghifar@hsu.ac.ir

Numerous studies have illustrated that vitamin E has a modulatory effect on the immune system. Xue *et al*. showed that this vitamin improved experimental autoimmune neuritis (EAN) in a rat model by suppressing the production of pro-inflammatory cytokines and inhibiting progressive oxidative damages (Kihara et al., 2019). It was also suggested that vitamin E modulates the phase conversion between naïve T cells and T helper1 (Th1) or T helper2 (Th2) cells, as a response to the stimulation of dendritic cells (Xue et al., 2016). The anti-inflammatory effects of vitamin E have also been reported *in vivo*, which seems to be independent of its antioxidant properties. Tahan *et al*., in 2011, found that vitamin E suppresses inflammatory cytokines and inhibits the acetic acid-induced chronic inflammation in a rat model (Tahan et al., 2011). Xue *et al*. in 2016, revealed that vitamin E decreases the number of inflammatory cells in lymph nodes and spleens of the animals *in vivo* and inhibits the proliferation of stimulated splenocytes *in vitro* (Xue et al., 2016).

Stem cell-based therapy is a proper strategy for controlling the symptoms of inflammatory and immune-mediated diseases. Mesenchymal stem/stromal cells (MSCs) have been widely used for allogeneic cell therapy to treat autoimmune diseases (Rad et al., 2019), inflammation-mediated disorders (Francis et al., 2019; Zhao et al., 2019), and cardiovascular diseases (Yun and Lee, 2019). The successful isolation of MSCs from a variety of adult tissues, e.g., bone marrow and adipose tissues, has provided a powerful tool for applied biological research (Wei et al., 2013).

Many studies revealed that some environmental and pharmacological stimuli (e.g., small molecules) or preconditioning strategies could influence the functional properties of MSCs in the context of immunotherapy (Linares et al., 2016; Pittenger and Martin, 2004; Schaefer et al., 2016). Furthermore, endogenous and exogenous oxidants that MSCs may expose to them during *ex vivo* expansion or *in vivo* transplantation procedures are considered as significant bottlenecks in cell therapy experiments (Yang et al., 2015). High levels of ROS are harmful to preserve self-renewal, reparative, and immunoregulatory functions of MSCs (Denu and Hematti, 2016; Yang et al., 2015). ROS, as a metabolic side product, increases adipogenic differentiation, enhances senescence, diminishes osteogenic differentiation, and hinders the immunomodulatory properties of MSCs (Denu and Hematti, 2016). Moreover, inflammatory responses, in addition to the production of ROS at the ischemic target sites, lead to the loss of transplanted MSCs. Hence, it is vital to reduce ROS either by manipulating the cells or their target sites (Devine et al., 2001; Pittenger and Martin, 2004; Yang et al., 2015).

Accordingly, understanding the effects of ROS on MSCs biology could shed light on the immunomodulatory behaviors of the cells under inflammatory conditions.

To the best of our knowledge, this is the first study that evaluates the effects of vitamin E on immunomodulatory and anti-inflammatory properties of human ASCs. Considering the vitamin E's evident antioxidant and anti-inflammatory properties, we anticipated that priming of ASCs with vitamin E could boost the beneficial effects of these therapeutically valuable cells.

Materials and Methods

Isolation and culture of human ASCs

Adipose tissues were obtained from three healthy donors undergoing elective liposuction at a private cosmetic day clinic in Mashhad, Iran. All three patients signed the informed consent form. The Academic Center for Education, Culture, and Research (ACECR) Biomedical Research Ethics Committee authorized all downstream protocols (IR.ACECR.JDM.REC.1398.009).

200 ml of adipose tissues were washed three times with phosphate-buffered saline (PBS) containing 0.1% penicillin-streptomycin (pen-strep) (Biowest, Canada) and incubated for one hour in constant–temperature bath at 37°C in the presence of 0.1% collagenase type I (Invitrogen, USA). Fetal bovine serum (FBS, Gibco, USA, 10%) was applied for collagenase I inactivation. Then, the mixture was centrifuged at 800 *g* for 10 min to remove adipose cell debris. In the following, pellets were suspended in Dulbecco's Modified Eagle Medium (DMEM, Biowest, Canada) contained 10% FBS and 0.1% pen-strep. Then, the cells were transferred into cell culture vessels and kept in a 5% CO_2 incubator at 37°C (Naderi-Meshkin et al., 2016). We changed the culture medium every three days. All the following experiments were conducted with the cells at passage number 3.

Characterization of human ASCs

Flowcytometric approach was applied for the identification of mesenchymal lineage-specific surface markers. A suspension of 10^6 single cells was transferred into the staining buffer contained PBS and 5% FBS. Then, anti-human monoclonal

antibodies (*all from* Cytognos, Spain) against clusters of differentiation 44 (CD44), CD90, CD73, CD13, CD14, CD34, and human leukocyte antigen– DR (HLA-DR) antigens were mixed with the cells and incubated for 45 min at 4 °C. FACS Calibur cytometer equipped with 488 nm argon laser (Bioscience, US) was used for data acquirements. Data analysis was performed using FlowJo (7.6.1) software.

The capacity of the cells for differentiation toward osteogenic and adipogenic lineages was qualitatively determined based on the previously described alizarin red and oil red O staining methods, respectively (Naderi-Meshkin et al., 2016). Briefly, adipogenesis was induced through the culture of ASCs in the presence of DMEM supplemented by 10% FBS, 200 mM indomethacin, 10 mM β-glycerophosphate, and 1 mM dexamethasone. After 14 days, the cells were rinsed with PBS and fixed in 10% formalin solution. Then, they were stained with 0.5% Oil Red O (Sigma, Germany) for 15 min.

The osteogenic inductive medium was composed of DMEM, 10% FBS, 0.5 mM acid ascorbic, 10 mM β-glycerophosphate, and 1 mM dexamethasone. The cells were incubated in this medium for 21 days. Then, they were fixed and stained with alizarin red (Sigma, Germany) for 30 min to detect the mineralized matrix of the bone, secreted by differentiated cells.

Preconditioning of human ASCs with vitamin E

Human ASCs were cultured in DMEM supplemented with 10% FBS and 1% pen-strep. Upon reaching 80% confluency, the proper concentration of vitamin E (Sigma, Germany) was added to the cultures. Untreated ASCs or cells that had been cultured with ethanol-containing media were applied as controls.

MTT assay

MTT (2, 3-bis (2-methoxy-4-nitro-5-5 sulfoxyphenyl)-2H-tetrazolium assay was carried out to evaluate the possible toxic effects of various concentrations of vitamin E against human ASCs. 10^4 cells were seeded in 96-well plates, and after reaching 80% confluency, they were treated with 200, 400, 600, 800, and 1000 µM of vitamin E for 24 to 72 hours. Cells cultured in the presence of DMEM or DMEM supplemented by an equal volume of ethanol were used as blank and control groups, respectively. Cell viabilities were determined following the addition of MTT dye (5 mg/ml) to the wells, incubating the vessels at 37°C for 4 hours, and recording optical densities (ODs) at 540nm by NanoDrop spectrophotometer (Nanodrop, BIO-TEK, Winooski, VT).

RNA extraction and quantitative PCR (qPCR)

Total RNAs were extracted from ASCs after 48 hours of treatment with 600 µM of vitamin E and control cells using TriPure according to the protocol provided by the manufacturer (Roche, Germany). The integrity of RNA samples was indicated using 1% agarose gel, and their concentrations were assessed via a NanoDrop spectrophotometer (Nanodrop, BIO-TEK, Winooski, VT).

One µg of DNase *I*-treated total RNA was used for cDNA synthesis in each case (Thermo Scientific, USA). cDNA synthesis steps were performed according to the kit instructions (Takara, Japan).

qPCR was accomplished by SYBR Green PCR Master Mix (amplicon, USA) according to the kit protocol with The CFX Connect™ Real-Time PCR Detection System (Bio-Rad, Germany). Ribosomal protein lateral stalk subunit P (*RPLP0*) gene was used as an internal control (reference gene) to normalize the transcript level of tested genes. Primers were designed by AlleleID 6 software and are shown in table 1.

Table 1. Primer sequences used for qPCR.

Genes	Primer sequences (5'→ 3')	product length (bp)
RPLP0	**F**: TGGTCATCCAGCAGGTGTTCGA **R**: ACAGACACTGGCAACATTGCGG	119
TGF-β1	**F**: GTTCAAGCAGAGTACACACAGC **R**: GTATTTCTGGTACAGCTCCACG	153
TSG-6	**F**: GCTGCTGGATGGATGGCTAAG **R**: CTCCTTTGCGTGTGGGTTGTAG	156
COX-2	**F**:CCAGAGCAGGCAGATGAAATACC **R**: ACCAGAAGGGCAGGATACAGC	168
IL-1β	**F**: CCTCTCTCACCTCTCCTACTCAC **R**: CTGCTACTTCTTGCCCCCTTTG	186
IL-17	**F:**CGGCAGGCACAAACTCATCC **R:**TTGTCCTCAGAATTTGGGCATCC	163
IL-10	**F:**GAGATGCCTTCAGCAGAGTGAAGA **R:**AGGCTTGGCAACCCAGGTAAC	114
TDO2	**F:** ACCTCCGTGCTTCTCAGACAG **R:** GACCTCCTTTGCTGGCTCTATTC	151
IL-6	**F**: ACTCACCTCTTCAGAACGAATT **R**: GCAAGTCTCCTCATTGAATCCAG	196

Statistical analysis

Statistical analysis was performed using GraphPad Prism 6. Data were expressed as mean of independent experiments±SEM. *One way* ANOVA and two samples T-test were used for statistical analysis. Events with *p* values less than 0.05 were considered significant.

Results

Characterization of human ASCs

Cultured ASCs were characterized through investigation of surface markers expression levels and their potential for multi-lineage differentiation. Flow cytometry analysis results indicated that > 98% of these cells expressed ASC specific markers including CD13, CD44, CD90 and CD73 and < 3% showed the expression of hematopoietic cell-specific markers including CD14, CD34, CD45, and HLA-DR (Figure 1).

The differentiation potential toward adipocytes and osteocytes was investigated using adipogenic and osteogenic differentiation media and staining with Oil Red O and Alizarin Red, respectively (figure 2 D, E & F).

Both lipid depositions and mineralization of the extracellular matrixes were visualized following the staining procedures, which confirmed the adipogenesis and osteogenesis of ASCs.

Investigating the toxic effects of vitamin E on ASCs

The effects of various concentrations of vitamin E (200-1000 µM) on ASCs' survival rate was explored by MTT assay. The results showed that after 24, 48, and 72 h, no significant difference (P<0.05) was observed between cell viabilities of control and sample groups among all concentrations and investigated time points (Figure 3).

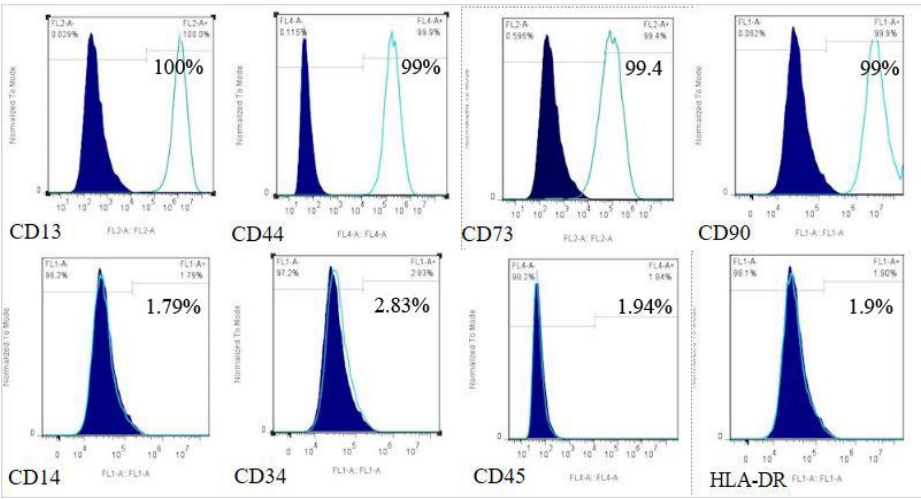

Figure 1. Immunophenotype characterization of sub-cultured MSCs at passage 3. Diagrams show flow cytometry data for MSC specific surface markers (CD13, CD44, CD73 & CD90) and hematopoietic markers (CD14, CD34, CD45 & HLA-DR). Data presents the percentages of the cells which were positive for each marker.

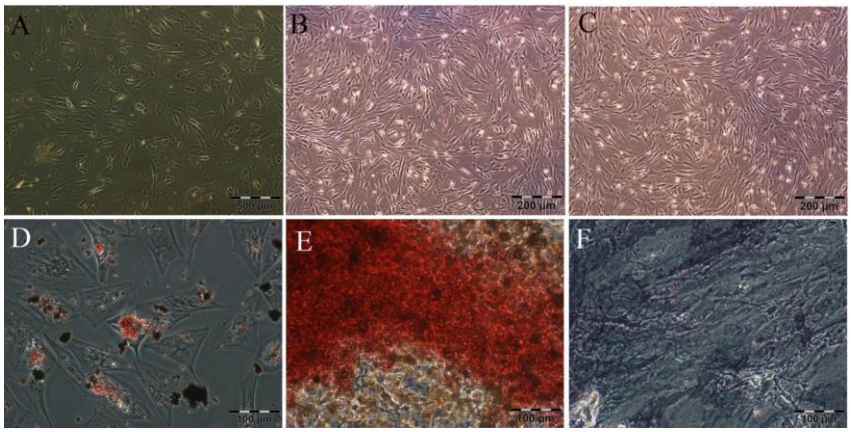

Figure 2. Characterization of human ASCs. Photomicrographs show the morphology and differentiation capacity of ASCs. A) Spindle-like morphology of human ASCs 8 days after harvesting from adipose tissues. B) Morphology of the control group after 48h. C) Morphology of ASCs preconditioned with 600 µM of vitamin E after 48 h. D) Oil Red O staining to detect adipogenic differentiation. E) Alizarin Red staining to measure osteogenic differentiation. F) Alkaline phosphatase assay to confirm osteogenic differentiation.

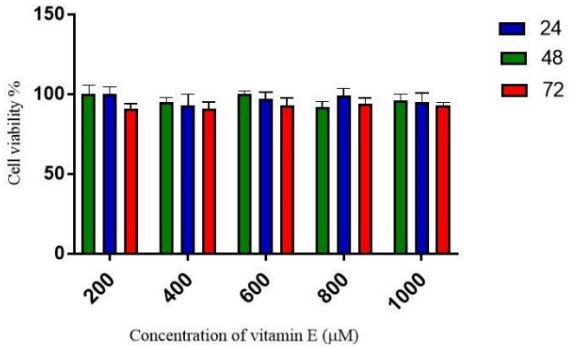

Figure 3. Mean of cell viabilities (%) calculated for pre-conditioned ASCs as obtained by MTT assay. As demonstrated, differences were not significant (p <0.05) in comparison to control groups at different concentrations and time points.

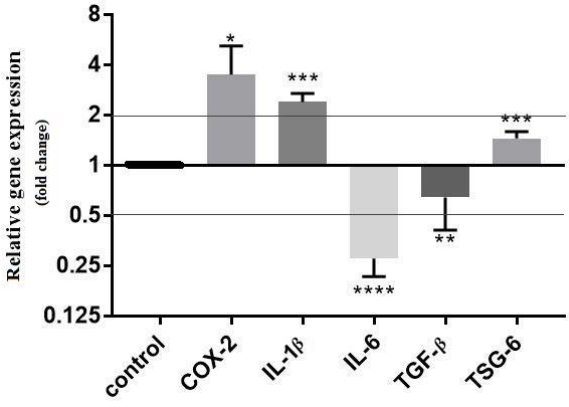

Figure 4. Vitamin E preconditioning of ASCs changed the expression of *IL-1β* and *IL-6* (inflammatory markers), in addition to *TSG-6*, *COX-2*, and *TGF-β* (immunomodulatory markers). Vitamin E treatment suppressed the expression of *IL-6* and *TGF- β* and enhanced the expression of *IL-1β*, *COX-2*, and *TSG-6* when compared to the control group. Results were expressed as mean±standard deviation (SD), and (*) represents $p < 0.05$, (**) represents $p < 0.01$, (***) represent $p < 0.001$ and (****) represent $p < 0.0001$. The expression levels of all investigated genes were considered equal to 1, conventionally.

Gene expression profiling of vitamin E stimulated ASCs

The expression levels of two categories of genes were investigated in this study: inflammatory-related genes including interleukin 1-betta (*IL-1β*), *IL-6*, *IL-17*, *IL-10* and immunomodulatory genes such as TNF-stimulated gene 6 (*TSG-6*), cyclooxygenase-2 (*COX-2*), tryptophan 2,3-dioxygenase (*TDO2*) and transforming growth factor- beta (*TGF-β*). The qPCR results showed that pretreatment with vitamin E markedly enhanced the gene expression of *TSG-6*, *IL-1β*, and *COX-2* at mRNA level and significantly (p<0.05) reduced the expressions of *IL-6* and *TGF-β* compared with the control group (Figure 4). In contrast, ASCs pretreatment did not affect *IL-10*, *IL-17*, and *TDO2* gene expressions compared to the control group.

Discussion

As a recommended supplement, vitamin E inhibits the production of ROS molecules and pro-inflammatory cytokines and depicts immunosuppressive properties (Lee and Han, 2018b). The findings of this study demonstrated that Vitamin E when applied as a small molecule for preconditioning of ASCs, altered the expression of some genes which are involved in immunomodulation and inflammation. Here, we argued that the pretreatment of stem cells with Vitamin E before cellular therapy could have beneficial effects on their immunoregulatory capacities.

ASCs are multipotent cells with a high capability for interacting with a variety of immune cells. These cells release various factors with immunomodulatory potential such as cytokines and chemokines, which make them a decent choice to treat numerous immune-mediated diseases accompanied by chronic inflammation (Baer et al., 2018). Priming MSCs with appropriate agents can promote the efficacy of some specific immunotherapeutic applications (Hu and Li, 2018; Silva et al., 2018; Tang et al., 2014; Wisel et al., 2009).

Vitamin E is recognized not only for its antioxidant properties but also for its regulatory effects on signaling pathways through the induction of gene expression modifications (Azzi, 2018; Sangiorgi et al., 2016; Zingg, 2015). We studied the consequences of vitamin E treatment at a high concentration (600 μM) on the cell proliferation rate and cytokine production status of the cells *in vitro*. Our findings showed that the preconditioning of MSCs by 600 μM of vitamin E significantly attenuated the expression of *IL-6* at least by two folds and altered the expression of *TGF-β* slightly. We also observed a significant increase in the expression of *COX-2*, *TSG6*, and *IL-1β*.

Wang *et al.* found that rat bone marrow-derived MSCs could ameliorate peritoneal injury by repairing mesothelial cells. They also showed that MSCs lacking *TSG-6* (TSG-6-siRNA MSCs) had no apparent effects on the peritoneal fibrosis. Thus, it was confirmed that the secretion of TSG-6 by MSCs made a significant contribution to their clinical outcomes (Wang et al., 2012). In line with their findings, Roddy *et al.* reported that

intravenous administration of human MSCs primed to express TSG-6 suppressed the inflammatory damages of the cornea following the induction of chemical injury in rats. Additionally, Roddy et al. demonstrated that the siRNA knockdown of TSG-6 impeded the anti-inflammatory effects of these cells on damaged corneal epithelial cells (Roddy et al., 2011). Given these observations, we suggest that preconditioning of MSCs with vitamin E could improve their immunomodulatory properties by enhancing the expression of TSG-6.

IL-6 is a pleiotropic and multifunctional cytokine involved in many physiological events, such as inflammation through NF-κB and signal transducers and activators of transcription (STAT) signaling pathways. It was shown that blockade of *IL-6* prevents the progression of autoimmune-based diseases and tumor formation (Barnes et al., 2011; Schaper and Rose-John, 2015; Tanaka et al., 2014). The blockade of *TGF-β1* also causes anti-tumor immunity and tumor regression (Mariathasan et al., 2018; Shangguan et al., 2012), which increases safety concerns in tumorigenesis. COX-2 is a crucial enzyme in prostaglandin E2 synthesis, which promotes the anti-inflammatory features of macrophages (M2) (Lu et al., 2017; Németh et al., 2009). The pro-inflammatory cytokine, IL-1*β*, is regulated through NF-κB and c-jun signaling pathways (Libby, 2017; Palomo et al., 2015; Rodriguez et al., 2019). In contrast, MSC pre-treatment did not affect *IL-10*, *IL-17*, and *TDO2* gene expressions in the current study. Their weak expression by naïve MSCs could explain it (Ben-Zwi et al., 2019).

There was a strong correlation between the changes in redox potential and the production of pro-inflammatory cytokines with the inflammatory pathways, e.g., NF-κB. NF-κB is a transcription factor thought to be modulated by oxidative stress (Behl et al., 1994; Lingappan, 2018). Antioxidants like vitamin E are believed to prevent the activation of NF-κB and other inflammatory pathways through the inhibition of lipid peroxidation (Saxena et al., 2019). Together, these findings support the notion that vitamin E improves the anti-inflammatory characteristics of ASCs. This effect could be due to inhibition of the activation of some inflammatory signaling pathways, such as NF-κB, in human MSCs that inhibits the production of pro-inflammatory cytokines.

Acknowledgments
This study was funded by ACECR-Khorasan Razavi. It was an Hakim Sabzevari University M.Sc thesis, Sabzevar, Iran. We are grateful to Dr. Naser Sanjar Mosavi for his kind contribution in collecting samples.

Conflict of interest
The authors declared no competing interest.

References

Azzi A. (2007) Molecular mechanism of α-tocopherol action. Free Radical Biology and Medicine 43:16-21.

Azzi A. (2018) Many tocopherols, one vitamin E. Molecular Aspects of Medicine 61:92-103.

Baer P. C., Overath J. M., Urbschat A., Schubert R., Koch B., Bohn A. A. and Geiger H. (2018) Effect of different preconditioning regimens on the expression profile of murine adipose-derived stromal/stem cells. International Journal of Molecular Sciences 19:1719.

Barnes T. C., Anderson M. E. and Moots R. J. (2011) The many faces of interleukin-6: the role of IL-6 in inflammation, vasculopathy, and fibrosis in systemic sclerosis. International Journal of Rheumatology.

Barrows I. R., Ramezani A. and Raj D. S. (2019) Inflammation, Immunity, and Oxidative Stress in Hypertension—Partners in Crime? Advances in Chronic Kidney Disease 26:122-130.

Behl C., Davis J., Lesley R., and Schubert D. (1994) Hydrogen peroxide mediates amyloid β protein toxicity. Cell 77:817-827.

Ben-Zwi M., Petrou P., Halimi M., Karussis D. and Kassis I. (2019) Neuralized mesenchymal stem cells (NMSC) exhibit phenotypical, and biological evidence of neuronal transdifferentiation and suppress EAE more effectively than unmodified MSC. Immunology Letters 212:6-13.

Biswas S. K. (2016) Does the interdependence between oxidative stress and inflammation explain the antioxidant paradox? Oxidative Medicine and Cellular Longevity.

Denu R. A. and Hematti P. (2016) Effects of oxidative stress on mesenchymal stem cell biology. Oxidative Medicine and Cellular Longevity.

Devine S. M., Bartholomew A. M., Mahmud N., Nelson M., Patil S., Hardy W., Sturgeon C., Hewett T., Chung T. and Stock W. (2001) Mesenchymal stem cells are capable of homing to the bone marrow of non-human primates following systemic infusion. Experimental hematology 29:244-255.

Droge W. (2002) Free radicals in the physiological control of cell function. Physiological Reviews 82:47-95.

Francis E., Kearney L. and Clover J. (2019) The effects of stem cells on burn wounds: a review. International Journal of Burns and Trauma 9:1.

Hu C. and Li L. (2018) Preconditioning influences mesenchymal stem cell properties in vitro and in vivo. Journal of Cellular and Molecular Medicine 22:1428-1442.

Kelly R. P., Poo Yeo K., Isaac H. B., Lee C.-Y. J., Huang S. H., Teng L., Halliwell B. and Wise S. D. (2008) Lack of effect of acute oral ingestion of vitamin C on oxidative stress, arterial stiffness or blood pressure in healthy subjects. Free Radical Research 42:514-522.

Kihara H., Konno S. and Fujioka T. (2019) Alpha-Tocopherol Ameliorates Experimental Autoimmune Neuritis (P1. 2-089). AAN Enterprises.

Lee G. Y. and Han S. N. (2018) The role of vitamin E in immunity. Nutrients 10:1614.

Libby P. (2017) Interleukin-1 beta as a target for atherosclerosis therapy: biological basis of CANTOS and beyond. Journal of the American College of Cardiology 70:2278-2289.

Linares G. R., Chiu C.-T., Scheuing L., Leng Y., Liao H.-M., Maric D. and Chuang D.-M. (2016) Preconditioning mesenchymal stem cells with the mood stabilizers lithium and valproic acid enhances therapeutic efficacy in a mouse model of Huntington's disease. Experimental Neurology 281:81-92.

Lingappan K. (2018) NF-κB in oxidative stress. Current Opinion in Toxicology 7:81-86.

Lu L. Y., Loi F., Nathan K., Lin T. h., Pajarinen J., Gibon E., Nabeshima A., Cordova L., Jämsen E. and Yao Z. (2017) Pro-inflammatory M1 macrophages promote Osteogenesis by mesenchymal stem cells via the COX-2prostaglandin E2 pathway. Journal of Orthopaedic Research 35:2378-2385.

Mahmood L. A., Al Saadi R. and Matthews L. (2018) Dietary and antioxidant therapy for autistic children: Does it really work? Archives of Medicine and Health Sciences 6:73.

Mariathasan S., Turley S. J., Nickles D., Castiglioni A., Yuen K., Wang Y., Kadel III E. E., Koeppen H., Astarita J. L. and Cubas R. (2018) TGFβ attenuates tumour response to PD-L1 blockade by contributing to exclusion of T cells. Nature 554:544.

Mishra G., Malik N., Paul A., Wadsworth M. and Bolton-Smith C. (2003) Childhood and adult dietary vitamin E intake and cardiovascular risk factors in mid-life in the 1946 British Birth Cohort. European Journal of Clinical Nutrition 57:1418-1425.

Naderi Meshkin H., Matin M. M., Heirani,Tabasi A., Mirahmadi M., Irfan-Maqsood M., Edalatmanesh M. A., Shahriyari M., Ahmadiankia N., Moussavi N. S. and Bidkhori H. R. (2016) Injectable hydrogel delivery plus preconditioning of mesenchymal stem cells: exploitation of SDF-1/CXCR4 axis toward enhancing the efficacy of stem cells' homing. Cell Biology International 40:730-741.

Németh K., Leelahavanichkul A., Yuen P. S., Mayer B., Parmelee A., Doi K., Robey P. G., Leelahavanichkul K., Koller B. H. and Brown J. M. (2009) Bone marrow stromal cells attenuate sepsis via prostaglandin E 2–dependent reprogramming of host macrophages to increase their interleukin-10 production. Nature Medicine 15:42.

Palomo J., Dietrich D., Martin P., Palmer G. and Gabay C. (2015) The interleukin (IL)-1 cytokine family–Balance between agonists and antagonists in inflammatory diseases. Cytokine 76:25-37.

Pittenger M. F. and Martin B. J. (2004)

Mesenchymal stem cells and their potential as cardiac therapeutics. Circulation Research 95:9-20.

Rad F., Ghorbani M., Roushandeh A. M. and Roudkenar M. H. (2019) Mesenchymal stem cell-based therapy for autoimmune diseases: emerging roles of extracellular vesicles. Molecular Biology Reports 46:1533-1549.

Roddy G. W., Oh J. Y., Lee R. H., Bartosh T. J., Ylostalo J., Coble K., Rosa R. H., Jr. and Prockop D. J. (2011) Action at a distance: systemically administered adult stem/progenitor cells (MSCs) reduce inflammatory damage to the cornea without engraftment and primarily by secretion of TNF-alpha stimulated gene/protein 6. Stem Cells 29:1572-1579.

Rodriguez L. A., Mohammadipoor A., Alvarado L., Kamucheka R. M., Asher A. M., Cancio L. C. and Antebi B. (2019) Preconditioning in an Inflammatory Milieu Augments the Immunotherapeutic Function of Mesenchymal Stromal Cells. Cells 8:462.

Sangiorgi B., De Freitas H. T., Schiavinato J. L. D. S., Leão V., Haddad R., Orellana M. D., Faça V. M., Ferreira G. A., Covas D. T. and Zago M. A. (2016) DSP30 enhances the immunosuppressive properties of mesenchymal stromal cells and protects their suppressive potential from lipopolysaccharide effects: a potential role of adenosine. Cytotherapy 18:846-859.

Saxena A., Sonowal H. and Ramana K. V. (2019) Transcriptional Factor Modulation by Lipid Peroxidation-Derived Aldehydes. In The Molecular Nutrition of Fats. Elsevier. 419-431.

Schaefer R., Spohn G. and Baer P. C. (2016) Mesenchymal stem/stromal cells in regenerative medicine: can preconditioning strategies improve therapeutic efficacy. Transfusion Medicine and Hemotherapy 43:256-267.

Schaper F. and Rose-John S. (2015) Interleukin-6: biology, signaling and strategies of blockade. Cytokine & growth factor reviews 26:475-487.

Schieber M. and Chandel N. S. (2014) ROS function in redox signaling and oxidative stress. Current biology 24:R453-R462.

Shangguan L., Ti X., Krause U., Hai B., Zhao Y., Yang Z. and Liu F. (2012) Inhibition of TGF-β/Smad signaling by BAMBI blocks differentiation of human mesenchymal stem cells to carcinoma-associated fibroblasts and abolishes their protumor effects. Stem cells 30:2810-2819.

Silva L. H., Antunes M. A., Dos Santos C. C., Weiss D. J., Cruz F. F. and Rocco P. R. (2018) Strategies to improve the therapeutic effects of mesenchymal stromal cells in respiratory diseases. Stem Cell Research & Therapy 9:45.

Tahan G., Aytac E., Aytekin H., Gunduz F., Dogusoy G., Aydin S., Tahan V. and Uzun H. (2011) Vitamin E has a dual effect of anti-inflammatory and antioxidant activities in acetic acid-induced ulcerative colitis in rats. Canadian Journal of Surgery 54:333.

Tanaka T., Narazaki M. and Kishimoto T. (2014) IL-6 in inflammation, immunity, and disease. Cold Spring Harbor Perspectives in Biology 6:a016295.

Tang J., Xiong J., Wu T., Tang Z., Ding G., Zhang C., Wang S. and Liu Y. (2014) Aspirin treatment improved mesenchymal stem cell immunomodulatory properties via the 15d-PGJ2/PPARγ/TGF-β1 pathway. Stem cells and Development 23:2093-2103.

Wang N., Li Q., Zhang L., Lin H., Hu J., Li D., Shi S., Cui S., Zhou J., Ji J., Wan J., Cai G. and Chen X. (2012) Mesenchymal stem cells attenuate peritoneal injury through secretion of TSG-6. PLoS One 7:e43768.

Wei X., Yang X., Han Z.-p., Qu F.-f., Shao L. and Shi Y.-f. (2013) Mesenchymal stem cells: a new trend for cell therapy. Acta Pharmacologica Sinica 34:747-754.

Wisel S., Khan M., Kuppusamy M. L., Mohan I. K., Chacko S. M., Rivera B. K., Sun B. C., Hideg K. and Kuppusamy P. (2009) Pharmacological preconditioning of mesenchymal stem cells with trimetazidine (1-[2, 3, 4-trimethoxybenzyl] piperazine) protects hypoxic cells against oxidative stress and enhances recovery of myocardial function in infarcted heart through Bcl-2 expression. Journal of Pharmacology and Experimental Therapeutics 329:543-550.

Xue H., Ren H., Zhang L., Sun X., Wang W., Zhang S., Zhao J. and Ming L. (2016) Alpha-tocopherol ameliorates experimental autoimmune encephalomyelitis through the regulation of Th1 cells. Iranian Journal of Basic Medical Sciences 19:561.

Yang S.-R., Park J.-R. and Kang K.-S. (2015) Reactive oxygen species in mesenchymal stem cell aging: implication to lung diseases. Oxidative Medicine and Cellular Longevity 2015.

Yuan T., Yang T., Chen H., Fu D., Hu Y., Wang J., Yuan Q., Yu H., Xu W. and Xie X. (2019) New insights into oxidative stress and inflammation during diabetes mellitus-accelerated atherosclerosis. Redox Biology 20:247-260.

Yun C. W. and Lee S. H. (2019) Enhancement of functionality and therapeutic efficacy of cell-based therapy using mesenchymal stem cells for cardiovascular disease. International Journal of Molecular Sciences 20:982.

Zhao L., Han F., Wang J. and Chen J. (2019) Current understanding of the administration of mesenchymal stem cells in acute kidney injury to chronic kidney disease transition: a review with a focus on preclinical models. Stem Cell Research & Therapy 10:385.

Zingg J.-M. (2015) Vitamin E: a role in signal transduction. Annual Review of Nutrition 35:135-173.

Note added in proof

COVID-19 outbreak has been a challenging global issue recently, and the early outcome of Sarilumab and Tocilizumab clinical trials as monoclonal antibodies, that work by inhibiting the IL-6, were successful. Hence, our results regarding the downregulation of IL-6 by vitamin E could be considered as a therapeutic option that needs to be evaluated by further studies.

Scientific Reviewers

MANUSCRIPT PREPARATION

Manuscripts should be prepared in accordance with the uniform requirements for Manuscript's Submission to **"Journal of Cell and Molecular Research".**

Language: Papers should be in English (either British or American spelling). The past tense should be used throughout the results description, and the present tense in referring to previously established and generally accepted results. Authors who are unsure of correct English usage should have their manuscript checked by somebody who is proficient in the language; manuscripts that are deficient in this respect may be returned to the author for revision before scientific review.

Typing: Manuscripts must be typewritten in a font size of at least 12 points, double-spaced (including References, Tables and Figure legends) with wide margins (2.5 cm from all sides) on one side of the paper. The beginning of each new paragraph must be clearly indicated by indentation. All pages should be numbered consecutively at the bottom starting with the title page.

Length: The length of research articles should be restricted to ten printed pages. Short communication should not exceed five pages of manuscript, including references, figures and tables. Letters should be 400-500 words having 7-10 references, one figure or table if necessary. Commentaries and news should also be 800-1000 words having 7-10 references and one figure or table if necessary.

Types of Manuscript: JCMR is accepting original research paper, short communication reports, invited reviews, letters to editor, biographies of scientific reviewers, commentaries and news.

Statement of Human and Animal Rights: Author's should declare regulatory statement regarding the experiments using animals, human cells/tissues that all in vivo experiments have been performed according to the guidelines (explained by WHO, international animal rights federations or your respective institute) to use animals in their research work.

Conflict of Interest Statement: Authors or corresponding author should declare statement of conflict of interest at the last of manuscript.

Manuscript Evaluation Time: All submitted manuscripts will be evaluated and reviewed according to following evaluation schedule.
Pre-Editorial Evaluation: All submitted manuscripts, right after their submission to JCMR will be evaluation by Editors for being according to the journal scope and format. This evaluation can take 2-7 days of submission.
Reviewer's Evaluation: Selected manuscripts after pre-editorial evaluation will be sent to minimum two blind reviewers assigned by Editor-in-Chief. This process may take 21-27 days.
Post Editorial Evaluation: After receiving reviewer's comments, editors evaluate the manuscripts considering the comments and decide their first decision. This process takes 3-5 days and then authors are informed regarding the editorial decision.

GENERAL ARRANGEMENT OF PAPERS

Title: In the first page, papers should be headed by a concise and informative title. The title should be followed by the authors' full first names, middle initials and last names and by names and addresses of laboratories where the work was carried out. Identify the affiliations of all authors and their institutions, departments or organization by use of Arabic numbers (1, 2, 3, etc.).

Footnotes: The name and full postal address, telephone, fax and E-mail number of corresponding author should be provided in a footnote.

Abbreviations: The Journal publishes a standard abbreviation list at the front of every issue. These standard abbreviations do not need to be spelled out within paper. However, non-standard and undefined abbreviations used five or more times should be listed in the footnote. Abbreviations should be defined where first mentioned in the text. Do not use abbreviations in the title or in the Abstract. However, they can be used in Figures and Tables with explanation in the Figure legend or in a footnote to the Table.

Abstract: In second page, abstract should follow the title (no authors' name) in structured format of not more than 250 words and must be able to stand independently and should state the Background, Methods, Results and Conclusion. Write the abstract in third person. References should not be cited and abbreviations should be avoided.

Keywords: A list of three to five keywords for indexing should be included at bottom of the abstract. Introduction should contain a description of the problem under investigation and a brief survey of the existing literature on the subject.

Materials and Methods: Sufficient details must be provided to allow the work to be repeated. Correct chemical names should be given and strains of organisms should be specified. Suppliers of materials need only be mentioned if this may affect the results. Use System International (SI) units and symbols.

Results: This section should describe concisely the rationale of the investigation and its outcomes. Data should not be repeated in both a Table and a Figure. Tables and Figures should be selected to illustrate specific points. Do not tabulate or illustrate points that can be adequately and concisely described in the text.

Discussion: This should not simply recapitulate the Results. It should relate results to previous work and interpret them. Combined Results and Discussion sections are encouraged when appropriate.

Acknowledgments: This optional part should include a statement thanking those who assisted substantially with work relevant to the study. Grant support should be included in this section.

References: References should be numbered and written in alphabetical order. Only published, "in press" papers, and books may be cited in the reference list (see the examples below). References to work "in press" must be accompanied by a copy of acceptance letter from the journal. References should not be given to personal communications, unpublished data, manuscripts in preparation, letters, company publications, patents pending, and URLs for websites. Abstracts of papers presented at meetings are not permissible. These references should appear as parenthetical expressions in the text, e.g. (unpublished data). Few example of referencing patterns are given as follows:

Bongso A., Lee E. H. and Brenner S. (2005) Stem cells from bench to bed side. World Scientific Publishing Co. Singapore, 38-55 pp.

Irfan-Maqsood M. (2013) Stem Cells of Epidermis: A Critical Introduction. Journal of Cell and Molecular Research 5(1): 1-2.

Note: All the reference should be in EndNote format (JCMR EndNote Style is available on JCMR's web site, Author's Guideline)

Tables and Figures: Tables and Figures should be numbered (1, 2, 3, etc.) as they appear in the text. Figures

should preferably be the size intended for publication. Tables and Figures should be carefully marked. Legends should be typed single-spaced separately from the figures. Photographs must be originals of high quality. Photocopies are not acceptable. Those wishing to submit color photographs should contact the Editor regarding charges.

Black Page Charges: There is no black page charges for publication in the Journal of Cell and Molecular Research.

Color Page Charges: All color pages being printed in color will cost 1,000,000 Iranian Rials/page.

JCMR Open Access Policy: Journal of Cell and Molecular Research follows the terms outlined by the Creative Common's Attribution-Only license (CC-BY) to be the standard terms for Open Access. Creative Commons License.

Note: All manuscripts submitted to JCMR are tracked by using "Plagiarism Tracker X" or "small tools" for possible plagiarism before acceptance to JCMR.

Table of Contents

Cost-effective Strategies for Depletion of Endogenous Extracellular Vesicles from Fetal Bovine Serum 42
Azadeh Haghighitalab, Maryam M. Matin, Fatemeh Khakrah, Ahmad Asoodeh, Ahmad Reza Bahrami

A Rapid Method for Analysis of cDNA Synthesis Using Ion-Pair Reversed-Phase High Performance Liquid Chromatography 55
Maryam M. Matin, David P. Hornby

Production of Silver Nanoparticles by Marigold Extract 59
Zohreh Sohrabi Nezhad, Hassan Marashi, Nasrin Moshtaghi

***In silico* Analysis of Determinant Factors in Microbial Protease Thermostability** 66
Parisa Farrokh, Fatemeh Salimi

Evaluation of IFN-γ and T-bet Expression Levels as Possible Molecular Markers of Schizophrenia 82
Roghaye Lorestani, Sohrab Boozarpour, Sakineh Alijanpour, Leila Ahangar

Immunosuppressive Effects of Human Chorionic Gonadotropin (hCG) on Mesenchymal Stromal Cells 90
Sepideh sadat Hosseini, Shadi Mehrzad, Halimeh Hassanzadeh, Hamid Reza Bidkhori, Mahdi Mirahmadi, Madjid Momeni-Moghaddam, Fatemeh Sadeghifar, Moein Farshchian

Vitamin E Pretreatment of Mesenchymal Stem Cells: The Interplay of Oxidative Stress and Inflammation 99
Shadi Mehrzad, Sepideh sadat Hosseini, Madjid Momeni-Moghaddam, Moein Farshchian, Halimeh Hassanzadeh, Mahdi Mirahmadi, Fatemeh Sadeghifar, Hamid Reza Bidkhor

Journal of Cell and Molecular Research

Volume 11, Number 2, Winter, 2020